

**SAKARYA UNIVERSITY  
INSTITUTE OF SCIENCE AND TECHNOLOGY**

**WIND TURBINE PROTECTION AND MODELLING**

**M.Sc. THESIS**

**Eric NDUWAYEZU**

**Department** : **ELECTRICAL & ELECTRONICS  
ENGINEERING**  
**Field of Science** : **ELECTRICAL**  
**Supervisor** : **(Assoc. Prof.) Dr. Mehmet BAYRAK**

**June 2015**

SAKARYA UNIVERSITY  
INSTITUTE OF SCIENCE AND TECHNOLOGY

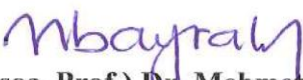
WIND TURBINE PROTECTION AND MODELLING

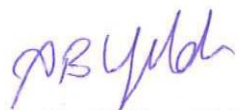
M.Sc. THESIS

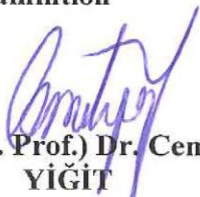
Eric NDUWAYEZU

Department : ELECTRICAL & ELECTRONICS ENGINEERING  
Field of Science : ELECTRICAL  
Supervisor : (Assoc. Prof.) Dr. Mehmet BAYRAK

This thesis has been accepted unanimously / ~~with majority of votes~~ by the examination committee on 10/06/2015

  
(Assoc. Prof.) Dr. Mehmet  
BAYRAK  
Head of Jury

  
(Assoc. Prof.) Dr. Ali Bekir  
YILDIZ  
Jury Member

  
(Assist. Prof.) Dr. Cemil  
YIGIT  
Jury Member

## **DECLARATION**

I declare that all the data in this thesis was obtained by myself in academic rules, all visual and written information and results were presented in accordance with academic and ethical rules, there is no distortion in the presented data, in case of utilizing other people's works they were refereed properly to scientific norms, the data presented in this thesis has not been used in any other thesis in this university or in any other university.

Eric NDUWAYEZU

10.06.2015

## **PREFACE**

This thesis is initiated from my daily work with Bereket Enerji-Uşak RES team and is carried out under the Türkiye Scholarship 2012RW005. The research started on the 23.06.2014 and ended at the 06.06.2015, where the writing of this thesis has been finished as well. The research got financially supported by Türkiye Burslari and scientifically by Bereket Enerji through the Uşak RES. The thesis is submitted to the Institute of natural sciences at Sakarya University as partial fulfilment of the requirements for gaining the Masters degree in Electrical and Electronics Engineering. There have been one main supervisor following the progress of the research, Associate Professor Mehmet BAYRAK from Sakarya University. I would like to thank him for his support, patient and help in finishing this ambitious research in the given time. I want to thank Mr. Hüseyin UYSAL and Mr.Zafer ARIKAN from Bereket Enerji for providing all required information regarding wind turbine technology and models during this study, the technical information given by them made it possible to achieve a complete wind turbine models. Furthermore I like to thank all the people I met on my way from cities all over Turkey, giving me the possibility to discuss my ideas and giving me feedback to my work and therewith having participated in the work. Especially I like to highlight the wonderful possibilities given by the ELIMSAN for HV/MV DS and switchgears training actively supported by Mr.Aykut ECİN and Mr. Sinan DÖNMEZ. I like to give further thanks to the R&D department of ELIMSAN in Kocaeli to help me clarifying some questions around machine technology and Assoc. Prof. Mehmet BAYRAK, who made this possible. Especially I want to thank Professor Ertan YANIKOĞLU, Assoc. Prof. Yılmaz Uyaroğlu, Assoc. Prof. Cemil YİĞİT, Assoc. Prof. Ali Bekir YILDIZ(Kocaeli University) and the Masters students from Sakarya University, helping me during my 3 years stay. Other thanks is to the Turkish people I became friends with during my stay in Turkey and who helped me staying motivated during the last phase of my work. Personally I want to thank Ms. Fatma KİRLİ and Görkem YUVARLAKLAR, who during my Masters became very good and close friends.

## TABLE OF CONTENTS

PREFACE .....	ii
TABLE OF CONTENTS .....	iii
LIST OF SYMBOLS AND ABBREVIATIONS .....	vi
LIST OF FIGURES.....	ix
LIST OF TABLES .....	xiii
SUMMARY .....	xiv
ÖZET .....	xv
CHAPTER 1.	
INTRODUCTION.....	1
1.1. Wind Turbine Technology.....	2
1.2. Work Motivation .....	6
1.3. Work Objective.....	8
1.4. Thesis Outline.....	10
CHAPTER 2.	
BACKGROUND AND LITERATURE REVIEW.....	11
2.1. Wind Turbine Development and Types of Turbines .....	11
2.1.1. Wind Turbine History .....	11
2.1.2. State-of-the-art Technologies .....	13
2.1.3. Power Control .....	22
2.2. Wind Farms .....	25
2.2.1. Wind Farm Definition and Siting.....	25
2.2.2. Requirements for the Interconnection of Wind Farms to the Power System .....	29
2.2.3. Discussing the Requirements .....	36

## CHAPTER 3.

SYSTEM MODELLING AND ANALYSIS .....	38
3.1. Asynchronous Generator Models .....	38
3.1.1. General Equations in ABC/abc Reference Frame .....	39
3.1.2. The Clark Transformation (a, b, 0 equivalent frame).....	49
3.1.3. The Park Transformation (d, q, 0 equivalent frame).....	52
3.1.4. Saturation Effects .....	55
3.1.5. Windage Losses and Friction Losses .....	61
3.1.6. The 3-ph – Model in Matlab/ Simulink.....	64
3.2. Modeling of Transformers .....	86
3.2.1. The 2-windings 3-phase Transformer Model.....	86
3.2.2. The 3-windings 3-phase Transformer Model.....	91
3.2.3. The 2-windings 3-phase Autotransformer.....	96
3.2.4. The transformer Models Implemented in Matlab/Simulink.....	99
3.3. Wind Turbine Modeling.....	106
3.3.1. Aerodynamic Model.....	106
3.3.2. Pitch Model .....	109
3.3.3. Mechanical Model.....	110

## CHAPTER 4.

WIND TURBINE PROTECTION.....	114
4.1. Overview of Electrical Faults in Wind Turbine Systems .....	114
4.2 Grid Faults .....	114
4.3. Protective Design for Wind Farm.....	116
4.3.1. Protection Functions.....	116
4.3.2. Rotor Protection System.....	118
4.3.3. Wind Turbine Controller Role .....	121
4.3.4. Local Step-up Transformer Protection .....	121
4.3.5. Collector Feeder Protection.....	122
4.4. Protection Challenges .....	122
4.4.1 Distribution System Topology .....	123
4.4.2 System Configuration Protection .....	123
4.4.3 Distributed Generation Effects.....	124

4.4.4 Control System Requirements.....	124
4.4.5 Aysnchronous Generator Dynamic Behavior.....	124
4.5. Simulated Illustrative Case Study.....	124
4.5.1 Modeling of Uşak RES- Bereket Enerji Wind Farm.....	124
4.5.2 Performance Evaluation of DFIG units.....	130
4.6. Aims for Improving Wind Farm Protection Systems .....	134
4.6.1 Distribution Network re-design.....	134
4.6.2 Employments more Protective Elements .....	136
4.6.3 Integrated Protection with Enhanced Communication Employment .....	136
 CHAPTER 5.	
CONCLUSION .....	137
5.1. The Work Summary .....	138
5.2. Results Obtained in the Work.....	140
5.2.1. Overview of Existing Grid Codes .....	140
5.2.2.Modelling and Analysis of the Asynchronous Machine Model.	140
5.2.3.Modelling of Electrical three-phase Components.....	141
5.2.4.Modelling of a Complete Wind Turbine System .....	141
5.2.5. Results Obtained from the Models.....	141
5.2.6. Wind Turbine Protection .....	142
5.3. Recommendation and Future Work .....	143
 REFERENCES.....	 145
RESUME.....	151

## LIST OF SYMBOLS AND ABBREVIATIONS

$a, j$	: complex Versors
$a_{12}, a_{23}, a_{13}$	: Transformer ratio between side 1-2, 2-3 and 1-3
$c_p$	: Power coefficient
$e$	: induced voltage
$f_1$	: Grid frequency
$f_1, f_2, f_3, f_4, f_5, f_6, f_7$	: Functions of angle difference between phases used in machine and transformer induction matrix
$i$	: current
$m$	: number of phase
$n$	: Number; gear ratio
$n_g$	: Generator speed
$n_0$	: Synchronous speed
$p_p$	: pairs of poles
$u$	: voltage
$u_e$	: ratio between stator and rotor winding
$s$	: slip
$v_w$	: Wind speed
$w_1, w_2$	: Primary, secondary winding turns
$D$	: damping factor
$D\omega_r$	: damping torque
$E_s$	: from stator induced voltage
$H$	: electric field strength
$I$	: Rms current
$I_r \text{ meas}$	: Measured rotor current amplitude
$I_{\text{ref}}$	: Desired rotor current
$J$	: Inertia



$J_{ges}$	: Total inertia
$L$	: inductance
$L_m, L_h$	: main flux inductance
$L_{ms}, L_{mr}$	: mutual inductance stator, rotor
$L_{msr}$	: stator – rotor couple inductance
$L_\sigma$	: leakage flux inductance
$N$	: number of turns
$N\xi$	: effective number of turns
$N_1, N_2$	: number of slots (stator, rotor)
$P$	: active power
$P_M$	: Mechanical power
$P_w$	: Power obtained from the wind
$Q$	: reactive power
$R$	: Resistance
$R_{ext'}$	: External rotor resistance
$S$	: Apparent power
$T_A$	: Aerodynamic torque
$T_e$	: electromagnetic torque
$T_m$	: mechanical load torque
$T_r$	: Generator time constant
$T_s$	: Shaft torque
$U$	: Rms voltage
$X$	: Reactance
$Z$	: Impedance
$\varepsilon$	: Permittivity
$\theta, \phi$	: General angle
$\gamma$	: Angle to arbitrary rotating reference frame
$\kappa_{fe}, \kappa_w$	: electrical conductivity of the core, winding material
$\lambda$	: Tip speed ratio
$\mu$	: order of rotor harmonics
$\mu_{fe}, \mu_{air}$	: Permeability of the core, air
$\nu\pi\omega$	: order of stator harmonics
$\omega_r$	: angular rotor speed

$\omega_e$	: electrical angular rotor speed
$\vartheta$	: Pitch angle
$\rho$	: rotor angle
$\dot{\rho}$	: rotor angle velocity = $\omega_r$
$\ddot{\rho}$	: rotor angle acceleration
$\sigma$	: Angle between rotor and flux reference frame
$\Phi$	: flux
$\Theta$	: mmf or magnetomotive force
$\Psi$	: Flux
s	: stator reference frame
r	: rotor reference frame flux
abc	: 3-phase rotor system of a machine
a, b, c	: Phase a, b, c
d,q	: components of Park's transformation
fw	: Friction and windage
gk	: generator
rtd, n	: Short circuit
o	: Rated/ nominal
ref	: reference
s, r	: Stator, rotor
ABC	: 3-phase stator system of a machine
0	: Zero component
123	: 3-phase systems of transformers
1, 2, 3	: Primary, secondary, tertiary
$\alpha, \beta$	: components of Clark's transformation
$\infty, m$	: Magnetizing parameter
DC	: Direct Current
DFIG	: Doubly Fed Induction Generator
DO L	: Direct On Line
EMK	: electromotive force
IG	: Induction Generator
2w3ph	: 2 winding 3 phase 3
3w3ph	: winding 3 phase

## LIST OF FIGURES

Figure 1.1. Power in wind varying with increasing wind speed .....	3
Figure 1.2. Wind speed, power in wind, power captured and rotor rpm correlations..	4
Figure 1.3. Power System Stability with a wind farm connected to a grid.....	7
Figure 1.4. Wind Turbine stress research.....	7
Figure 2.1. Wind turbine with three blades which rotate at high speed .....	12
Figure 2.2. Wind Energy Conversion process .....	13
Figure 2.3. Aerodynamic Lift and Aerodynamic Drag .....	14
Figure 2.4. Internal equipment in a horizontal axis wind turbine .....	15
Figure 2.5. Horizontal-axis and vertical-axis wind turbines configurations .....	16
Figure 2.6. $C_p$ Vs. $\lambda$ for a typical wind turbine.....	21
Figure 2.7. Feedback loop for Pitch angle control .....	25
Figure 2.8. Onshore wind farm .....	27
Figure 2.9. Offshore wind farm.....	28
Figure 2.10. Single line diagram of a simple radial power system .....	32
Figure 2.11. Typical reactive power limiting curve .....	33
Figure 3.1. Magnetic axes, concentric stator and rotor windings, currents and voltage and angle dependencies of a 3-ph asynchronous generator .....	40
Figure 3.2. Space vector constructed from a 3-ph system .....	44
Figure 3.3. Phase currents in a time based system .....	45
Figure 3.4. Dynamical per phase equivalent diagram for asynchronous generator ..	49
Figure 3.5. Equivalent two-phase machine showing Clark-Transformation .....	49
Figure 3.6. Equivalent circuit diagram for $\alpha$ and $\beta$ – components.....	51
Figure 3.7. Equivalent circuit diagram for the zero component .....	51
Figure 3.8. Park's – transformation.....	53
Figure 3.9. Equivalent circuit diagram for d, q – components.....	55
Figure 3.10. Example of a measured no load.....	56

Figure 3.11. Current circle diagram showing the effect of main inductance saturation .....	57
Figure 3.12. Main inductance dependency of the magnetizing current .....	58
Figure 3.13. Current circle diagram showing the effect of leakage reactance saturation .....	60
Figure 3.14. Different exponential dependencies of D .....	63
Figure 3.15. Different exponential dependencies of D at over speed .....	63
Figure 3.16. The unmasked Machine model in Matlab/ Simulink.....	64
Figure 3.17. Block angle – friction .....	65
Figure 3.18. Block flux – current used in the machine model .....	66
Figure 3.20. Stator current related to rated stator current .....	69
Figure 3.21. Stator reactive power related to rated reactive stator power.....	70
Figure 3.22. Measured Grid voltages/Stator voltages during the DOL of a 850/800 kW generator.....	71
Figure 3.23. Speed during DOL start of a 850/800 kW generator .....	72
Figure 3.24. Zoom into the stator currents at start of the DOL-start .....	73
Figure 3.25. Window of the stator currents in the middle of the DOL-start.....	74
Figure 3.27. Example of stator (solid line) and rotor (dashed line) leakage inductance.....	76
Figure 3.28. Modified Matlab/ Simulink block “flux – current” including leakage inductance saturation .....	77
Figure 3.29. Speed during DOL start .....	78
Figure 3.30. Zoom into stator currents simulation at start of the DOL start.....	79
Figure 3.31. Window of Stator currents in the quasi stationary state of the DOL-start.....	80
Figure 3.32. Zoom into stator currents at no load operation after DOL- start .....	81
Figure 3.33. 3-ph equivalent ABC/abc circuit diagram of a doubly fed asynchronous generator.....	82
Figure 3.34. Voltage at generator stator terminal during a two-phase short circuit...	84
Figure 3.35. Stator currents of the generator.....	85
Figure 3.36. 2-windings 2-phase Transformer.....	88
Figure 3.37. Equivalent circuit of a transformer referred to primary side .....	89
Figure 3.38. Equivalent circuit of a transformer referred to secondary side.....	90

Figure 3.39. Simplification of 3w3ph transformer.....	93
Figure 3.40. Simple equivalent circuit of a 3w3ph transformer .....	94
Figure 3.41. Simple equivalent diagram of the 3-ph three-windings autotransformer .....	97
Figure 3.42. Coupling of the second and third winding in an autotransformer .....	98
Figure 3.43. The 2w3ph transformer model in Matlab/ Simulink .....	99
Figure 3.45. Ideal (thin line) and real secondary voltage (thick line) at no load and full loaded .....	101
Figure 3.46. Primary (thick line) and secondary current (thin line) at no load and loaded.....	101
Figure 3.47. The 2w3ph transformer inclusive grounding system.....	102
Figure 3.48. The 3w3ph transformer model in Matlab/ Simulink including star point grounding .....	103
Figure 3.49. Magnetizing curve of a 2.1 MVA 3w3ph transformer related to the rated current.....	104
Figure 3.50. Main inductance saturation curve of a 2.1 MVA 3w3ph transformer .	105
Figure 3.51. Block flux – current of a 3w3ph transformer with main saturation ....	105
Figure 3.52. Cross section of a wind turbine blade ( $\alpha$ -angle of attack). .....	107
Figure 3.53. The power coefficient – tip speed ratio curve as a function of the pitch angle .....	108
Figure 3.54. The aerodynamical model implemented in Matlab/ Simulink .....	109
Figure 3.55. Model of the pitch system implemented in Matlab/ Simulink .....	109
Figure 3.56. Drive train schematic for modeling of a wind turbine.....	110
Figure 3.57. Drive train model implemented in Matlab/ Simulink.....	112
Figure 4.1. Frequency of Different fault types on 132KV overheadlines.....	115
Figure 4.2. Typical wind farm construction with its protection zones.....	116
Figure 4.3. Crowbar protection system for DFIG units .....	120
Figure 4.4. Chopper rotor protection system for DFIG units.....	120
Figure 4.5. Fault location effects on the protection of the collecting feeder .....	123
Figure 4.6. Uşak RES- Bereket Enerji Wind Farm location .....	125
Figure 4.7. The SLD of Uşak RES- Bereket Enerji Wind Farm.....	126
Figure 4.8. Uşak RES- Bereket Enerji Wind Farm - DFIG Detailed Model .....	128

Figure 4.9. Simulation response due to a solid 3-phase grid-fault without crowbar initialization.....	131
Figure 4.10. Simulation response due to a solid 3-phase grid-fault with crowbar initialization.....	132
Figure 4.11. Simulation response due to a solid 2-phase fault beyond the local transformer.....	134
Figure 4.12. Proposed communication-based relaying employment .....	135

## LIST OF TABLES

Table 1.1. Average wind power densities and speeds of turkey over various regions .	5
Table 1.2. Typical study description for wind turbines models .....	8
Table 2.1. The comparative parameters of Horizontal-axis and vertical axis wind turbines .....	18
Table 2.2. Advantages of Offshore wind Farm .....	28
Table 2.3. Vestas Type Development during the last 34 years .....	31
Table 3.1. Leakage inductance saturation reference .....	76
Table 3.2. The parameters of the 3w3ph transformer .....	92

## SUMMARY

Keywords: Wind Turbine, Protection and Modelling

Wind energy is fast becoming the most preferable alternative to conventional sources of electric power. Owing to the perennial availability of wind and the considerable range of power control, wind turbines are now coming up in almost all parts of the world. In the early days of development, wind turbines were designed to rotate at constant speed through pitch control or stall control. The modern wind turbines implement pitch control in order to tap maximum energy at wind speeds lower than rated wind speed. These developments raise a number of challenges to be dealt with now and in the future. The penetration of wind energy in the grid system raises questions about the compatibility of the wind turbine power generation with the grid. In particular, the contribution to grid stability, power quality and behavior during fault situations plays therefore as important a role as the reliability. The main motivations of this thesis are the challenges related to grid connection of wind turbines, protection and modeling. The second chapter clarifies recent thinking in the area of wind turbine development by discussing several grid codes/grid requirements. In the discussion, this thesis tried to demonstrate the view of the transmission line operation as well as the challenges wind turbine manufacturing. However, since wind turbine technology only has recently had to address grid related faults, models do not satisfy the demands peculiar to this technology. The improvement of the large asynchronous generator model as an interface between the mechanical and electrical characteristics of a wind turbine takes a central part in this research process. Chapter 3 presents the development and implementation of a detailed analytical asynchronous generator model. Although the generator model is of primary interest for improving the wind turbine model, the implementation of the other elements completing a total wind turbine model have been challenging as well. The development of a three-phase transformer model and especially a three-phase autotransformer is also shown. The wind turbine models are completed by modeling the mechanical and aerodynamical parts of the wind turbine and include the basic control system. Chapter 4 deals with the protection approach based on Relaying Unit which executes protection and control functions for a whole wind farm. This approach reduces the total installed costs for protection and control systems, while increasing system reliability which enable the possibility to create a small electrical network and thereby give the possibilities to research the dynamics introduced by a fault in the grid. Finally fault situations have been studied with the developed wind turbine models. The influences on the generator as well as the behavior of the wind turbine during these faults are briefly discussed based on the simulation results. It can be concluded, that it has been possible to build advanced wind turbine models in Matlab/ Simulink for researching fault situations.



## ÖZET

Anahtar kelimeler: Rüzgar Türbinleri, Koruma ve Modelleme

Rüzgâr enerjisi geleneksel enerji kaynaklarına göre en çok tercih edilen alternatif enerji kaynağı haline gelmektedir. Rüzgârın sürekli elde edilebilir ve geniş aralıklarda kontrol edilebilir bir enerji türü olması sayesinde günümüzde rüzgar türbinleri dünyanın büyük kesiminde yaygınlık kazanmaktadır. İlk zamanlarda, rüzgar türbinleri pitch ve stall kontrol vasıtasıyla sabit hızda dönmeleri doğrultusunda tasarlanmışlardır. Modern rüzgar türbinleri ise nominal rüzgar hızından düşük hızlarda da maksimum enerji elde edilmesi amacıyla pitch kontrolün uygulanması esasına dayanır. Bu konudaki ilerlemeler şimdi ve gelecekte karşılaşılması muhtemel birçok zorluğu ortadan kaldırmaktadır. Şebeke sistemlerindeki rüzgar enerji “etki”si, şebeke ile rüzgar türbininin enerji üretimi arasındaki uyumluluk hakkında soruları gündeme getirmektedir. Özellikle, şebeke kararlılığına katkı olarak, enerji kalitesi ve hata durumlarındaki davranış güvenilirlik gibi önemli bir rol oynar. Bu tez çalışmasının giriş bölümü kısaca türbin teknolojisinin gelişimini açıklar. Çalışma kapsamında farklı türbin türleri ele alınmıştır. Bu tez çalışmasının asıl amacı ise rüzgâr türbinlerinin şebeke bağlantısı, koruma ve modellenmesine dair durumların incelenmesidir.

İkinci bölüm rüzgâr türbini alanındaki son gelişmeleri birçok şebeke yönetmeliği üzerinden ele alarak açıklığa kavuşturmayı amaçlar. Bu çalışma, rüzgâr türbini imalatı & tasarımının yanı sıra iletim hatlarında karşılaşılan sorunlara da bir bakış getirmeye çalışmıştır. Modelleme, yanıtlanması gereken birçok soruyu da beraberinde getiriyor olması dolayısıyla sistem araştırma ve geliştirme çalışmalarında önemli bir yer edinmektedir. Böyle bir modelleme sırasında karşılaşılabilecek çeşitli zorluklar tek bir modelleme yazılımı ile giderilemeyebilir.

Birçok farklı uluslararası şirketin yayınlamış olduğu kurum içi programa ek olarak, enerji sistemleri üzerine en yaygın olarak bilinenleri EMTDC/PSCAD ve PSS/E yazılımlarıdır. Araştırma ve özellikle koruma ve kontrol işlemleri için genellikle Matlab / Simulink yazılımı kullanılır. Bütün bu programlar, günümüzdeki kullanılmakta olan farklı araştırma amaçları doğrultusunda geliştirilmiş olan genel veya özel amaçlı modelleri basitleştirmektedir. Son dönemde, rüzgâr türbin teknolojisi sadece şebeke kaynaklı hataları ele aldığından; geliştirilen modeller bu teknolojiye özgü talepleri karşılamamaktadır. Özellikle, rüzgar türbini ve şebekenin; birbirlerine olan etkileri, etkileşimleri ve şebeke hataları ile asimetric işlem altındaki davranışları daha fazla araştırmaya ihtiyaç duymaktadır. Bu tez çalışması bu sebeple geliştirilmiş bir rüzgâr türbini tasarımına da değinmektedir. Modelleme için bilinen ve yaygın olarak kullanılan Matlab / Simulink programı seçilmiştir. Program matematiksel diferansiyel denklemlerin çözümü ve açıklanması için güçlü bir araçtır ve bu sayede oldukça geniş bir aralıkta

modelleme olanağı sağlamaktadır. Rüzgar türbininin elektriksel ve mekaniksel karakteristikleri arasında bir arayüz olarak asenkron generatörün tasarlanması bu araştırma çalışmasının merkez noktasını oluşturmaktadır.

Üçüncü bölüm, bir asenkron generatör modelinin tasarım ve geliştirilmesini detaylı bir şekilde açıklar. Model sadece generatör imalatçıları tarafından uygulanan bir minimum parametre setini kullanır. Simülasyonun kesinliği; deney ölçümleri ile doğrulanan ana ve kaçak endüktans doyumlarını içermesiyle sağlanır. Generatör doyum sonuçlarının etkisi generatörün kendisinin ve tüm rüzgar türbininin davranışına ilişkin olarak tartışılmıştır. Her ne kadar generatör modellemesi rüzgar türbin modeli tasarımı için öncelikli olsa da rüzgar türbinini tamamlayan diğer ekipmanların tasarlanması da ayrıca önem arz etmektedir.

Üç fazlı bir transformatör ve özellikle üç fazlı bir ototransformatör tasarımı ayrıca incelenmiştir. Rüzgâr türbin modelleri, temel kontrol sistemini içeren mekanik ve aerodinamik kısımların modellenmesiyle tamamlanır. Dördüncü bölüm, tüm rüzgâr santrali için koruma ve kontrol fonksiyonlarını üstlenen röle ünitesini esas alan koruma yaklaşımını açıklar. Bu yaklaşım, şebekede oluşan bir arıza sebebiyle oluşan dinamiklerin incelenmesi ve dolayısıyla küçük bir elektrik ağı oluşturulmasına olanak tanıyan sistem güvenilirliğini arttırırken koruma ve kontrol sistem giderlerini düşürür. Son olarak, geliştirilen rüzgâr türbin modelleri ile hata durumları incelenmiştir. Hata durumu sırasında rüzgâr türbininin davranışının yanı sıra generatör üzerindeki etkileri de simülasyon sonuçlarına bağlı olarak kısaca ele alınmıştır. Matlab / Simulink programında hata durumları araştırmaları için gelişmiş rüzgâr türbin modellerinin geliştirilebilmesinin muhtemel olduğu sonucuna varılabilir. Bununla beraber bu tez çalışmasının başka bir sonucu da küçük bir enerji sistemindeki bir rüzgâr türbininin detaylı modellemesi için Matlab / Simulink programının ideal modelleme aracı olamayabileceği yönünde.

Diferansiyel denklemlerin karmaşıklığı yüksek sayıdaki iterasyon işlemi ile birleşince modelin kullanımını kısıtlayan sistem kararsızlıklarına yol açmaktadır. Diğer bir yandan geliştirilen modeller daha sonraları yapılacak olan modelleme çalışmaları için temel olarak görülebilir. Sunulan modeller, farklı amaçlarla -harmonik araştırmaları gibi- geliştirilmeye açık durumdadırlar. Makinenin kontrolüne dair azaltılmış doyum etkisi, temel olarak makinenin doğal davranışından kaynaklanan hatayı kompanze eder. Doyum etkisi çok güçlü bir koruma ile çift besleme işlemi sırasında özellikle azalır. Tüm türbin sisteminin doğrulanması veya kontrol sistemi üzerindeki etkilerin araştırılmasına dair daha fazla çalışma gerçekleştirilebilir. Dahası, geliştirilen rüzgâr türbin modelleri şebeke hatalarının araştırılmasında kullanılabilir.

Kabaca yapılmış tahminlere göre yatırım yapılmasına karar verilemez. Bu nedenle her ülkede veya bölgede, rüzgâr enerjisi kaynağını ortaya çıkaracak daha detaylı analizler yapılmalıdır. Durumun ayrıca çevresel şartlara göre de değerlendirilmesi, düşük veya yüksek sıcaklık, buz, kar, havada üflenen kum ve havanın tuz ihtiva ettiği yerlerin dikkatle incelenmesine gerek vardır. Türbinlerin değerlendirilmesi, test metodları için pratik tavsiyelerin geliştirilmesi, karma sistemler, deniz rüzgâr sistemleri, türbülans etkisi ve rüzgâr meteorolojisini de kapsayan projelerin yürütülmesi için bir iş bölümü yapılmalıdır. Rüzgâr türbinlerinin güç kalitesi, elektriksel karakteristikleri tarafından tanımlanır. Rüzgar türbinlerinin güç kalitesinin belirlenmesi konusunda uluslararası ve

farklı ülkelerin ulusal standartları güç kalite ölçümlerine ilişkin şartları belirlemektedir. Anahtarlama işlemlerinin söz konusu olduğu durumdaki güç tepeleri, harmonik yayın, reaktif güç, kırpışma ve elektriksel davranış bu standartlara göre ölçülmektedir. Değişken-hızlı rüzgâr türbinleri ve sabit-hızlı rüzgâr türbinleriyle karşılaştırıldığında daha yumuşak bir güç çıkışına sahiptir ve aktif ve reaktif gücü kontrol edebilir. Ancak değişken-hızlı türbinler, harmonik yayın üretme dezavantajına sahiptir. Lokal seviyede, kararlı- durum değişimi, genelde şebeke bağlantısı için sınırlayıcı faktördür. Şebeke arızaları, aktif ve reaktif gücün kontrolü söz konusu olduğunda, şebekenin desteği gibi rüzgâr türbinlerinin ve rüzgâr çiftliklerinin şebeke bağlantısına ilişkin olarak ilâve hususlar ülkelerin şebeke kodu dokümanlarında mevcuttur. Genel olarak, rüzgâr enerjisi endüstrisi, yeni enterkoneksiyon standartlarında verilen artırılmış şartlara uygundur. Ancak, bazı durumlarda, bu, bir rüzgâr türbininin ya da rüzgâr çiftliğinin toplam maliyetini büyük ölçüde artırabilir. Dünyada sanayideki gelişmeler ve artan nüfus karşısında enerji harcamaları hızlı bir şekilde artmış ve yıllardır kullanılan fosil kaynaklar tükenmeye başlamış ve ayrıca beraberinde büyük çevresel sorunlar da getirmiştir. Bunun sonucu olarak yeni ve yenilenebilir enerji kaynaklarından yararlanma gündeme gelmiştir. Bu çalışmada; yenilenebilir enerji kaynaklarından biri olan ve son yıllarda ülkemizde de yaygın olarak kullanılan rüzgâr enerjisi konusu ele alınmıştır. Burada önemli olan rüzgâr enerjisi potansiyelinden daha verimli yararlanabilmektir. Küçük çapta enerji üretimi için kullanılan Savonius rüzgâr çarkları ile ilgili çalışmalar ve özellikle düşük rüzgâr hızlarında kullanımı üzerinde durulmuştur. Fakat büyük ölçekte enerji üretimi söz konusu olduğunda Darrieus tipi rüzgâr türbinlerinin kullanımı ön plana çıkmaktadır.

Dünya'da araştırmaların sürdürüldüğü Darrieus rüzgâr türbinleri yavaş yavaş dünyaya yayılmaya ve özellikle Çin'de kullanılmaya başlanmıştır. Bu türbinler hem yapım ve hem de işletim kolaylıkları yanında MW mertebesinde tesislerin yapımı içinde uygundur. Düşey eksenli olduğu için bir kuleye ihtiyaç duyulmadığı gibi dişli kutusu ve jeneratör gibi büyük hacimdeki düzeneklerin kule tarafından taşınması da söz konusu değildir. Jeneratör ve kontrol mekanizması yeryüzüne yakın olduğu için montaj ve bakımları daha kolaydır. Bu türbinlerin kendi kendine ilk harekete başlama gibi sorunları ise birleşik Savonius-Darrieus türbini ile giderilmiştir. Darrieus rüzgâr türbinlerinin kanat tipleri ile ilgili hesap yöntemleri için metin içinde verilen literatürlerden yararlanılabilir. Bunlar içinde en uygun tiplerden biri Sandia Laboratuvarında geliştirilen tiptir. Kanat profilleri için simetrik NACA 65-018 ve NACA 0012 örnek olarak verilmeli ve bunlara ait iki profil örneği gösterilmelidir. Mukavemet açısından NACA 65-018 profili daha uygundur. Uygun kanat profili seçilerek tip projeler geliştirmek suretiyle deniz kıyısında ve düz arazilerde uygulamalar yaygınlaştırılabilir. Yüksek rüzgâr hızlarında Darrieus rüzgâr çarklarının mukavemetleri yatay rüzgâr çarklarınıninkine göre daha iyidir. Kanat uçları olmadığından ve ayrıca tahrik mekanizmaları yer seviyesinde monte edildiğinden daha sessiz çalışırlar.

Normal işletme koşulları altında modelin davranışı, kararlı hal ölçümlerinin karşılaştırılmasıyla ve dinamik hata durumları sırasında makine modelinin uygulanabilirliği, makinenin bir deney düzeneğinde doğrudan çalıştırılmasıyla doğrulanır. Görülmektedir ki, makinenin kaçak endüktans doyumunu düşüncesi özellikle hata durumları sırasında önemlidir. Ana ve kaçak endüktans doyum etkilerini içeren bir makine modeli ile simule edilmiş bir stator akımı test düzeneğindeki ölçümleri ile karşılaştırıldığında; yüksek akımlarda pik değerlerde %20 oranında bir hata gözlenirken; %2 den daha az

bir hata göstermektedir. Her ne kadar %20 oranındaki hata büyük olsa da, diğer bütün etkilerin ihmal edildiği basit bir makine modeli ile yapılan bir simülasyon karşılaştırmasında hatada %10 oranında bir düşüm görülür. Yakınlık etkisi (proximity effect) ve demir kayıpları gibi bu çalışmada yer almayan ek etkilerin göz önünde bulundurulmasıyla hata oranında daha fazla azalma elde edilebilir.

Üç fazlı generatör modeline ek olarak, üç fazlı bir sistemdeki tüm elektrik ağı tasvirlenmiştir. Üç fazlı modellerin geliştirilmesi ve Matlab/Simulink programı ile gerçekleştirilmesi oldukça zorlayıcı bir işlem haline gelmiştir. Sistemlerin matematiksel temsili basitleştirmek için kullanılan “Park Dönüşümü” gibi dönüşümler kontrol strateji tasarımı gibi amaçlar için uygun olmakla birlikte bu modellerin gereksinimleri için yetersizdir. Dq-bileşen temeline dayanan bir sistem modeli (örneğin Park Transformation) ile rüzgar türbininin simetrik hata durumlarının incelenmesi mümkün olsa da, tüm sistem konfigürasyonları hakkında detaylı bir bilgi ve asimetrik simülasyon gibi çeşitli kullanım ve gelişimlere adaptasyon için kısıtlı bir kapsam olduğunu varsayar.

Üç fazlı bir sistem kullanımı dönüşüm teorisiyle anlatılan her türlü geçersiz varsayımlardan uzaklaşır ve model için öncelikli olan fiziksel sisteme oldukça yaklaşır ve daha az hata olanağı sağlar. Üçüncü bölümde makine modellemesi sayesinde kazanılan deneyim kullanılarak; üç faz-iki sargılı, üç faz-üç sargılı ve üç fazlı ototransformatör tasarımı anlatılmaktadır. Rüzgâr türbinini tamamiyle simüle etmeye yarayacak olan jeneratör, transformatör, şebeke elemanları ve kaynak gibi elektriksel elemanları bağlamak için kullanılan modelleme metodu, bu çalışmada incelenmiştir ancak çalışma kapsamında yer almamaktadır.

Rüzgar türbin modellemesinin gerçekleştirilmesi, aerodinamikler için kullanılan modeller (Rüzgar gücü modellemesi, kanatların eğimi ve 3p- etkisi), mekanik modelleme (iki kitle kullanarak: kanatların ve sürüş yatağının kütlesi ve jeneratör eksen) ve kontrol sistemleri modellemeleri kullanılarak tamamlanmıştır. Aerodinamik ve mekanik elemanlar modellemeleri ve kontrol sistemleri, yayınlanan farklı makale/yayınlar kullanılarak ve çeşitli doğrulama prosedürleri kullanılarak geliştirilmiştir. Bu çalışma kapsamında karşılaşılan en büyük zorluk, mevcut modellerle, çalışma kapsamında geliştirilen ileri seviye elektriksel modellerin, etkili bir bütünlük gösteren modelde harmanlanmasıdır. Zira, araştırılan rüzgar türbini korumaları çok fark göstermektedir, Sinovel rüzgar türbini modeli içindir. Röle koruması içeren rüzgar türbini koruma sistemi, ilgili bölümde açıklanmış ve beyan edilmiştir.

Geliştirilen modellerde, rüzgâr türbininin mevcut şebeke bağlantısı gereklerinden kaynaklanan hata simülasyonları gerçekleştirilmiştir. Sunulan birçok gereklilikten ötürü, bir “2 faz kısa devre” ve bir “gerilim dalgalanma” hataları incelenmiştir. “2 faz kısa devre” hatası, ilgi çekici bir durumdur çünkü görece sıklıkla görülür ve asimetrik bir olaydır. İlaveten, operasyon limitleri içerisinde bir “gerilim dalgalanması” da incelenmiştir. Her iki hata da, doyma etkisini içerebilen ve çıkartabilen bir jeneratör modellemesi ile incelenmiştir. Koruması olmayan bir makinenin simülasyonu sırasında, bu etkiler önemli bir rol oynamaktadır, fakat korunan bir türbinde minimal bir etkisi olmaktadır. Normal çalışma şartları altında, makine doyma etkisi minimaldir ve çalışılan makine tipinde ihmal edilebilir.

Ancak, hata durumlarında, doyma etkileri bazı makinelerde çok daha büyük bir etkiye sahiptir. Araştırılan bu iki spesifik örnek, genel bir kanıya varmak için yeterli bir temel oluşturmamaktadır. Bu nedenle, şebeke hata durumu çalışmalarında, genel bir kanıya varılana dek bu durum doyma etkilerini göz önünde bulundurma adına bir avantajdır.

## **CHAPTER 1. INTRODUCTION**

Wind power has become cost-competitive with other conventional means of power generation. It can provide a significant amount of energy from a renewable resource with minimum adverse impacts on the environment and is the focus of “green power” marketing programs throughout Turkey. Wind generation and wind farms are rapidly becoming an important part of the generating capacity of the modern utility grid. Emerging trends such as government incentives, carbon limits, and decreasing costs of wind turbine technology will all lead to increased number of wind farms in the coming years [1]. There are two kinds of wind farms: (1) large wind farms located onshore or offshore consisting of numerous wind turbines connected together and distributed over several square kilometers, with a single interface to the transmission system; and (2) a single wind turbine directly connected to the distribution utility’s system. The focus of this work shall be the large wind turbine farm. Typically modern wind farm consist of 20-150 individual wind turbines clustered into many groups depending on the total number of turbines. The capacity of each turbine is in the range of 0.5–3MW, with some turbines as large as 5MW. A typical wind turbine generator unit consists of the wind turbine itself, an asynchronous generator, turbine/generator control, generator breaker, and step-up transformer. Recently power converters have been employed to permit variable speed operation in order to maximize the output power and provide reactive power. Generation voltage is typically 690V and this is stepped up to 34.5kV. Numerous wind turbine outputs are connected together and tied to the collector bus through a circuit breaker. Multiple collector feeders are combined and fed to a utility transformer, which steps up the voltage to transmission level and transfers the power. Often, reactive power compensation units such as capacitor banks are also provided at the collector bus [1][2]. There are other modern ways such as the use of FACTS devices or advanced control of asynchronous generator for providing reactive power support. When it comes to protection and control requirements of a

wind turbine, the wind power industry has been using conventional and simple approaches. Even though rapid advancements are being introduced in various fields related to wind power such as wind turbine and asynchronous generator design, wind turbine/asynchronous generator control, ride-through ability, and reactive power control, approaches adopted for implementing protection have not seen significant advancement. It is not that protection and control industry has not made technology breakthroughs; in fact there have been remarkable developments. However, there might have been a gap in tuning these to the needs of wind turbine application. The objective of this thesis is to present a new approach for wind turbine model, protection and control implementation. Advancements in the protection and control industry have to be brought into the domain of wind turbine application to address the specific needs and challenges of this application. This work ends by presenting an over view of protection requirements for a wind turbine highlighting the key challenges. The technology evolution in protective relays and the direction for future technology is explained. It is important to note that the capacity of individual wind turbine generators and wind farms as a whole continue to increase [2][3]. The simple and basic protection approaches such as fuses will no longer be sufficient to protect these systems. More elaborate protection functions and schemes will be required in order to enhance the availability and reliability of wind turbines. The time is ripe for the wind power industry to look at innovative technology that not just meets their protection and control needs, but goes beyond to solve their various other economic, operation and maintenance challenges, while remaining simple and using proven methods.

### **1.1. Wind Turbine Technology**

Wind turbines are essentially thermo-dynamical [8] control volumes just like every other modern engineering applications today, which means they all can be simplified into input and output problems. In our case of wind turbines, this simplification is decreed by the first law of thermodynamics: Energy is conserved within a control volume. Most wind turbines start generating electricity at wind speeds of around 3-4 meters per second (m/s), (8 miles per hour); generate maximum 'rated' power at around 15 m/s (30mph); and shut down to prevent storm damage at 25 m/s or above (50mph) [4][9]. For the energy collecting purposes of wind turbine applications, equations of

thermodynamics are simplified into to Equations below; Wind energy (E) of streaming air can be calculated as:  $E = \frac{1}{2} \cdot m \cdot v^2$ ; where m: mass of the air and v: air speed. Power extracted by the turbine can be calculated as:  $P_{\text{turbine}} = \frac{1}{2} \cdot \rho \cdot \pi \cdot r^2 \cdot v^3 \cdot c_p$ ; where  $\rho$ : density of the air; r: radius of the rotor; v: air speed and  $c_p$ : Power Coefficient. The Power Coefficient ( $c_p$ ) is the efficiency or the proportion of kinetic energy extracted by the turbine [4]. Figure 1.1 visualizes how power in the wind varies with wind speed for a turbine of 40m rotor diameter and conditions of 20°C temperature and 1 atm. of pressure.

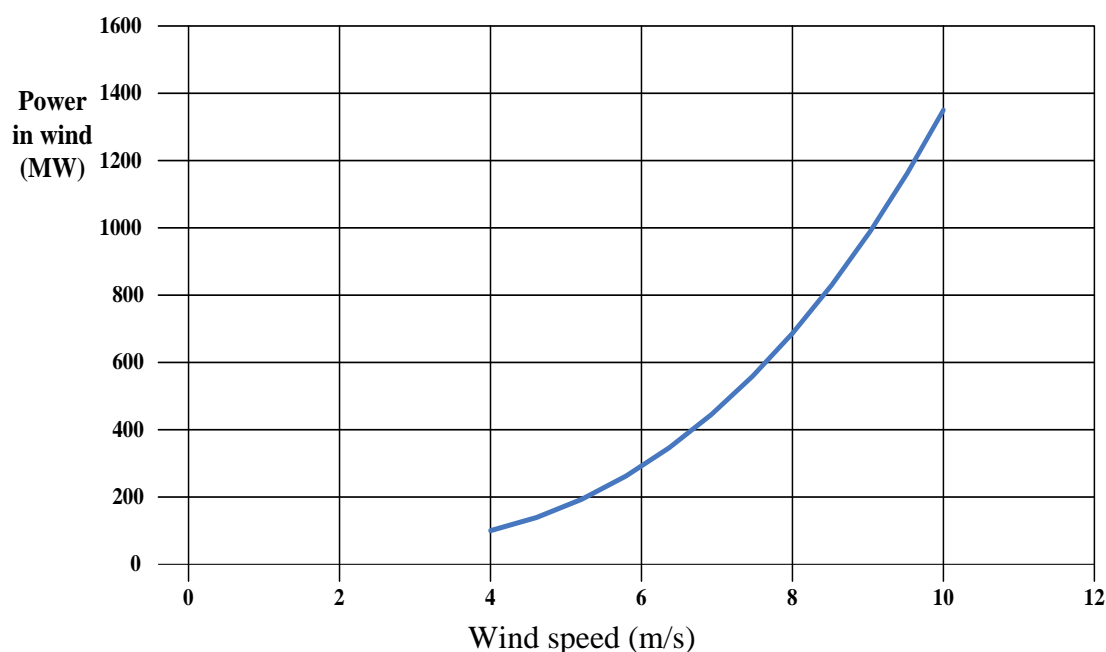


Figure 1.1. Power in wind varying with increasing wind speed

Dramatically increasing trend can be seen when the wind speed increases. Power embodied in wind increases seven times when wind speed is doubled from 4 m/s to 8 m/s. As stated above, power in wind increases cubically when wind velocity is increased. However, wind turbines have three distinct regions of operation depending on the wind speed. With low velocities, wind turbines remain static, this is labeled as Region I, hence a `cut-in` speed is required to start a turbine`s revolution. Between the cut-in speed and rated speed of the specific turbine, power harvested from wind employs the same cubic trend with the power in wind itself. This cubic power generation properties lie within Region II [9]. During Region II, rotors are spinning with increasing RPM.



When the rated speed of the turbine is reached, rotors spin with a fixed RPM and power output is also fixed, this is called the rated output of the wind turbine. After the rated speed, increasing wind speed doesn't affect the power output or rotation speed of the rotors until wind gets too fierce and turbine has to protect itself by shutting down. This mark in wind speed is called `cut-out` speed and between the rated speed and cut-out speed is the Region III. Figure 1.2 shows the wind speed, wind power, rotor RPM and power captured from wind [8][9].

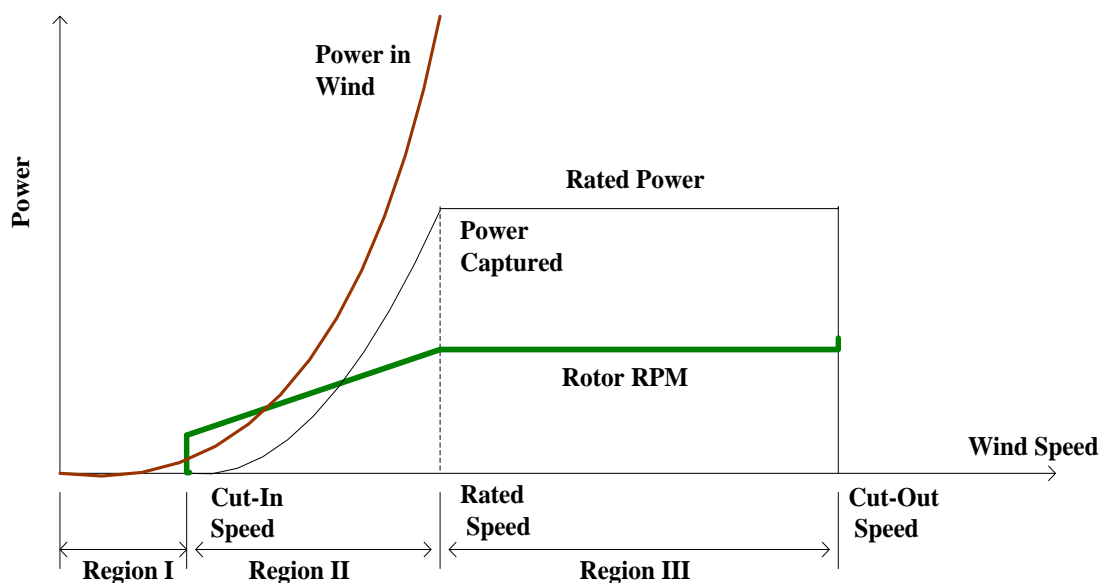


Figure 1.2. Wind speed, power in wind, power captured and rotor rpm correlations

The rated power output of a wind turbine directly depends on a specific wind speed and it requires the wind to be constantly available at that speed. On the other hand, wind histograms and common sense dictates that wind speed and wind direction constantly changes throughout a day, a week, a month and a year. Change of wind direction is remedied by changing the hub of the turbine to direct the rotor blades perpendicular to the wind whereas change in wind speed cannot be controlled. Therefore, a 54 wind turbine cannot operate at its rated power all the time unlike other means of energy production. Annual change of power generation is referred to as Capacity Factor and it is a function of wind speed and/or elevation [9]. Generating electricity from the wind is simple since wind passes over the blades exerting a turning force. The rotating blades turn a shaft inside the nacelle, which goes into a gearbox. The gearbox increases the rotation speed for the generator, which uses magnetic fields to convert

the rotational energy into electrical energy. The power output goes to a transformer, which converts the electricity from the generator at around 690 Volts (V) to the right voltage for the distribution system, typically between 11 kV and 154 kV. The National Grid transmit the electricity around the country, and on into homes and businesses. The amount of electricity produced from a wind turbine depends on three factors [5][6]:

-The power available from the wind is a function of the cube of the wind speed. Therefore if the wind blows at twice the speed, its energy content will increase eight-fold. Turbines at a site where the wind speed averages 8 m/s produce around 75-100% more electricity than those where the average wind speed is 6 m/s.

Table 1.1. Average wind power densities and speeds of turkey over various regions [7]

Region	Annual mean wind speed (m/s)	Annual mean power density (W/m <sup>2</sup> )
Mediterranean region	2.45	21.36
Middle Anatolia region	2.46	20.14
Aegean region	2.65	23.47
Black Sea region	2.38	21.31
Eastern Anatolia region	2.12	13.19
South-Eastern Anatolia	2.69	29.33
Marmara region	3.29	51.91

-This is the capability to operate when the wind is blowing, i.e. when the wind turbine is not undergoing maintenance. This is typically 98% or above for modern Turkish machines.

-Wind farms are laid out so that one turbine does not take the wind away from another. However other factors such as environmental considerations, visibility and grid connection requirements often take precedence over the optimum wind capture layout.

## 1.2. Work Motivation

Wind energy is one of the fastest growing renewable energies in the world. The generation of wind power is clean and non-polluting; it does not produce any byproducts harmful to the environment. Nowadays, modeling is the basic tool for analysis, such as optimization, project, design and protection. Wind energy conversion systems are very different in nature from conventional generators, and therefore dynamic studies must be addressed in order to integrate wind power into the power system. In the case of power systems with classical sources of energy analysis, the modeling is relatively simple because the models of objects and protection devices are well known and even standardized; the data are available [13]. But in the case of wind turbine modeling, researchers meet problems related to the lack of data and lack of protection-system structures due to strong competition between wind turbine manufacturers. This leads to the situation in which many researchers model the wind energy conversion systems in relatively simple form, almost neglecting the protection systems, which significantly influence the reliability of the analytical results. Researches in wind turbine technology made necessary the design of more powerful protection systems, to improve wind turbines behavior and make them more profitable and reliable. However, protecting modern turbines to minimize the cost of wind energy is a complex task, and much research remains to be done to improve protection devices [14]. An interesting characteristic of wind energy systems is that wind speed determines the point of operation; it simply defines the available amount of energy that can be converted into electricity. The wind cannot be protected; in other words the system is driven by noise, which makes wind turbine systems essentially different from most other systems. This explains the need for robust protection and control design [15]. However, the requirements are for all turbine types and the development of wind turbine models for the study of variable speed wind turbines with DFIG is still being developed. Wind turbines with DFIG have the advantage of fast electrical control and protection. This gives the opportunity to use a wind turbine like a power plant. With special control strategies the wind turbine can even support the grid e.g. the power factor [10][11][12]. However existing models are mainly made with the purpose to develop control and protection strategies and therefore do not express the dynamic behavior of the whole turbine on the grid.

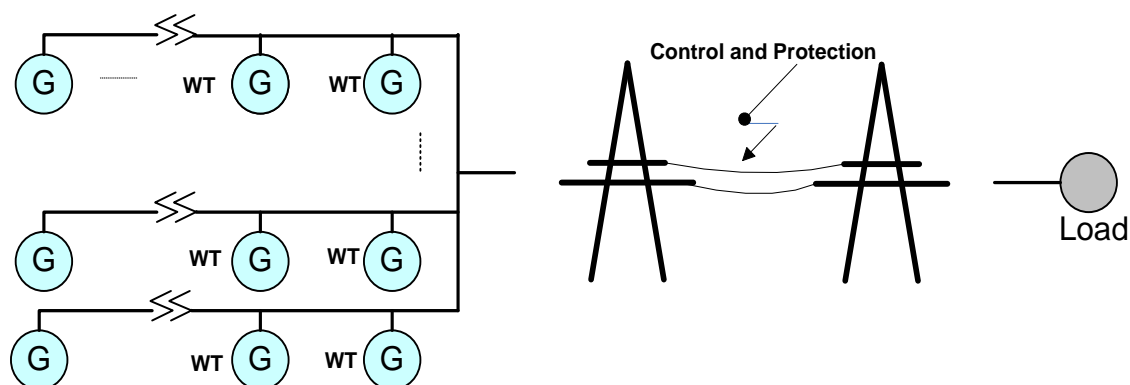


Figure 1.3. Power System Stability with a wind farm connected to a grid

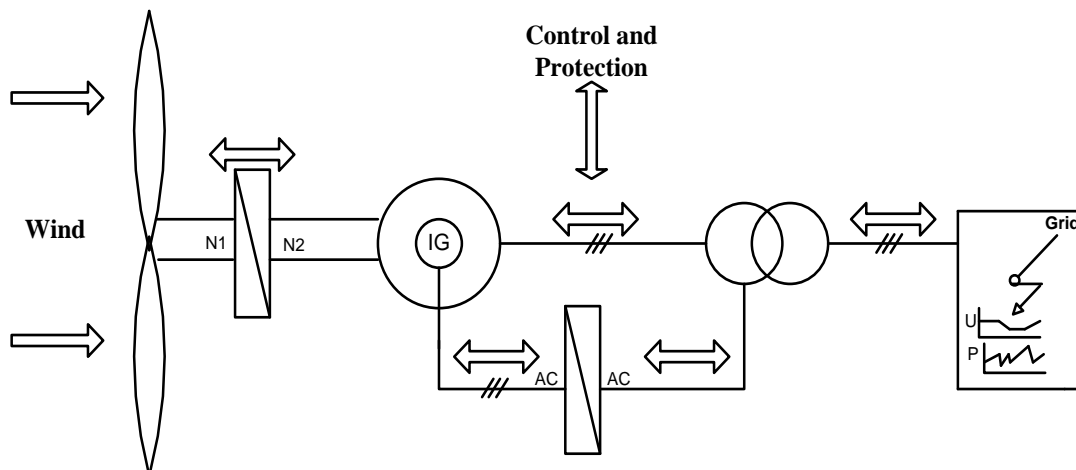


Figure 1.4. Wind Turbine stress research

As the wind turbine affects the grid, the grid affects the function of the wind turbine itself. Determining the load caused by voltage sags, asymmetries or short circuits on the electrical as well as mechanical system require detailed models (Figure 1.4). These models contribute with a detailed knowledge about the torque on the wind turbine shaft caused by faults in the grid or transient current rises which is important for the estimation of the load on the wind turbines[16]. An accurate as possible knowledge ensures the availability of the turbine for the estimated lifetime and low costs as well as help for the design of new wind turbines. The typical model studies requirements are summarized in Table 1.2.

Table 1.2. Typical study description for wind turbines models

	Network operator models	Wind turbine manufacturer
Type of analysis	Power system stability - Steady state (load flow) - Transient dynamics (large disturbances) - Small signal stability (small disturbances) - Stability studies including short and long thermodynamics (angular, frequency, voltage stability)	Wind turbine stability - Transient dynamics - Load analysis
Time scale	0...ms...10s...min	0...us...ms...s
Model type	- turbine model as wind turbine unit -> several units in wind farm	- detailed turbine model with detailed transformer model, generator model

Wind turbine modeling is therefore an important part in the study of control, design, production and grid integration of wind turbines. One important issue while developing models is the clarification of the purpose of the model. Any assumptions made during the model development, which lead to simplifications of the model itself, are important in order to validate the correctness of the results [16]. On the other hand, theoretically, the electrical output from a wind turbine should be smooth and non-fluctuating [17]. But electricity generated from wind farms can be highly variable on different time scales: from hour-to-hour, daily and seasonally. This represents a considerable challenge when incorporating wind power into a grid system, since in order to maintain grid stability energy supply and demand must remain in balance.

### 1.3. Work Objective

The main objective of this work is to present a new approach for wind turbine model, protection and control implementation by developing an accurate model for a wind

turbine and based on this model contemplate protection system. The scientific objectives of this work by considering the different aspects towards wind turbine simulations for a wind turbine manufacturer such as Sinovel include the following requirements to a wind turbine model.

- Development of a total wind turbine protection and model which is appropriate for fault simulations into one programme.

- Modeling and dynamic behavior investigation of the aerodynamic, mechanical and electrical parts of a variable speed wind turbine equipped with an asynchronous generator and blade pitch angle control.

- Development of an open wind turbine protection and model with an ability to add features for future wind turbine development.

- Development of a detailed generator and transformer model able to handle asymmetries, fault operations, a huge range of different generators and a minimum data input.

The main goals of the project is concluded in the following points:

- Clarification about the requirements due to wind turbines operation with focus on non-normal operation modes.

- Achievement of a generator and transformer model in Matlab/ Simulink handling the above mentioned requirements.

- Implementation of total specific wind turbine models in Matlab/ Simulink appropriate for grid fault simulation studies.

The wind turbine configuration considered throughout this work is an aerodynamic lift, 3 blade, horizontal-axis, variable speed, pitch controlled wind turbine.

## 1.4. Thesis Outline

The thesis is divided into five chapters including this introduction chapter. The paper is structured as follows. Chapter 2 contains a background on theoretical fundamentals regarding wind turbines and wind farms. The first part gives an overview of the wind turbine history and development. The main types of wind turbines and their configurations are explained in detail. Furthermore, the different power control techniques available to control the wind turbine power output are exposed. Wind farms are introduced and classified accordingly to their siting. The main wind farm control structures are described and the requirements for the interconnection of wind farms to the power system are discussed. Chapter 3 presents detailed mathematical models that describe the dynamic behavior of a wind energy system, including aerodynamic, mechanical and electrical parts. Simulation results of the overall wind turbine model are given for a base case, as well as for wind speed and blade pitch angle step changes. Chapter 4 contains the formulation of an explicit parametric protection strategy for a wind turbine. The properties and potential benefits of this protection method for wind energy systems are investigated. Moreover, the protection devices are to be implemented and tested. Finally, Chapter 5 provides conclusions on the research done and offers recommendations for future work.

## **CHAPTER 2. BACKGROUND AND LITERATURE REVIEW**

This chapter is aimed at presenting a review on the wind turbines and wind farm state of the art technologies.

### **2.1. Wind Turbine Development and Types of Turbines**

#### **2.1.1. Wind turbine history**

Energy from wind has been utilized for many centuries in the traditional agricultural societies around the world as supplement to the muscle power of humans and animals. Until the 20th century wind power was used to provide mechanical power to pump water or to grind grain. The earliest recorded windmills are vertical-axis mills and were used in Afghanistan in the seventh century BC. Horizontal-axis windmills are found in historical documents from Persia, Tibet and China around 1000 AD. From Persia and the Middle-East, the horizontal-axis windmill spread across Europe in the 12th century, where windmill performance was constantly improved; by the 19th century a considerable part of the power used in the industry in Europe was based on wind energy. Industrialization then led to a gradual decline in windmills, as the use of fluctuating wind energy was substituted by fossil fuel fired engines which provided a more consistent power source[19].



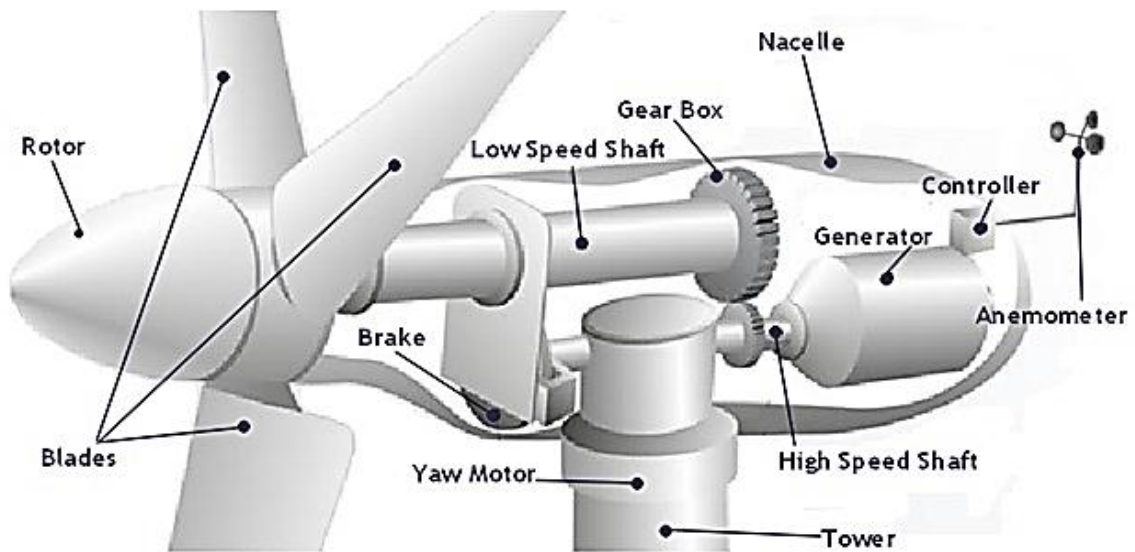


Figure 2.1. Wind turbine with three blades which rotate at high speed [18]

In the 1970s, with the first oil price shock, the modern era of wind turbine generators began, focusing in producing electricity instead of mechanical energy. Conventional methods to generate electricity burn fuel to provide the energy to drive a generator, creating pollution, acid rain and contributing to global warming. In recent years there has been a growing interest in wind energy power systems because of the environmental benefits and the economic benefits of fuel savings[20]. The wind is a clean source and it will never run out. Wind developing fast; turbines are becoming cheaper and more powerful, bringing the cost of renewably-generated electricity down[21]. The cost of generating electricity from wind has fallen almost 90% since the 1980s[22]. Nowadays, wind energy is one of the most important sustainable energy resources and has become an acceptable alternative for electrical energy generation by fossil or nuclear power plants[23]. Progress in wind energy technology is increasing steadily year over year and with the initiative to provide an increasing percentage of wind energy available year over year, advances in wind power are expected to continue.

## 2.1.2. State-of-the-art Technologies

### 2.1.2.1. Definition of a wind turbine

A wind turbine is a machine that converts the kinetic energy from the wind into mechanical energy. If the mechanical energy is used directly by machinery, such as a pump or grinding stones, the machine is so called a windmill. If the mechanical energy is then converted to electricity, the machine is called a wind generator.

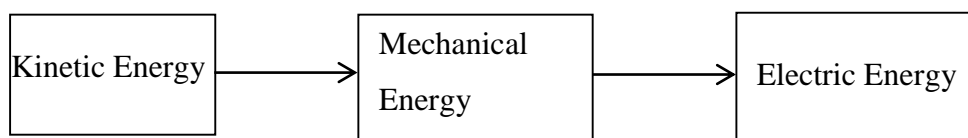


Figure 2.2. Wind Energy Conversion process

Utility-scale turbines range in size from 100 kilowatts to as large as several megawatts[24]. Larger wind turbines are more cost effective and are grouped together into wind farms, which provide bulk power to the electrical grid. Single small turbines, below 100 kilowatts, are used for homes, telecommunications dishes, or water pumping. Small turbines are sometimes used in connection with diesel generators, batteries, and photovoltaic systems. These systems are called hybrid wind systems and are typically used in remote, off-grid locations, where a connection to the utility grid is not available.

### 2.1.2.2. Aerodynamic lift and aerodynamic drag wind turbines

There are two different types of wind energy conversion devices: those which depend mainly on aerodynamic lift and those which use mainly aerodynamic drag.

Wind turbines exploit the aerodynamic forces which arise when the wind blows on the rotor blades, and the blades move relative to the wind. Drag is air resistance, the force that is working against the blades, causing them to slow down. It is required to design your blades so that they have as little drag as possible. Drag increases with the area

facing the wind. Changing the angle of the blades will change the area facing the apparent wind (the real wind combined with the wind created with the blades movement or headwind). Changing the angle of the blades changes the area facing the wind[26]. A blade pitch angle between  $10\text{-}20^\circ$  has less drag than greater angles. Drag also increases with wind speed, so the faster the blades move through the air, the more drag force it experiences. The tips of the blade move faster than the base which is why the shape changes along the length of the blade.

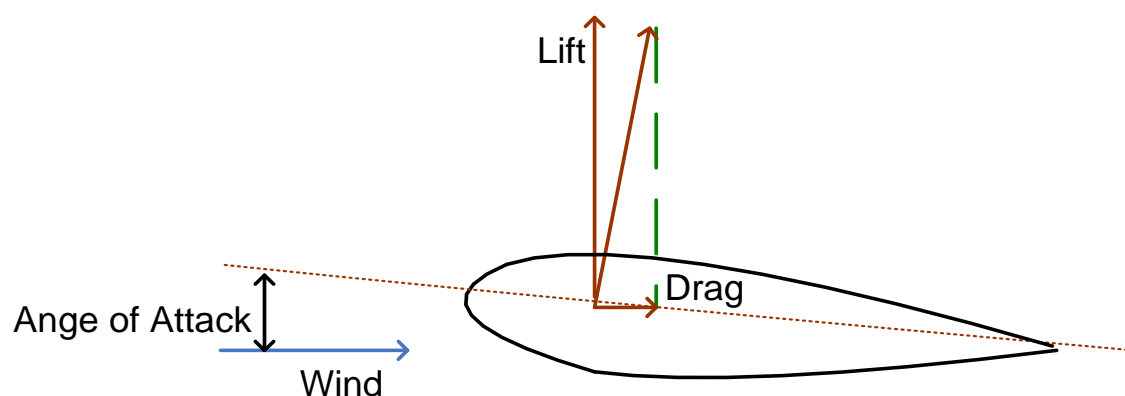


Figure 2.3. Aerodynamic Lift and Aerodynamic Drag

Lift is the force that opposes drag. The goal is to generate as much lift while minimizing the drag. The amount of lift a blade can generate is determined by shape, speed of air passing around blade and the angle of the blade relative to the apparent wind. High speed turbines rely on lift forces to move the blades. To generate electricity from a wind turbine, it is usually desirable that the driving shaft of the generator operates at considerable speed (1500 revolutions per minute). This, together with the higher aerodynamic efficiency of lift devices, means that turbines which rely in aerodynamic drag are not commonly used[25].

### 2.1.2.3. Horizontal-axis and vertical-axis wind turbines

Wind turbines can further be classified into horizontal-axis or vertical-axis. The earliest windmills in antiquity rotated about a vertical axis and they were driven by drag.

### 2.1.2.3.1. Horizontal-axis wind turbine

The main rotor shaft and electrical generator are generally at the top of a tower for a horizontal axis wind turbine (HAWT). A horizontal axis wind turbine has a design which demands that it should be pointed to the wind to capture maximum power. This process is called yawing. The turbine shaft is generally coupled to the shaft of the generator through a gearbox which turns the slow rotation of the blades into a quicker rotation that is more suitable to drive an electrical generator. At present, horizontal-axis wind turbines dominate the market. Figure 2.4 shows the internal equipment in a horizontal axis wind turbine.

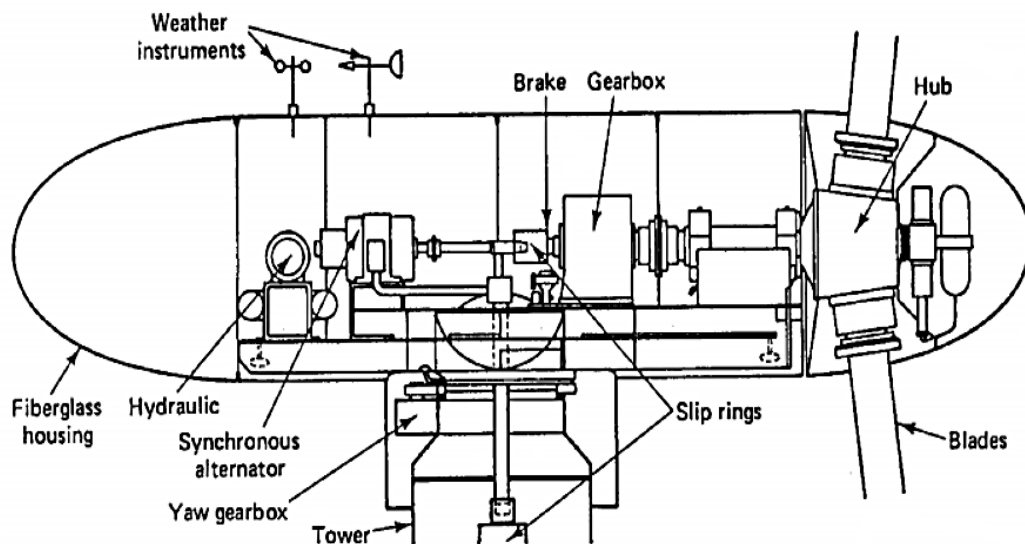


Figure 2.4. Internal equipment in a horizontal axis wind turbine [R Vijay, 2011]

A horizontal-axis wind energy conversion system mainly consists of [27]:

- The rotor blades, which extract the kinetic energy present in the wind and transform it into mechanical power.

- The nacelle, with a power control system that limits and conditions the extracted power; a gear box that transfers the load and increases the rotational speed to drive the generator; and an electrical system which converts the mechanical energy into electrical energy.

–A tower that supports the nacelle.

The yaw mechanism turns the turbine so that it faces the wind. Sensors are used to monitor wind direction and the tower head is turned accordingly. Wind turbines can have three, two or just one rotor blades. Two or three blades are usually used for electricity power generation. Two blades cost less than three blades, but they need to operate at higher rotational speed than three-bladed wind turbines. As a result, the individual blades need to be lighter and hence more expensive on a two bladed turbine[29]. Besides, three-bladed turbines are generally accepted as more aesthetic than two or one bladed turbines. Hence, turbines with three blades dominate the wind industry.

At present, horizontal-axis wind turbines dominate the market; Figure 2.5 illustrates the different configuration between a horizontal-axis and a vertical axis turbine.

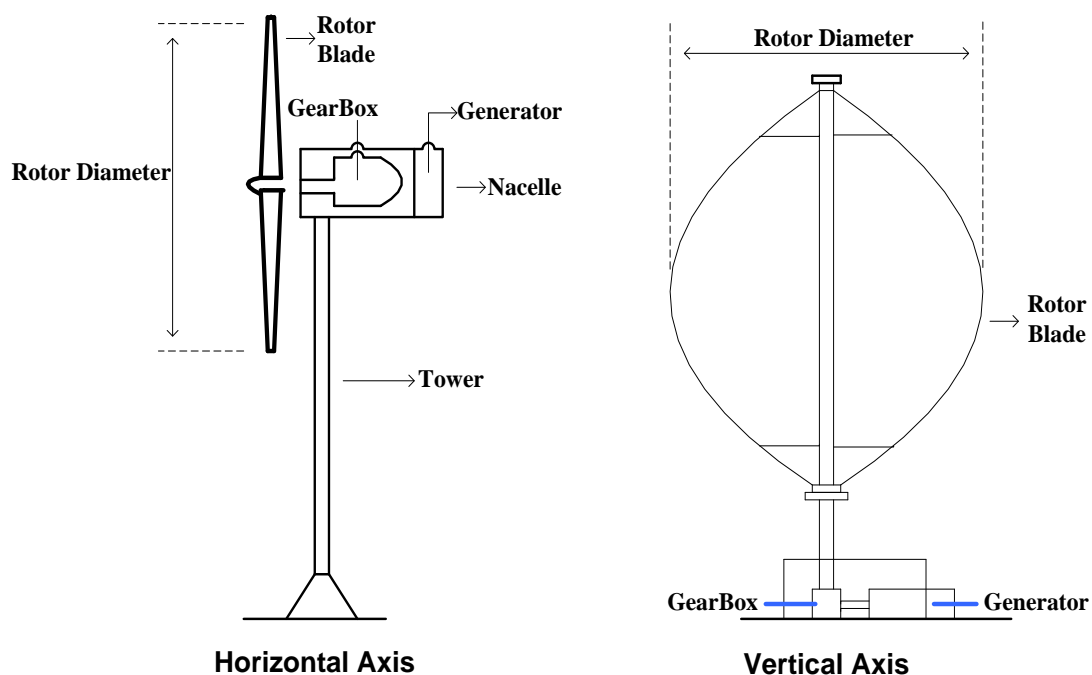


Figure 2.5. Horizontal-axis and vertical-axis wind turbines configurations

Horizontal-axis wind turbines have the advantages that Variable pitch is possible by which the angle of attack of the turbine blades can be controlled; since the blades are present at a considerable height, they are able to capture stronger winds. Wind speed

can increase by 20% and the power output by 34% for every 10 meters in elevation; the blades always move perpendicular to the wind. This leads to higher efficiency as the blades receive power throughout the rotation [28].

But they have also disadvantages: The tall towers of the HAWT are difficult to transport and install; the downwind HAWT suffers from fatigue; the large HAWTs require additional yaw control systems to point them into the wind; Rotations of blades result in cyclic stresses and vibrations in the main bearings of the turbine

### **2.1.2.3.2. Vertical axis wind turbine**

The vertical axis wind turbines, as shown in Figure 2.5, have the main rotor shaft arranged vertically. The structure of these wind turbines are such that they can capture wind irrespective of its direction. Thus, it is of great benefit in places where the wind direction keeps varying. Unlike the HAWT where the gearbox and generator are placed on top of the tower, the generator and gearbox are generally placed near the ground[28]. This makes it more accessible and easier for maintenance. But they do not come without any drawbacks. Some designs produce pulsating torque which results in fatigue. It is also difficult to mount vertical-axis turbines on towers. They are often installed nearer to the base on which they rest. As the wind speed is slower at a lower altitude, so less wind energy is available for a given size turbine. The only vertical-axis turbine which has been manufactured commercially at any volume is the Darrieus machine, named after the French engineer Georges Darrieus who patented the design in 1931. The conventional Darrieus turbine has curved blades connected at the top and at the bottom and rotates like an “egg whisk”[27]. The darrieus type of VAWT that was invented by French inventor Georges Darrieus has features of Good efficiency; Produces large torque ripple and cyclic stress; Starting torque is very less and the external superstructures are needed to hold them up. Vertical-axis wind turbines have the advantages that no tower is needed; they operate independently of the wind direction (a yawing mechanism is not needed); heavy gearboxes and generators can be installed at ground level; Massive superstructures are rarely required; Wind start-up speeds are lower than HAWTs and Noise signature is lower than HAWTs. But they have many disadvantages: they are not self-starting; the torque fluctuates with each revolution as

the blades move into and away from the wind; changing parts is very difficult and speed regulation in high winds can be difficult. Vertical-axis turbines were developed and commercially produced in the 1970s until the end of the 1980s. But since the end of the 1980s the research and production of vertical-axis wind turbines has practically stopped worldwide[19]. At present, horizontal-axis wind turbines dominate the market due to their advantageous features as seen in the comparative parameters of table 2.1.

Table 2.1. The comparative parameters of Horizontal-axis and vertical axis wind turbines[30]

Performance	Horizontal-axis wind Turbine	Vertical-axis wind Turbine
Power generation Efficiency	50%-60%	Above 70%
Electromagnetic Interference	YES	NO
Steering mechanism of the wind	YES	NO
Gear box	Above 10KW: Yes	NO
Blade rotation space	Quite large	Quite small
Wind-resistance capability	Weak	Strong (it can resist the typhoon up to 12-14 class)
Noise	5-60dB	0-10dB
Starting wind speed	High (2.5-5 m/s)	Low (1.5-3 m/s)
Ground projection effects on human beings	Dizziness	No effect
Failure rate	High	Low
Maintenance	Complicated	Convenient
Rotating speed	High	Low
Effect on birds	Great	Small
Cable standing Problem	Yes	NO
Power curve	Depressed	Full

#### 2.1.2.4. Variable-speed and constant-speed wind turbines

Initially, most wind turbines operated at fixed speed when producing power. In a start-up sequence the rotor may be parked (held stopped), and on release of the brakes would be accelerated by the wind until the required fixed speed was reached. At this point, a connection to the electricity grid would be made and then the grid (through the generator) would hold the speed constant. When the wind speed increased beyond the level at which rated power was generated, power would be regulated in either of the ways previously described, by stall or by pitching the blades. Subsequently, variable speed operation was introduced. This allowed the rotor and wind speed to be matched, and the rotor could thereby maintain the best flow geometry for maximum efficiency. The rotor could be connected to the grid at low speeds in very light winds and would speed up in proportion to wind speed. As rated power was approached, and certainly after rated power was being produced, the rotor would revert to nearly constant speed operation, with the blades being pitched as necessary to regulate power. The important differences between variable speed operation, as employed in modern large wind turbines and the older conventional fixed speed operation are:

- Variable speed in operation below rated power can enable increased energy capture; and
- Variable speed capability above rated power (even over quite a small speed range) can substantially relieve loads, ease pitch system duty and much reduce output power variability.

The design issues of pitch versus stall and degree of rotor speed variation are evidently connected. Although the power electronics needed for variable speed wind turbines are more expensive, this type of turbines can spend more time operating at maximum aerodynamic efficiency than constant speed turbines. This can be seen clearly if the performance coefficient,  $C_p$  of a wind turbine is plotted against the tip speed ratio,  $\lambda$ .

The tip speed ratio,  $\lambda$ , is defined as the ratio between the speed of the tips of the blades of a wind turbine and the speed of the wind.



$$\lambda = \frac{V_{TIP}}{V_{WIND}} = \frac{\omega \cdot R}{V} \quad (2.1)$$

Where  $\omega$  is the blades angular velocity (rad/s),  $R$  the rotor radius (m) and  $v$  the wind speed (m/s).

The coefficient of performance,  $C_p$ , is defined as the fraction of energy extracted by the wind turbine of the total energy that would have flowed through the area swept by the rotor if the turbine had not been there.

$$C_p = \frac{P_{EXTRACTED}}{P_{WIND}} \quad (2.2)$$

The coefficient of performance  $C_p$  has a theoretical optimum of 0.59. Only a portion of the power in the wind can be converted to useful energy by a wind turbine. The power available for a wind turbine is equal to the change in kinetic energy of the air as it passes through the rotor. This maximum theoretical  $C_p$  was first formulated in 1919 by Betz and applies to all types of wind turbines. It is conventional to plot the variation of the performance coefficient,  $C_p$ , against the tip speed ratio,  $\lambda$ , rather than against the wind velocity, as this creates a dimensionless graph. A typical  $C_p$  vs.  $\lambda$  curve is shown in Figure 2.6.

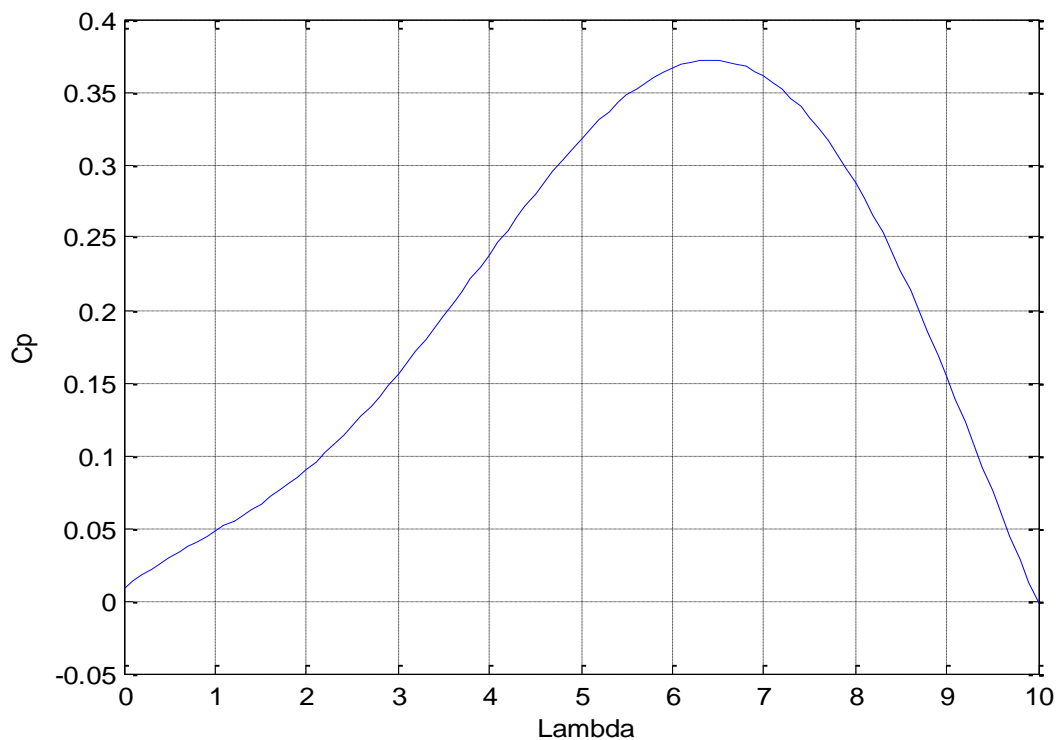


Figure 2.6.  $C_p$  Vs.  $\lambda$  for a typical wind turbine

This curve illustrates that the power coefficient  $C_p(\lambda)$  becomes the maximum. The maximum  $C_p$  is 0.37 when  $\lambda=6.7$ . For a fixed-speed wind turbine, where  $\omega$  is constant, this corresponds to a particular wind speed. For all other wind speeds the efficiency of the turbine is reduced[25]. The aim of variable-speed wind turbines is to always run at optimal efficiency, keeping constant the particular  $\lambda$  that corresponds to the maximum  $C_p$ , by adapting the blades velocity to the wind speed changes. Hence, variable speed wind turbines are designed to operate at optimum energy efficiency, regardless of the wind speed. Variable speed has some attractions, but also brings cost and reliability concerns. It was seen as a way of the future, with expected cost reduction and performance improvements in variable speed drive technology. To some extent this has been realized. However, there was never a clear case for variable speed on economic grounds, with small energy gains being offset by extra costs and also additional losses in the variable speed drive. The current drive towards variable speed in new large wind turbines relates to greater operational flexibility and concerns about power quality of traditional stall regulated wind turbines. Two-speed systems emerged during the 1980s

and 1990s as a compromise, improving the energy capture and noise emission characteristics of stall regulated wind turbines. The stall-regulated design remains viable, but variable speed technology offers better output power quality to the grid and this is now driving the design route of the largest machines. Some experiments are under way with the combination of variable speed and stall regulation, although variable speed combines naturally with pitch regulation. For reasons related to the methods of power control, an electrical variable speed system allows pitch control to be effective and not over-active. Another significant impetus to the application of pitch control, and specifically pitch control with independent pitching of each blade is the acceptance by certification authorities that this allows the rotor to be considered as having two independent braking systems acting on the low speed shaft.

Hence, only a parking brake is required for the overall safety of the machine. Pitch control entered wind turbine technology primarily as a means of power regulation, which avoided stall when stall, from the experience of industries outside wind technology, was seen as problematic if not disastrous. However, in combination with variable speed and advanced control strategies, stall offers unique capabilities to limit loads and fatigue in the wind turbine system and is almost universally employed in new large wind turbine designs. The load-limiting capability of the pitch system improves the power to weight ratio of the wind turbine system and compensates effectively for the additional cost and reliability issues involved with pitch systems. This, together with the increased energy capture obtained by using a variable-speed wind turbine provides enough benefit to make the power electronics (frequency converter) cost effective[14]. Therefore, the wind industry trend is to design and construct variable-speed wind turbines.

### 2.1.3. Power control

The power contained in the wind is the kinetic energy of the flowing air mass per unit time. If  $V_{wind}$  is the velocity of the wind,  $A$  is the rotor swept area and  $\rho$  is the density of air, then Kinetic energy of the wind is given by

$$KE = \frac{1}{2} \cdot m \cdot V_{wind}^2 \quad (2.3)$$

Volume of air passing through swept area per unit time  $= A \cdot V_{wind}$ , Mass flow rate  $= \rho \cdot A \cdot V_{wind}$ . Power contained in the wind:  $P = \frac{1}{2}(\text{mass flow rate}) V_{wind}^3$

$$P = \frac{1}{2} \cdot \rho \cdot A \cdot V_{wind}^3 \quad (2.4)$$

Where  $\rho$  is the air density ( $\text{kg/m}^3$ ),  $A$  the area ( $\text{m}^2$ ) and  $v$  the wind speed ( $\text{m/s}$ ), and  $P$  the power of the wind (watts or  $\text{J/s}$ ). From the latter equation, the power available from the wind is a function of the cube of the wind speed. That means that a doubling of the wind speed gives eight times the power output from the turbine. Therefore, turbines have to be designed to support higher wind loads than those from which they can generate electricity, to prevent them from damage. Wind turbines reach the highest efficiency at a wind speed between 10 and 15  $\text{m/s}$ . Above this wind speed, the power output of the rotor must be controlled to reduce driving forces on the rotor blades as well as the load on the whole wind turbine structure [19]. High winds occur only for short periods and hence have little influence in terms of energy production but, if not controlled, they would dominate the design and cost of the drive train and the generator [27]. While power is being captured from the wind it is desired that the power captured may be maximized. Also, it is to be made sure that the turbine safety is not compromised under any circumstances. Thus, power control is a very important feature of a wind turbine. To avoid damage to the wind turbine at very high wind speeds, the aerodynamic forces on the rotor can be controlled to limit the power captured [31]. The following techniques are employed for the same.

### **2.1.3.1. Stall control**

#### **2.1.3.1.1. Passive stall control**

Stall control is the simplest, cheapest and most robust control method [31] for a wind turbine which the blades are bolted onto the hub at a certain angle. The blades of the rotor are fashioned such that when the wind speeds exceed a certain level, stalling takes place. That is, the lift force on the rotor decreases causing the turbine to stall and restrain itself in the permissible speed limit. Thus, at high wind speeds the turbine is

protected. It is the simplest and a very robust technique of power control. It has long been the preferred control method for small and medium sized Turkish commercial turbines and it is also known as passive control, since there are no moving parts to adjust. The drawback faced is that the turbines operate at efficiency lower than the rated value at low wind speeds. And no assisted start-up [31][33][34]. Besides, this type of control requires the use of a constant speed turbine which, as already explained, has lower energy efficiency than the variable speed turbine.

#### **2.1.3.1.2. Active stall control**

The active stall control comes in as a development over the passive stall control. Instead of natural stalling, this system uses pitching to actively control the stall of the blade. Thus, at low wind speeds, maximum efficiency is achieved by pitching the blades as in a pitch controlled wind turbine[31][34]. On the other hand, at high wind speeds the blades are pitched slightly into the direction opposite to that of a pitch-controlled turbine to make them go into a deeper stall. The advantages of this system are: Smoother limited power can be achieved without high power fluctuations, Can compensate variations in air density, Easier for the system to carry out emergency stops and to start up the wind turbine.

#### **2.1.3.2. Pitch Control**

Through pitch control, the blades can be turned out or into the wind. This results in variation of the force exerted by the wind on the rotor shaft. The main advantages of this type of control are Good power control, assisted startup, and Emergency stop. The angle of the rotor blades can be actively adjusted by the control system in order to shed the unwanted power. Pitch control is relatively fast and can be used to limit the rotor speed by regulating input aerodynamic power flow[17]. Besides, stall controlled turbines have to be shut down beyond a certain speed, whereas pitch controlled turbines can adjust the angle of the blades to reduce the aerodynamic forces.

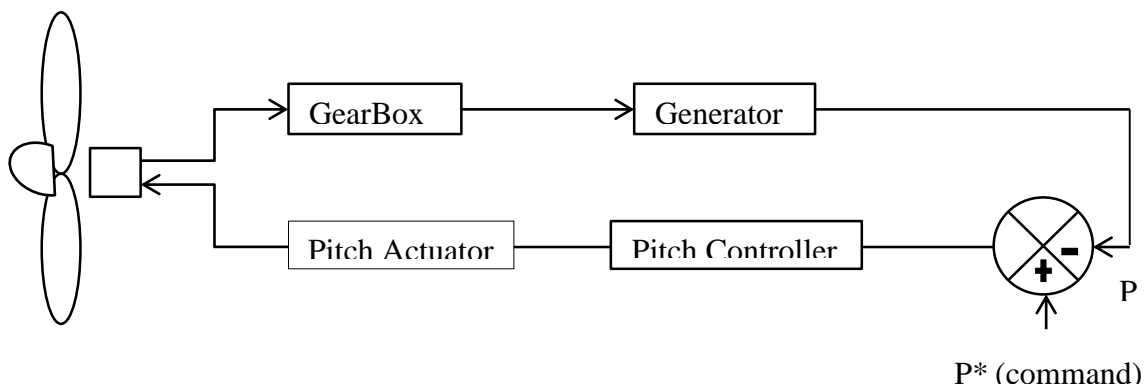


Figure 2.7. Feedback loop for Pitch angle control(Bhadra S N, 2010)

In low and medium wind speeds, the pitch angle is regulated to allow the wind turbine to operate at its optimum condition. In high wind speeds, the pitch angle is increased in order to shed some of the aerodynamic power and maintain the rotor speed within a controllable limit. As pitch angle increases, the wind turbine operates at lower efficiency[17]. The drawback in this case is extra system complexity in the pitch mechanism and the higher power fluctuations at high wind speeds[31][32]. Nowadays, large wind turbines are increasingly being operated with pitch control systems. Due to presence of gusts, the instantaneous power fluctuates around the rated mean value of the power.

## 2.2. Wind Farms

### 2.2.1. Wind farm definition and siting

#### 2.2.1.1. Definition of wind farm

A wind farm is a group of wind turbines in the same location used to produce energy. Installing several turbines in groups at a site leads to large-scale utilization of wind energy. This has operation, maintenance as well as economic advantages. Any wind energy project will incur fixed costs such as the preparation of the environmental statement, legal fees and project management costs. They are largely independent of the size of the wind farms, so it is desirable to spread them over as large a project as possible[25]. This had led to the construction of large wind farms. A large wind farm may

consist of several hundred individual wind turbines which produce an output of hundreds of megawatts and cover an extended area of hundreds of square miles [24], but the land between the turbines may be used for agricultural or other purposes.

#### **2.2.1.2. Wind farm siting**

Siting wind energy projects is a crucial part of wind power development and operations. Effective siting can help Turkey wind energy industry to continue the dramatic growth, as well as related economic and environmental benefits, that the country has experienced over the last several years.

To successfully site wind projects, a developer must consider:

- Adequate wind: Turbines usually need wind that blows at least 11 miles per hour on average. Small changes in wind speed can make a dramatic difference in the output of a wind farm.

- Land rights: Developers need to secure adequate land rights from private owners or public agencies, so lease agreements come into play.

- Permits: Developers must secure proper permits from all levels of government.

- Transmission: Access to adequate and available transmission capacity is essential, and proximity to existing lines keeps costs down.

- A buyer for the wind power: Developers must secure a utility or other entity to purchase the power generated from the wind project.

- Financing: In order to build and operate a wind farm, developers need an investor or investors.

Each of these six elements must be secured to move a wind project from development, through construction, and into operation. Failure to successfully navigate any one of

these issues can result in a shelved project[34]. On average, only one in ten projects originally conceived by a developer will actually get constructed and put into operation. Wind farms can be classified by the location in which they are installed: Onshore developments (Figure 2.8), where wind farms are constructed inland, usually in hilly or mountainous regions to favor windy conditions.



Figure 2.8. Onshore wind farm (Said Webber, Feb 2014)

Offshore developments (Figure 2.9), where wind farms are installed in the sea, at least 10 kilometers away from the land. This is attractive because of higher wind speeds over the sea but mainly because of the reduced environmental impact. The major disadvantage of this type of wind farm development is the higher cost involved in terms of foundations, power collection cables, installation and maintenance [25].





Figure 2.9. Offshore wind farm (Øresund between Malmö and Copenhagen, Sweden)

Table 2.2. Advantages of Offshore wind Farm

Aesthetics	Offshore wind turbines are obviously coming into much less human contact than those on land. Thus, people do not need to deal with the noise pollution and eye sore that turbine cause for some. Farmers have complained that the whirring noise of turbines scare their livestock, while others simply do not like the sight of the turbines. Thus, with a move off land, the sounds and images of the turbines are nearly unnoticeable.
Less Harm to Birds	Thousands of birds each year die by flying into wind turbines on land in Turkey. Though this number is relatively very small in comparison to the number of deaths associated with pesticides, power lines, and other man-made structures, it is still an unacceptable statistic. Fortunately, offshore wind turbines mitigate this danger. In an attempt to cut down on bird deaths, offshore wind farms are located in specific areas of the ocean where birds do not frequently fly.
More Wind	One of the greatest advantages that offshore wind farms have over those on land is the frequency of strong winds over the ocean. Studies have shown that winds offshore blow nearly 40 percent more often than on land. Consequently, offshore wind farms can outpace those on land in terms of capacity and possibly offset the higher construction costs.

The combination of all three offshore advantages make a significant reason for developers to maintain the development of onshore wind farms in places where there is an economic (i.e. enough wind), aesthetic and environmental sense, and to intensify their

support for offshore wind[35]. The current trend in offshore wind investment reflects this. Turkey is increasing its investments in this clean technology, showing that with time, It is becoming not only more efficient but also smarter about the way it creates energy.

#### **2.2.1.2.1. Operation and maintenance**

Both onshore and offshore wind turbines have instruments on top of the nacelle, an anemometer and a wind vane, which respectively measure wind speed and direction. When the wind changes direction, motors turn the nacelle, and the blades along with it, around to face into the wind. The blades also ‘pitch’ or angle to ensure that the optimum amount of power is extracted from the wind[36]. All this information is recorded by computers and transmitted to a control center, which can be many miles away. Wind turbines are not physically staffed, although each will have periodic mechanical checks, often carried out by local firms. The onboard computers also monitor the performance of each turbine component, and will automatically shut the turbine down if any problems are detected; alerting an engineer that an onsite visit is required.

#### **2.2.2. Requirements for the interconnection of wind farms to the power system**

Even though power production from wind turbines has been known for several years the discussion for connection of wind turbines has arisen in recent years as the produced power by wind turbines increases. Furthermore, it became more and more common to install several wind turbines connected in wind farms, which changes the view from wind power as a supplementary power source to the issue of possible substitution of conventional power plants with wind power. Connection requirements for electrical devices to the grid have a long history in order to ensure stable operation of the grid. These requirements are besides juristic terms concerning frequency, voltage, power production and many others characteristics of the system. Because common power plants are usually equipped with large synchronous machines, grid connection requirements are fitted to meet the operation from electrical networks with synchronous machines. Most commonly wind turbines are equipped with asynchronous generators. Historically asynchronous generators have been treated as consumer of the electrical

grid and not as supplier. Experiences with asynchronous generators connected in large numbers of wind turbines as energy supplier on the grid have just recently been studied[37][38] and there are still many questions to answer. Another important difference from conventional power plants is the energy resource for production. Unlike power production from nuclear power plants or coal power plants, where the possible power production is dependent on the mass of raw material and the consumed power, wind turbines are dependent on wind forecasting to guarantee a predicted power production. This forecasting of power production from wind turbines is not a simple task. However it is quite important for system operators, who need to have reliable energy sources. They have to ensure the produced power offer is fitting to the power demand, in order to keep the power system stable. Varying power demands can cause voltage and frequency changes in the system. These changes can be normalized with controlling the active and reactive power supply and therewith is another requirement the transmission system operators have towards power plants.

#### **2.2.2.1. Wind turbine producers' view**

A wind turbine is a state of the art product, which all the time should meet the market demands. In addition, the cost per kilowatt should be low. Therefore it is important to know the loads in the turbine and the behavior of the turbine exactly. Only with precise knowledge is it possible to avoid over- or under sizing of the product, which will lead to either rather expensive solutions or of not holding the life time expectancies of 20 years for the turbine. It takes typically three to five years to develop a new wind turbine type fitting to the new demands from design to sale. As an example, the Vestas products over the past years are shown in Table 2.2.

Table 2.3. Vestas Type Development during the last 34 years [16]

First Installation	Rotor	Tower	Control	Capacity	MWh/year
1981	15/16m	22m	Stall	55KW	217
1984	17m	22m	Stall	75KW	265
1986	19m	22m	Stall	90 KW	301
1987	20m	31m	Stall	100 KW	346
1988	25m	31m	Stall	200 KW	662
1989	27/29m	39m	Pitch	225 KW	860
1991	39m	50m	Pitch/OptiSlip	500 KW	1671
1995	44m	50m	Pitch/OptiSlip	600 KW	1904
1997	47m	55m	Pitch/OptiSlip	660 KW	2372
2000	52m	49-65m	Pitch/OptiSpeed	850 KW	2998
1999	66m	60-78m	Pitch/OptiSpeed	1750 KW	5303
2000	80m	60-100m	Pitch/OptiSpeed	2000 KW	7041
2002	90m	80m	Pitch/OptiSpeed	3000 KW	-

While the development demands in recent years have been driven by mainly extracting most power out of the wind, the recent developments moved the focus to grid compliance. Unfortunately the recent requirements to wind turbines or wind farms acting like conventional power plants are not necessarily easy to combine with the ideas and challenges that wind turbines have been designed in line with in years[16]. A balance between the wind turbines handling the fluctuating wind energy resource and on the other hand being a reliable energy source supporting the electrical network has to be found. In this process the general requirements to produce a cheap product with low maintenance costs and high reliability have to be met.

#### 2.2.2.2. Connection Requirements

However, the lack of experience enforces the use of existing grid codes of common generating units or power plants, which can be quite challenging for wind turbines. Special connection conditions for wind turbines have to be discussed. A few countries including Turkey are already working on grid codes specifically for wind turbines or

wind farms, or a modification of the existing code, which also meets wind turbine characteristics[39]. Unfortunately not all countries where wind turbines are installed have specific or modified grid codes. This makes the development of future wind turbines very difficult. There is a big risk involved in developing new techniques to fulfill unspecified demands. Most wind turbine producers today deliver wind turbines to an international market and are faced with various numbers of grid requirements. Looking at a few of the existing grid codes it appears that they are very different in the most important characteristics.

### 2.2.2.2.1. Voltage and reactive power control

The voltage in power systems can vary due to load changes or fault occurrence. To avoid loss of power generation in especially critical situations a voltage operation range is defined. The voltage tolerances can be seen from two aspects. Firstly, how much voltage variation should the wind turbine system be able to withstand, without tripping out and secondly, when and how should the disconnection from the grid occur. In order to understand voltage control as it applies to grid modeling, it is useful to describe a simple model of a power system. An example of a simplified power system model that has a generator at the sending end, a power line and a load at the receiving end is annotated in Figure 2.10.

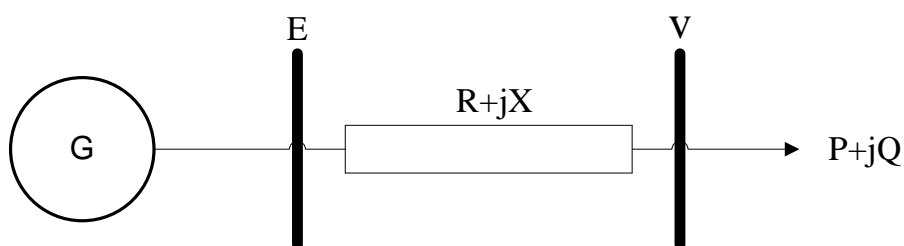


Figure 2.10. Single line diagram of a simple radial power system

Let  $E$  and  $V$  be the voltage at the sending and receiving end, respectively. The power line has a resistance  $R$  and a reactance  $X$ .  $P$  and  $Q$  are the transmitted active and reactive power at the receiving end. Thus, the voltage gradient from sending end to receiving end is represented by the following equation:

$$\Delta V = E - V = ZI = (R + jX) \left( \frac{P - jQ}{E} \right) \quad (2.5)$$

$$= \frac{RP+XQ}{E} + j \frac{XP-RQ}{E} = \Delta V_p + j \Delta V_q \approx \Delta V_p$$

Where

$$\Delta V_p = \frac{RP+XQ}{E} \quad \text{in most networks } X \gg Q; \text{ hence } Q \propto \Delta V$$

This means that the magnitude of the voltage is controlled by the reactive power exchange, whereas the phase difference between sending and receiving end is dictated by the active power. The active and reactive power flow between the generation and the load in the power system must be balanced in order to avoid large voltage and frequency excursions[40]. Voltage or reactive power requirements in the grid codes are usually specified with a limiting curve such as that shown in Figure 2.11:

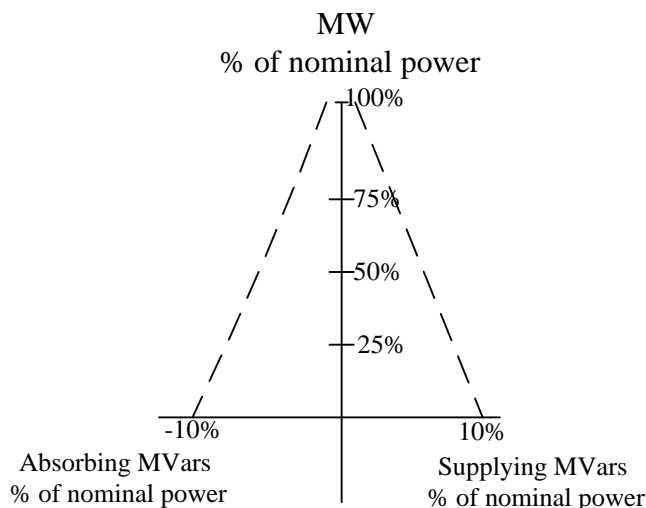


Figure 2.11. Typical reactive power limiting curve

According to Figure 2.10 and Figure 2.11, the mean value of the reactive power over several seconds should stay within the limits of the curve. When the generating unit is providing low active power the power factor may deviate from unity because it can support additional leading or lagging currents due to the reactive power demanded by the utility. When the generating unit is working under nominal conditions, the power factor must be kept close to unity or else there will be excessive currents. Thus, the occurrence of a fault leads to a voltage drop along the circuit proportional to current and to distance from the substation. Wind farms are often located in remote locations, the distance to the substation may be very long and the connection may be radial. In

this case the impedance is usually high and the voltage drop may be important. The regulator in the substation may not be able to raise the voltage at the connection of the wind farm without exceeding its voltage limits. Voltage control capability of the wind farm is very useful to keep the voltage profile along the system. In Turkey, wind farms have to be able to afford automatic voltage control at the point of connection by continuous control of the reactive power at their terminals, according to a certain characteristic specified in a site specific bilateral agreement. However, handling a voltage to a certain rest voltage is less complicated than the handling of no voltage. Thus, the wind farm should have the capability to control the voltage and/or the reactive power at the connection point. This is essential in order to ensure secure operation of the system. The wind farm operator has the opportunity to gain additional payments for providing reactive power.

#### **2.2.2.2.2. Frequency requirement**

Historically power plants use big synchronous generators. Direct grid connected synchronous machines have stability problems due to load changes and frequency changes. In the case of a machine overload, the synchronous machines will drop in speed, which means either they decrease the grid frequency as well or become unstable and drop out. The frequency change in a grid can be caused by loss of transmission, sudden demand changes or some problems of bigger power plants (loss of generation), which would normally stabilize the grid frequency. A change in grid frequency will affect all other machines connected to it. Therefore an important issue is to operate in a wide range of frequencies. Wind turbines with asynchronous generators have no problem with asynchronous operation. The frequency operation range is more an issue of control strategy. A high frequency operation range for wind turbines and frequency control is therefore only interesting, if the power system operator uses the wind farm for stabilizing the grid frequency. Although wind turbines are able to tolerate major frequency changes they have difficulties to support the frequency control operation in a wide range, hence the inertia in the system is very small. It is possible to initiate a sudden supply or reduction of power, which will actively help to stabilize the grid again[41]. However, it has to be mentioned, that a supply of power into the grid is only

possible, if the wind turbine is using an advanced operation at reduced power and thereby has enough power reserve or using another new control strategy.

#### **2.2.2.2.3. Wind farm protection**

Recommendations for the connection of wind farms to distribution networks usually include the disconnection of wind farms in the case of a fault in the network. However, this does not apply for large wind farms, for which an immediate disconnection would put additional stress on the already troubled system. After severe disturbances, several transmission lines may be disconnected and part of the network may be isolated, leading to an imbalance between production and consumption in this part of the network. As a rule, wind farms are not required to disconnect, as long as certain voltage and frequency limits are not exceeded. Undervoltages/overvoltages and overfrequency/underfrequency after a fault can also damage wind turbines and associated equipment. The protection system of the wind farm should therefore be design to pursue two goals [31]:

- To comply with requirements for normal network operation and support the network during and after a failure.
- To secure wind farms against damage from impacts originating from faults in the network.

The interaction between wind farm and power system during faults in the power system is usually verified through simulations.

#### **2.2.2.2.4. Communication and external control**

In most regulations, the wind farm owner is required to provide the signals necessary for the operation of the power system, such as: voltage, active power, reactive power, operating status, wind speed, wind direction, ambient temperature and pressure, generator transformer tap position, regulation capability, frequency control status, abnormalities and external control possibilities[31]. It is important to note that interconnec-



tion regulations vary considerably and it is difficult to find a general technical justification for the different technical regulations that are currently in use worldwide. Many of the differences in the technical regulations are caused by different wind power penetration levels and different power system robustness depending on the countries[31].

### 2.2.3. Discussing the requirements

The specifications given in this chapter to voltage, frequency and reactive power requirements show clearly the discrepancy and the variety in the grid codes. It also has to be mentioned that all requirements are in a rapid development, and these are changing at this moment. However, every grid is different and it might not be a good idea just copying the requirements. Although it is a good example for the Turkish grid, a more practical solution could be a separation into two groups – wind turbines connected to strong grids, wind turbines connected to weak grids and the introduction of special requirements depend on the case. Grid codes should not have the purpose to avoid the connection of wind turbines to the grid. They should be open enough for discussion project specific issues. The following points should be treated.

- Turbine should start automatically with a pre-defined time delay and power ramp
- Turbine should stop automatically with a pre-defined disconnection procedure (high wind or fault) and power ramp
- The continuous frequency range should be defined.
- A distinction between synchronous and asynchronous generator should be made.
- A dynamical description during rated operation and fault situations regarding voltage, active power and reactive power should be made.
- Considering the possible power production dependent on the wind input

The problem however stays. Wind turbine producers have a numbered product range, which should be able to fulfill as many grid requirements as possible. With the lack of

conformability wind turbines will be designed for the codes for the biggest market and the outer limits. This consequently limits the price reduction of wind turbine technology.

Therefore a continuous positive discussion between all grid operators, customers and wind turbine producers is required to find acceptable demands and solutions in the future. One step forward is to gain knowledge of the behavior of wind turbines with asynchronous generators during situations such as voltage sags. In a test bench it is hard to produce the necessary operation modes. Therefore the development of wind turbine models as presented in this thesis is a necessary step on the way to define grid codes and design wind turbines.

## **CHAPTER 3. SYSTEM MODELLING AND ANALYSIS**

### **3.1. Asynchronous Generator Models**

The mechanical power of the wind turbine is converted into electric power by an alternating current (AC) generator or a direct current (DC) generator. The AC generator can be either a synchronous machine or an asynchronous machine. The latter is most widely used in the wind power industry and was selected for this thesis. The electrical machine works on the principle of action and reaction of electromagnetic induction. The resulting electromechanical energy conversion is reversible. The same machine can be used as a motor for converting electrical power into mechanical power or as a generator for converting mechanical power into electric power. As explained in the chapters above, one main interest of wind turbine manufacturers is the precise and strong knowledge about the influence of certain grid conditions to the wind turbine itself. Detailed knowledge about the torque on the wind turbine shaft caused by faults in the grid or transient current rises is important for the estimation of the load on the wind turbines. Accurate knowledge of these effects ensures low costs and the availability for the estimated life time of the wind turbine. Therewith the generator as connection point between the electrical grid and the mechanical wind turbine plays an important role. Though for understanding and calculation of the dynamic behavior in a wind turbine, the realistic representation of the generator is important. However wind turbine producers face several problems which are limiting the information gained from a machine model. Because many wind turbine manufacturers don't produce their own generators, there is only a minimum access to data. Representing a range of generators in a model, facing the additional variation in each generator's dimension and material, detailed FEM studies of the generator are not sufficient since an appropriate model of the asynchronous generator is the most complicated part of the total wind generation model. Therefore the main purpose of the presented thesis is to find an

analytical asynchronous generator model for the simulation of fault conditions on variable speed Wind Turbines like asymmetrical voltage supply or 1-ph, 2-ph , 3-ph short circuit using Matlab. The mathematical model of an asynchronous generator for power system analysis is usually based on the following assumptions:

### 3.1.1. General equations in abc/abc reference frame

To make a mathematical description of the asynchronous generator it will be assumed that a uniform air gap machine can be modeled initially as two concentric cylinders with an air gap of constant radial length[42]. The stator and rotor have wounded 3-ph windings. Furthermore iron losses, and changing of parameters with temperature, are not considered. A balanced 3-ph machine is expressed in Figure 3.1. The conceptual windings are placed along the magnetic axes of the windings. The subscript 's' indicates the stator windings with effective number of turns  $N_s \xi_s$  and 'r' the rotor windings with effective number of turns  $N_r \xi_r$ . The couplings between the phases are depending from the electrical angle between the phases  $\theta$ . If the 3 windings subscripted with 'a, b, c' are displaced by  $\pm 120^\circ$  the angle  $\theta$  is only dependent from the rotor displacement angle  $\rho$ . The basic equations for developing a 3-ph model can be found in various books about electrical machines and drives[43][44]. The variables of the machine are defined in vectors, where each element is represented per phase: The equation for stator and rotor voltages has to be written as:

$$\vec{u}_s^s = R_s \cdot \vec{i}_s^s + \frac{d\vec{\Psi}_s^s}{dt} \quad (3.1)$$

$$\vec{u}_r^r = R_r \cdot \vec{i}_r^r + \frac{d\vec{\Psi}_r^r}{dt} \quad (3.2)$$

Where the voltages  $u$ , the currents  $i$  and Flux  $\Psi$  are vectors exemplified for stator values defined by (3.3). The same definition has to be written for rotor values.

$$\vec{u}_s = \begin{pmatrix} \vec{u}_{as} \\ \vec{u}_{bs} \\ \vec{u}_{cs} \end{pmatrix}, \vec{i}_s = \begin{pmatrix} \vec{i}_{as} \\ \vec{i}_{bs} \\ \vec{i}_{cs} \end{pmatrix}, \vec{\Psi}_s = \begin{pmatrix} \vec{\Psi}_{as} \\ \vec{\Psi}_{bs} \\ \vec{\Psi}_{cs} \end{pmatrix} \quad (3.3)$$

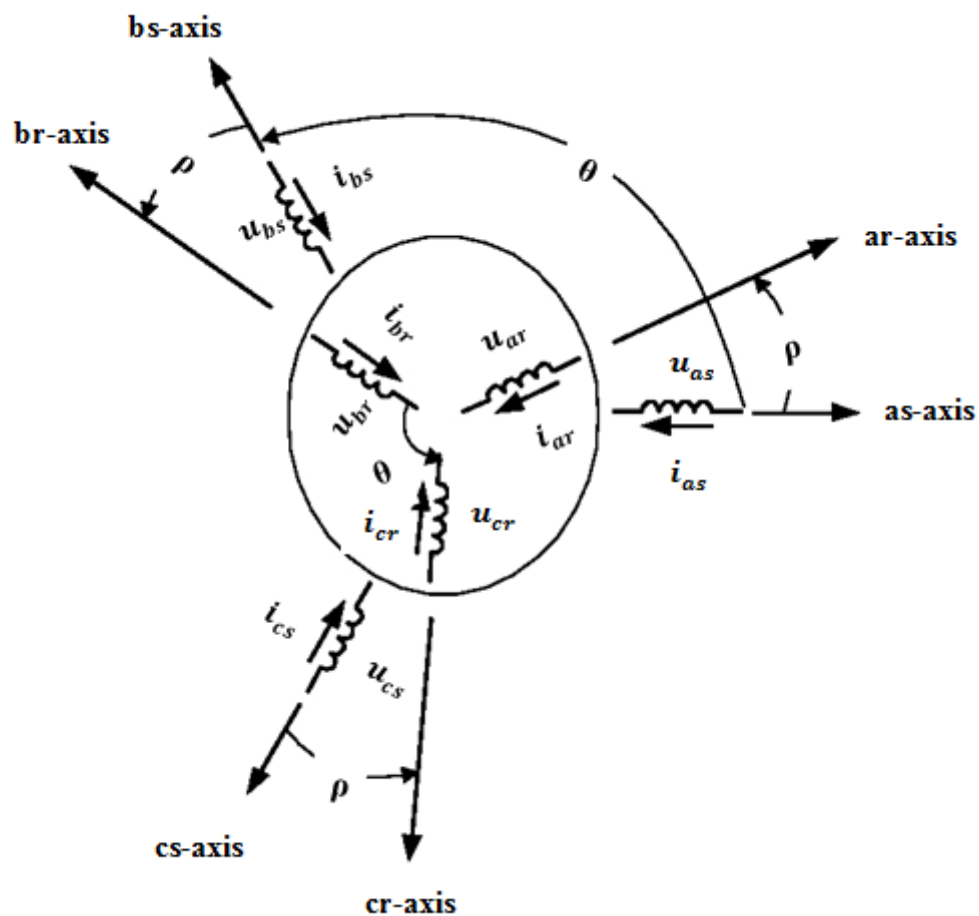


Figure 3.1. Magnetic axes, concentric stator and rotor windings, currents and voltages and angle dependencies of a 3-ph asynchronous generator[45]

The flux in stator of the machine has to be expressed with the flux created by the stator phases itself and the flux part influencing the stator originated from the rotor phases. In the same way the rotor flux has to be separated into the flux belonging to the rotor and a part penetrating the rotor windings originating from the stator phases.

$$\vec{\Psi}_s = \vec{\Psi}_{s(s)} + \vec{\Psi}_{s(r)} \quad (3.4)$$

$$\vec{\Psi}_r = \vec{\Psi}_{r(r)} + \vec{\Psi}_{r(s)} \quad (3.5)$$

The flux has to be expressed as a product of an inductance matrix and the current vector  $\vec{i}$ . The flux created from the stator windings is expressed in equation (3.6).

$$\vec{\Psi}_{s(s)} = \begin{pmatrix} L_{\sigma s} + L_{ms} & -\frac{L_{ms}}{2} & -\frac{L_{ms}}{2} \\ -\frac{L_{ms}}{2} & L_{\sigma s} + L_{ms} & -\frac{L_{ms}}{2} \\ -\frac{L_{ms}}{2} & -\frac{L_{ms}}{2} & L_{\sigma s} + L_{ms} \end{pmatrix} \cdot \vec{i}_s \quad (3.6)$$

In the same way the flux created from the rotor windings is expressed in equation (3.7).

$$\vec{\Psi}_{r(r)} = \begin{pmatrix} L_{\sigma r} + \left(\frac{N_r \xi_r}{N_s \xi_s}\right)^2 L_{ms} & -\frac{L_{ms}}{2} \left(\frac{N_r \xi_r}{N_s \xi_s}\right)^2 & -\frac{L_{ms}}{2} \left(\frac{N_r \xi_r}{N_s \xi_s}\right)^2 \\ -\frac{L_{ms}}{2} \left(\frac{N_r \xi_r}{N_s \xi_s}\right)^2 & L_{\sigma r} + \left(\frac{N_r \xi_r}{N_s \xi_s}\right)^2 L_{ms} & -\frac{L_{ms}}{2} \left(\frac{N_r \xi_r}{N_s \xi_s}\right)^2 \\ -\frac{L_{ms}}{2} \left(\frac{N_r \xi_r}{N_s \xi_s}\right)^2 & -\frac{L_{ms}}{2} \left(\frac{N_r \xi_r}{N_s \xi_s}\right)^2 & L_{\sigma r} + \left(\frac{N_r \xi_r}{N_s \xi_s}\right)^2 L_{ms} \end{pmatrix} \cdot \vec{I}_s \quad (3.7)$$

The coupling between the rotor and stator is depending from the rotor displacement angle. The flux penetrating the stator initiated in the rotor is shown in equation (3.7) and the stator flux penetrating the rotor is shown in equation (3.8)

$$\vec{\Psi}_{s(r)} = \left(\frac{N_r \xi_r}{N_s \xi_s}\right) \cdot L_{ms} \cdot \begin{pmatrix} \cos \rho & \cos(\rho + 2\pi/3) & \cos(\rho - 2\pi/3) \\ \cos(\rho - 2\pi/3) & \cos \rho & \cos(\rho + 2\pi/3) \\ \cos(\rho + 2\pi/3) & \cos(\rho - 2\pi/3) & \cos \rho \end{pmatrix} \cdot \vec{I}_r \quad (3.8)$$

$$\vec{\Psi}_{r(s)} = \left(\frac{N_r \xi_r}{N_s \xi_s}\right) \cdot L_{ms} \cdot \begin{pmatrix} \cos \rho & \cos(\rho - 2\pi/3) & \cos(\rho + 2\pi/3) \\ \cos(\rho + 2\pi/3) & \cos \rho & \cos(\rho - 2\pi/3) \\ \cos(\rho - 2\pi/3) & \cos(\rho + 2\pi/3) & \cos \rho \end{pmatrix} \cdot \vec{I}_s \quad (3.9)$$

The winding turns in stator and rotor are mostly different. For expression of the stator and rotor system in an equivalent coupled system the ratio  $ue$  is introduced in (3.10). This ratio is already implied in the flux equations.

$$ue = \left(\frac{N_r \xi_r}{N_s \xi_s}\right) \quad (3.10)$$

$$ue \cdot \underline{u}_r = \underline{u}'_r \quad (3.11) \quad ue \cdot \underline{\Psi}_r = \underline{\Psi}'_r \quad (3.12)$$

$$\frac{i_r}{ue} = i'_r \quad (3.13) \quad ue^2 \cdot L_{mr} = L_{ms} = ue \cdot L_{msr} \quad (3.14)$$

With  $L_{msr} = \sqrt{L_{ms} \cdot L_{mr}}$

$$ue^2 \cdot R_r = R'_r \quad (3.15) \quad ue^2 \cdot L_{\sigma r} = L'_{\sigma r} \quad (3.16)$$

When using the ratio  $ue$  the flux equations are simplified to:

$$\vec{\Psi}_s = \begin{pmatrix} L_{\sigma s} + L_{ms} & -\frac{L_{ms}}{2} & -\frac{L_{ms}}{2} \\ -\frac{L_{ms}}{2} & L_{\sigma s} + L_{ms} & -\frac{L_{ms}}{2} \\ -\frac{L_{ms}}{2} & -\frac{L_{ms}}{2} & L_{\sigma s} + L_{ms} \end{pmatrix} \cdot \vec{i}_s + L_{msr} \cdot \begin{pmatrix} \cos \rho & \cos(\rho + 2\pi/3) & \cos(\rho - 2\pi/3) \\ \cos(\rho - 2\pi/3) & \cos \rho & \cos(\rho + 2\pi/3) \\ \cos(\rho + 2\pi/3) & \cos(\rho - 2\pi/3) & \cos \rho \end{pmatrix} \cdot \vec{i}_r \quad (3.17)$$

$$\vec{\Psi}_r = \begin{pmatrix} L_{\sigma s} + L_{ms} & -\frac{L_{ms}}{2} & -\frac{L_{ms}}{2} \\ -\frac{L_{ms}}{2} & L_{\sigma s} + L_{ms} & -\frac{L_{ms}}{2} \\ -\frac{L_{ms}}{2} & -\frac{L_{ms}}{2} & L_{\sigma s} + L_{ms} \end{pmatrix} \cdot \vec{i}_s + L_{msr} \cdot \begin{pmatrix} \cos \rho & \cos(\rho - 2\pi/3) & \cos(\rho + 2\pi/3) \\ \cos(\rho + 2\pi/3) & \cos \rho & \cos(\rho - 2\pi/3) \\ \cos(\rho - 2\pi/3) & \cos(\rho + 2\pi/3) & \cos \rho \end{pmatrix} \cdot \vec{i}_r \quad (3.18)$$

Often the expression in one matrix is used [46][47] expressing the angle dependency in a function:

$$f_1 = \cos \rho \quad (3.19)$$

$$f_2 = \cos(\rho + 2\pi/3) \quad (3.20)$$

$$f_3 = \cos(\rho - 2\pi/3) \quad (3.21)$$

$$\begin{pmatrix} \Psi_{as} \\ \Psi_{bs} \\ \Psi_{cs} \\ \Psi'_{as} \\ \Psi'_{bs} \\ \Psi'_{cs} \end{pmatrix} = \begin{pmatrix} L_{\sigma s} + L_{ms} & -\frac{L_{ms}}{2} & -\frac{L_{ms}}{2} & L_{msr} \cdot f_1 & L_{msr} \cdot f_2 & L_{msr} \cdot f_3 \\ -\frac{L_{ms}}{2} & L_{\sigma s} + L_{ms} & -\frac{L_{ms}}{2} & L_{msr} \cdot f_3 & L_{msr} \cdot f_1 & L_{msr} \cdot f_2 \\ -\frac{L_{ms}}{2} & -\frac{L_{ms}}{2} & L_{\sigma s} + L_{ms} & L_{msr} \cdot f_2 & L_{msr} \cdot f_3 & L_{msr} \cdot f_1 \\ L_{msr} \cdot f_1 & L_{msr} \cdot f_3 & L_{msr} \cdot f_2 & L'_{\sigma s} + L_{ms} & -\frac{L_{ms}}{2} & -\frac{L_{ms}}{2} \\ L_{msr} \cdot f_2 & L_{msr} \cdot f_1 & L_{msr} \cdot f_3 & -\frac{L_{ms}}{2} & L'_{\sigma s} + L_{ms} & -\frac{L_{ms}}{2} \\ L_{msr} \cdot f_3 & L_{msr} \cdot f_3 & L_{msr} \cdot f_1 & -\frac{L_{ms}}{2} & -\frac{L_{ms}}{2} & L'_{\sigma s} + L_{ms} \end{pmatrix} \cdot \begin{pmatrix} i_{as} \\ i_{bs} \\ i_{cs} \\ i'_{as} \\ i'_{bs} \\ i'_{cs} \end{pmatrix} \quad (3.22)$$

The inductance matrix is expressing the coupling of the flux in the stator and rotor windings. It takes an important position in the machine modeling. Depending on the form of the inductance matrix, the machine model is more or less detailed. In progress of this chapter, consideration of saturation effects will change the constant inductances in this matrix to time dependent functions.

### 3.1.1.1. Complex space vector representation

Many authors[43][45][48] introduced the method of complex space vector for a more convenient mathematical description of the machine variables. It is widely used in the field of machine modeling and machine protection.

The phase currents of the 3 machine windings displaced by  $\pm 120^\circ$  as already shown in Figure 3.2 is described as complex vectors. With the help of the complex vector (28) this complex vectors is expressed by (3.24). For convenience the real part of the complex space vector is aligned to phase a of the 3 phase stator system or 3 phase rotor system.

$$\underline{a} = 1 \angle 120^\circ = \frac{1}{2} + \frac{\sqrt{3}}{2} \cdot j = e^{j \frac{2}{3} \pi} \quad (3.23)$$



$$\underline{i}_a = i_a, \underline{i}_b = \underline{a} \cdot i_b, \underline{i}_c = \underline{a}^2 \cdot i_c \quad (3.24)$$

Where  $i_a, i_b, i_c$  are the absolute values of the current time vector. A resulting current vector is achieved through an addition of the 3 phase current vectors (3.24).

$$\underline{i} = \underline{i}_a + \underline{i}_b + \underline{i}_c = i_a + \underline{a} \cdot i_b + \underline{a}^2 \cdot i_c \quad (3.25)$$

Most electrical engineers[37][49] interpret this equation as a definition for the complex space vector. In interpretation as complex space vector the time vectors itself may be complex vectors. Instead of the definition (3.25) a more common definition is achieved through multiplying (3.25) by the factor  $\frac{2}{3}$ (3.26).

$$\underline{i}_s = \frac{2}{3} \cdot (i_{as} + \underline{a} \cdot i_{bs} + \underline{a}^2 \cdot i_{cs}) \quad (3.26)$$

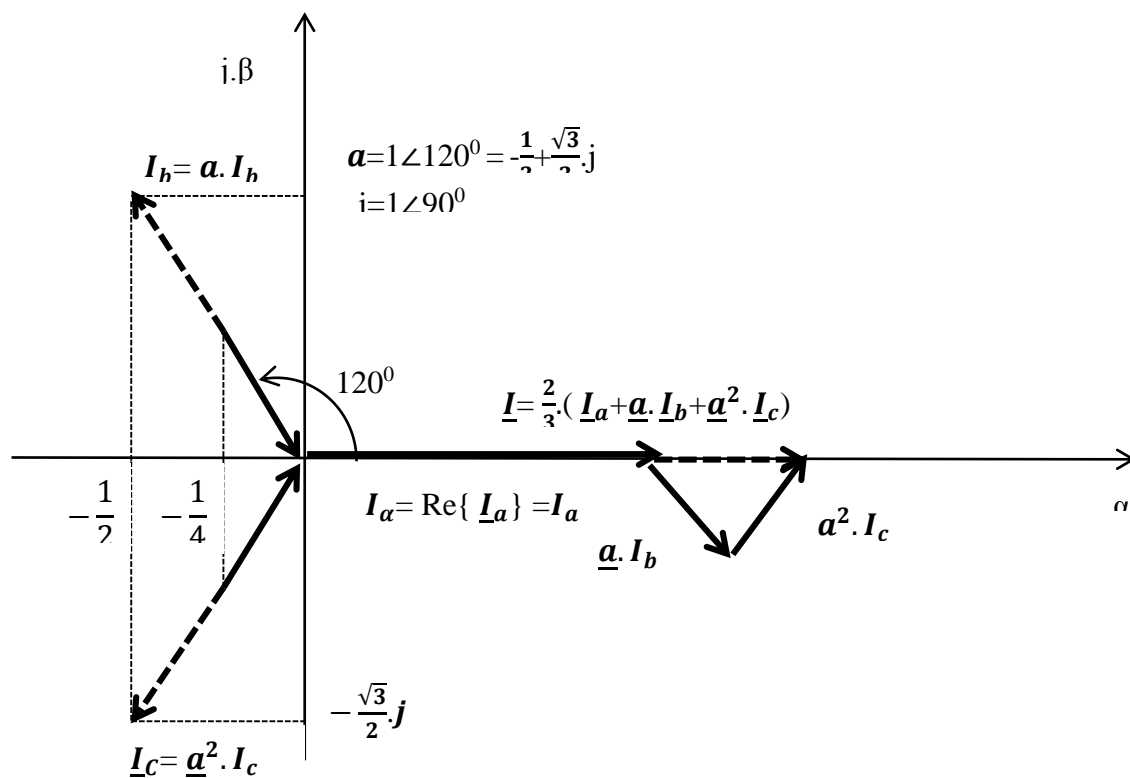


Figure 3.2. Space vector constructed from a 3-ph system

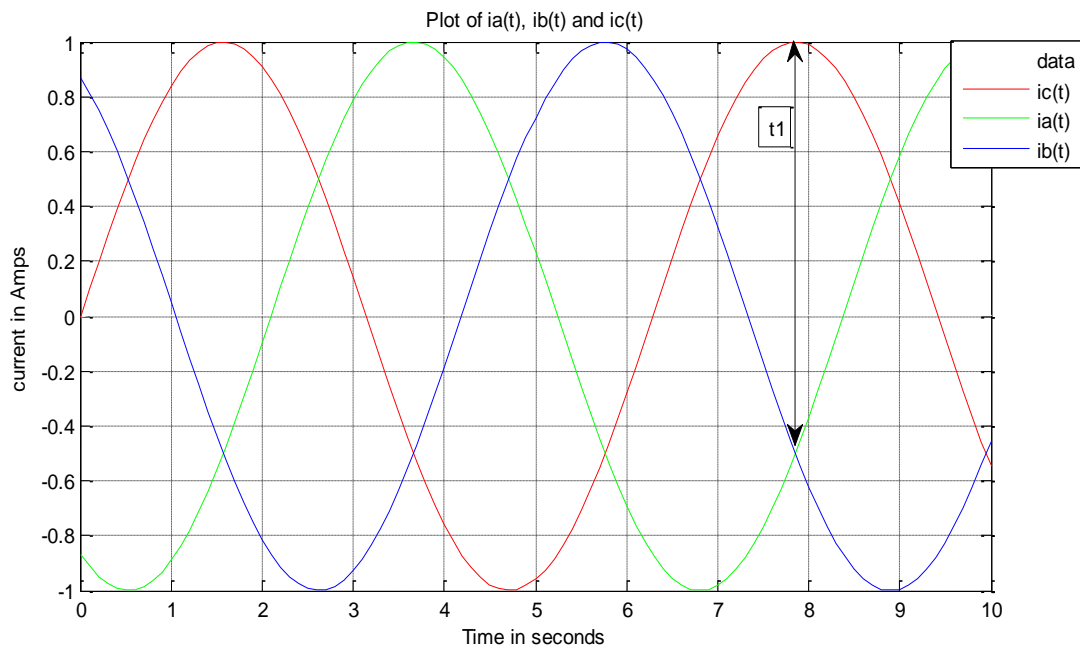


Figure 3.3. Phase currents in a time based system

The main advantages of using definition (3.26) are that the projections from the space vector  $\underline{i}_s$  to the magnetic axes achieve the absolute time values of the existing axes-currents (3.27). The vector changes its length and position with the phase currents (Figure 3.1, Figure 3.2). In addition, the space vector is used for voltages and fluxes in the same way as for the currents (3.28), (3.29). The calculated power using the vectors defined as in (31), (3.28) is non-variant. The calculation of power and torque (see equations (3.32), (3.33), (3.34) gives the same expressions like the general equations of symmetrical 3-ph systems[48]. Therefore this definition is often called the real or correct power definition.

$$i_{as} = \text{Re}\{\underline{i}_s\}, i_{bs} = \text{Re}\{\underline{a}^2 \cdot \underline{i}_s\}, i_{cs} = \text{Re}\{\underline{a} \cdot \underline{i}_s\} \quad (3.27)$$

$$\underline{u}_s = \frac{2}{3} \cdot (u_{as} + \underline{a} \cdot u_{bs} + \underline{a}^2 \cdot u_{cs}) \quad (3.28)$$

$$\underline{\Psi}_s = \frac{2}{3} \cdot (\Psi_{as} + \underline{a} \cdot \Psi_{bs} + \underline{a}^2 \cdot \Psi_{cs}) \quad (3.29)$$

The power calculated using the method of complex space vector is shown in equation

$$S_s = \frac{3}{2} \cdot \{ \underline{u}_s \cdot \underline{i}_s^* \} = \frac{3}{2} \cdot \left\{ \frac{2}{3} \cdot (u_{as} + \underline{a} \cdot u_{bs} + \underline{a}^2 \cdot u_{cs}) \cdot \frac{2}{3} \cdot (i_{as} + \underline{a} \cdot i_{bs} + \underline{a}^2 \cdot i_{cs}) \right\}$$

$$S_s = \frac{3}{2} \cdot \left\{ \begin{aligned} &\frac{4}{9} \cdot \{ (u_{as} \cdot i_{as} + u_{bs} \cdot i_{bs} + u_{cs} \cdot i_{cs}) - \frac{1}{2} (u_{as}(i_{bs} + i_{cs}) + u_{bs}(i_{as} + i_{cs}) + u_{cs}(i_{as} + i_{bs})) \} \\ &+ \frac{4}{9} \cdot \frac{\sqrt{3}}{2} \cdot j \cdot (i_{as}(u_{bs} - u_{cs}) + i_{bs}(u_{cs} - u_{as}) + i_{cs}(u_{as} - u_{bs})) \end{aligned} \right\} \quad (3.30)$$

Assuming that the phase currents are added to zero, as shown in equation (3.31). The active stator power in equation (3.32) and reactive stator power equation (3.33) are achieved as real and imaginary part of the total power shown in equation (3.30). The assumption of equation (3.31) means there is no zero component existing, or the zero component is not considered in the calculation. It can be easily considered separately on a later (see sub-chapter 3.1.2).

$$i_a + i_b + i_c = 0 \quad (3.31)$$

$$P_s = \frac{3}{2} \cdot \text{Re} \{ \underline{u}_s \cdot \underline{i}_s^* \}$$

$$= \frac{4}{9} \cdot \{ (u_{as} \cdot i_{as} + u_{bs} \cdot i_{bs} + u_{cs} \cdot i_{cs}) - \frac{1}{2} (u_{as}(i_{bs} + i_{cs}) + u_{bs}(i_{as} + i_{cs}) + u_{cs}(i_{as} + i_{bs})) \} \quad (3.32)$$

$$Q_s = \frac{3}{2} \cdot \text{Im} \{ \underline{u}_s \cdot \underline{i}_s^* \}$$

$$= \frac{1}{\sqrt{3}} \cdot (i_{as}(u_{bs} - u_{cs}) + i_{bs}(u_{cs} - u_{as}) + i_{cs}(u_{as} - u_{bs})) \quad (3.33)$$

and the torque in an analogous manner (damping due to friction and windage is not included).

$$T_e = \frac{3}{2} \cdot p_p \cdot \text{Im} \{ \underline{\Psi}_s^* \cdot \underline{i}_s^s \}$$

$$= \frac{p_p}{\sqrt{3}} \cdot (i_{as}(\Psi_{bs} - \Psi_{cs}) + i_{bs}(\Psi_{cs} - \Psi_{as}) + i_{cs}(\Psi_{as} - \Psi_{bs})) \quad (3.34)$$

### 3.1.1.2. Using space vector for the general machine equations

By using the above introduced complex space vector, the general machine equation is expressed more conveniently compared to the vector presentation for the per phase

presentation. The voltage equations (3.35), (3.36) using the complex space vector representation for the stator and rotor are expressed through the stator flux  $\underline{\Psi}_s^s$  and rotor flux  $\underline{\Psi}_r^r$  transient and winding losses:

$$\underline{u}_s^s = R_s \cdot \underline{i}_s^s + \frac{d\underline{\Psi}_s^s}{dt} \quad (3.35)$$

$$\underline{u}_r^r = R_r \cdot \underline{i}_r^r + \frac{d\underline{\Psi}_r^r}{dt} \quad (3.36)$$

The flux is defined with the following equations [3.45]:

$$\underline{\Psi}_s^s = \underline{\Psi}_{s(s)} + \underline{\Psi}_{s(r)} \quad (3.37)$$

$$\underline{\Psi}_r^r = \underline{\Psi}_{r(r)} + \underline{\Psi}_{r(s)} \quad (3.38)$$

Where the flux components are expressed as:

$$\underline{\Psi}_{s(s)} = (L_{\sigma s} + \frac{3}{2} \cdot L_{ms}) \cdot \underline{i}_s \quad (3.39)$$

$$\underline{\Psi}_{r(r)} = (L_{\sigma r} + \frac{3}{2} \cdot L_{mr}) \cdot \underline{i}_r \quad (3.40)$$

$$\underline{\Psi}_{r(s)} = \frac{3}{2} \cdot L_{msr} \cdot \underline{i}_s \cdot e^{-jp} \quad (3.41)$$

$$\underline{\Psi}_{s(r)} = \frac{3}{2} \cdot L_{msr} \cdot \underline{i}_r \cdot e^{-jp} \quad (3.42)$$

If the mutual inductances and couple inductances are equal as assumed in a 1-ph equivalent diagram, then the magnetizing inductance has to be written as:

$$L_m = \frac{3}{2} \cdot L_{ms} = \frac{3}{2} \cdot L'_{mr} = \frac{3}{2} \cdot L_{msr} \quad (3.43)$$

The flux equations become:

$$\underline{\Psi}_s = (L_{\sigma s} + L_m) \cdot \underline{i}_s + L_m \cdot \underline{i}'_r \cdot e^{jp} \quad (3.44)$$

$$\underline{\Psi}'_r = (L_{\sigma r} + L_m) \cdot \underline{i}'_r + L_m \cdot \underline{i}_s \cdot e^{-jp} \quad (3.45)$$

The rotor voltage equation related to the stator becomes:

$$\underline{u}_r^{r'} = R_r' \cdot \underline{i}_r^{r'} + \frac{d\Psi_r^{s'}}{dt} \quad (3.46)$$

The vectors expressing the rotor current, voltage and flux are still related to their own reference frame, marked by the upper index 'r', while the stator vectors are related to the stator reference frame, marked by the upper index 's'. This difference of the two coordinate systems is expressed with the rotor angle  $\rho$  (Figure 3.1). With using vector transformation and this angle, the rotor voltage equation has to be written as:

$$\underline{u}_r^{s'} = R_r' \cdot \underline{i}_r^{s'} + \frac{d\Psi_r^{s'}}{dt} - j \cdot \dot{\rho} \cdot \underline{\Psi}_r^{s'} \quad (3.47)$$

Finally all general equations for modeling an asynchronous generator using the representation of complex space vectors are:

$$\underline{u}_s^s = R_s \cdot \underline{i}_s^s + \frac{d\Psi_s^s}{dt} \quad (3.48)$$

$$\underline{u}_r^{s'} = R_r' \cdot \underline{i}_r^{s'} + \frac{d\Psi_r^{s'}}{dt} - j \cdot \dot{\rho} \cdot \underline{\Psi}_r^{s'} \quad (3.49)$$

$$\underline{\Psi}_s = (L_{\sigma s} + L_m) \cdot \underline{i}_s + L_m \cdot \underline{i}_r' \cdot e^{j\rho} \quad (3.50)$$

$$\underline{\Psi}_r' = (L_{\sigma r} + L_m) \cdot \underline{i}_r' + L_m \cdot \underline{i}_s \cdot e^{-j\rho} \quad (3.51)$$

$$T_e = \frac{3}{2} \cdot p_p \cdot \text{Im}\{\underline{\Psi}_s^{s*} \cdot \underline{i}_s^s\} \quad (3.52)$$

$$T_e - T_m = J \frac{d\omega_r}{dt} + D\omega_r [55] \quad (3.53)$$

$$\ddot{\rho} = \frac{d\omega_e}{dt} - \frac{d\omega_r \cdot p_p}{dt} = \frac{p_p}{J} \cdot (T_e - T_m - D\omega_r) \quad (3.54)$$

The achieved equations and parameters is visualized in the dynamical 1-ph equivalent diagram seen in Figure 3.4.

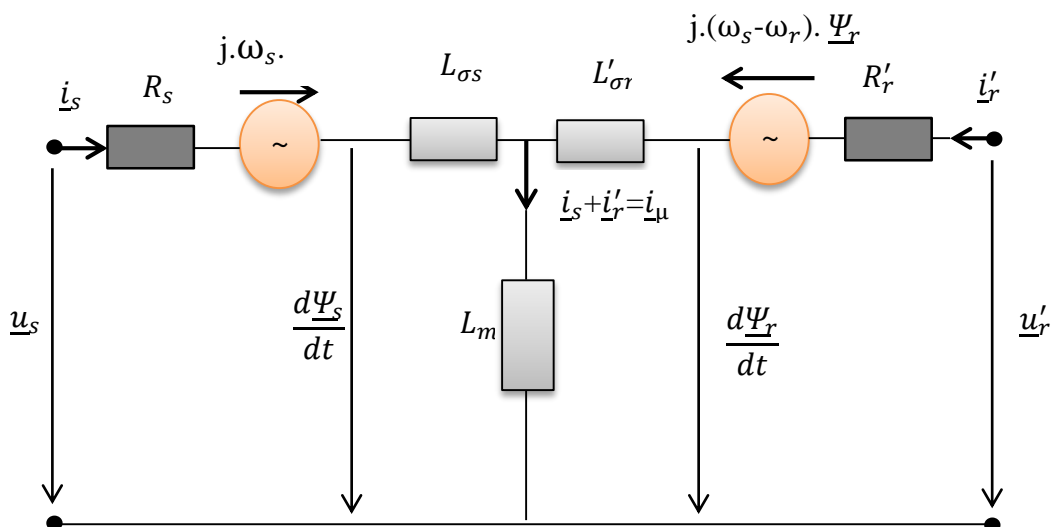


Figure 3.4. Dynamical per phase equivalent diagram for asynchronous generator

### 3.1.2. The Clark transformation (a, b, 0 equivalent frame)

The complex space vector representation is the base for several different descriptions of an electrical machine. One of the possible interpretations with the complex space vector deduced machine equations are the so-called  $\alpha$ ,  $\beta$ -components. The  $\alpha$ ,  $\beta$ -components, also known as Clark Transformation, are deduced by separating the complex space vectors of the machine into their real and imaginary parts and referring them to a stationary reference system. The so-achieved components are physically imagined as two fields in normative direction to each other, meaning the 3-ph machine has been deduced to an equivalent 2-ph machine, see Figure 3.5.

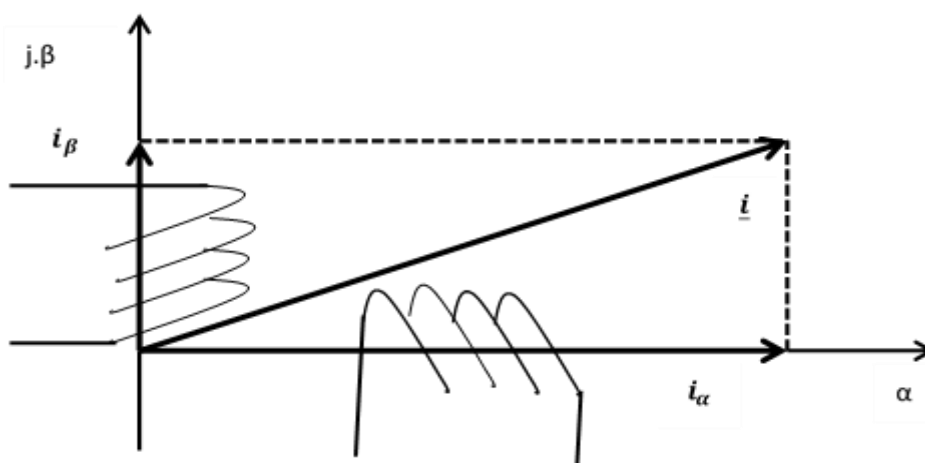


Figure 3.5. Equivalent two-phase machine showing Clark-Transformation

The real component is calculated as shown in equation (3.55) and the imaginary part equation (3.56).

$$i_{\alpha} = \text{Re}\{\underline{i}\} = \text{Re}\left\{\frac{2}{3}(i_a + \underline{a}i_b + \underline{a}^2i_c)\right\} = \frac{2}{3}(i_a - \frac{i_b + i_c}{2}) \quad (3.55)$$

$$i_{\beta} = \text{Im}\{\underline{i}\} = \text{Im}\left\{\frac{2}{3}(i_a + \underline{a}i_b + \underline{a}^2i_c)\right\} = \frac{1}{\sqrt{3}}(i_b - i_c) \quad (3.56)$$

The complex space vector has to be written as:

$$\underline{i} = i_{\alpha} + j \cdot i_{\beta} \quad (3.57)$$

If the addition of the 3-phs does not equate to zero an additional component the so called zero component has to be used as well.

$$i_0 = \frac{i_a + i_b + i_c}{3} \quad (3.58)$$

The truth is the fact that in case of no existing zero component the real part is identical to the phase a of the 3-ph system.

$$i_{\alpha} = \text{Re}\{\underline{i}\} = \frac{2}{3}(i_a - \frac{i_b + i_c}{2}) = \frac{2}{3}(i_a - \frac{i_a + i_c - i_c}{2}) \Big|_{i_a + i_b + i_c = 0} = i_a \quad (3.59)$$

In the following matrices the complete transformation (including zero component) is shown.

$$\begin{pmatrix} i_{\alpha} \\ i_{\beta} \\ i_0 \end{pmatrix} = \frac{1}{3} \begin{pmatrix} 2 & -1 & -1 \\ 0 & \sqrt{3} & -\sqrt{3} \\ 1 & 1 & 1 \end{pmatrix} \cdot \begin{pmatrix} i_a \\ i_b \\ i_c \end{pmatrix} \quad (3.60)$$

$$\begin{pmatrix} i_a \\ i_b \\ i_c \end{pmatrix} = \frac{1}{3} \begin{pmatrix} 2 & 0 & 2 \\ -1 & \sqrt{3} & 2 \\ -1 & -\sqrt{3} & 2 \end{pmatrix} \cdot \begin{pmatrix} i_{\alpha} \\ i_{\beta} \\ i_0 \end{pmatrix} \quad (3.61)$$

in which equation (3.60) is used for the transformation of the 3-ph system into  $\alpha$ ,  $\beta$ -components the equation (3.61) is used for the clark transformation. The equivalent diagrams for the machine representation is seen in Figure 3.6 and Figure 3.7.

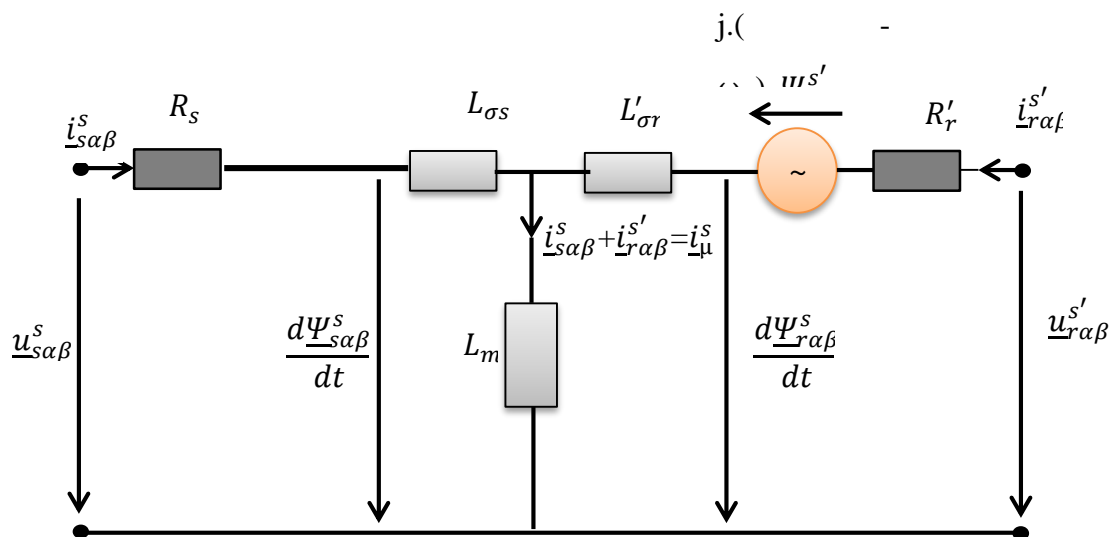


Figure 3.6. Equivalent circuit diagram for  $\alpha$  and  $\beta$  – components

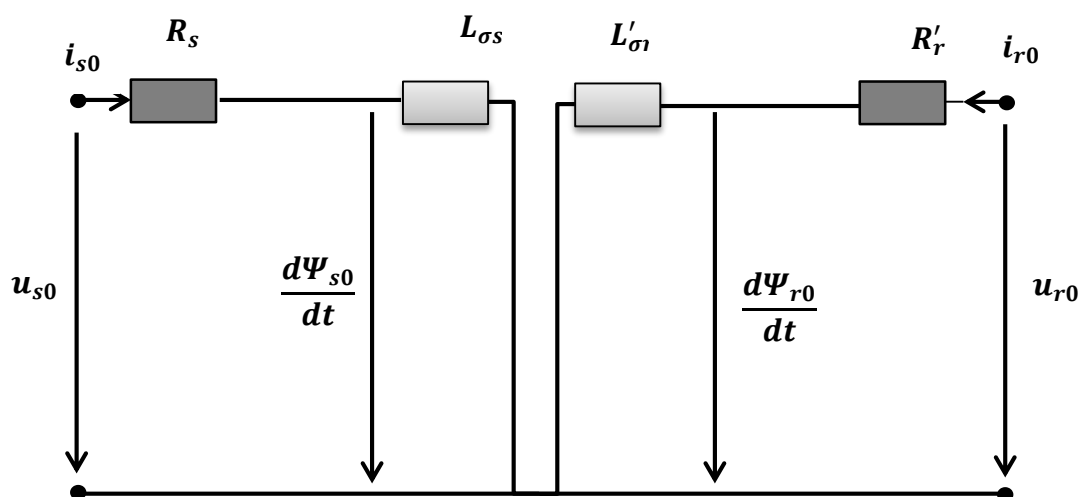


Figure 3.7. Equivalent circuit diagram for the zero component

The equations for description of the machine are concluded in equation (3.62) to (3.72). The zero components are assumed to be only linked via the leakage field.



$$\underline{u}_s^s = R_s \cdot \underline{i}_s^s + \frac{d\Psi_s^s}{dt} \quad (3.62)$$

$$u_{s0} = R_s \cdot i_{s0} + \frac{d\Psi_{s0}}{dt} \quad (3.63)$$

$$\underline{u}_r^{s'} = R_r' \cdot \underline{i}_r^{s'} + \frac{d\Psi_r^{s'}}{dt} - j \cdot \dot{p} \cdot \Psi_r^{s'} \quad (3.64)$$

$$u_{r0} = R_r \cdot i_{r0} + \frac{d\Psi_{r0}}{dt} \quad (3.65)$$

$$\underline{\Psi}_s = (L_{\sigma s} + L_m) \cdot \underline{i}_s + L_m \cdot \underline{i}_r' \cdot e^{jp} \quad (3.66)$$

$$\Psi_{s0} = L_{\sigma s} \cdot i_{s0} \quad (3.67)$$

$$\underline{\Psi}_r' = (L_{\sigma r} + L_m) \cdot \underline{i}_r' + L_m \cdot \underline{i}_s \cdot e^{-jp} \quad (3.68)$$

$$\Psi_{r0} = L_{\sigma r} \cdot i_{r0} \quad (3.69)$$

$$T_e = \frac{3}{2} \cdot p_p \cdot \text{Im} \{ \underline{\Psi}_s^* \cdot \underline{i}_s^s \} = \frac{3}{2} \cdot p_p \cdot (\Psi_{s\alpha} i_{s\beta} - \Psi_{s\beta} i_{s\alpha}) \quad (3.70)$$

$$T_e - T_m = J \frac{d\omega_r}{dt} + D\omega_r \quad (3.71)$$

$$\ddot{p} = \frac{d\omega_e}{dt} = \frac{d\omega_r \cdot p_p}{dt} = \frac{p_p}{J} \cdot (T_e - T_m - D\omega_r) \quad (3.72)$$

The power is calculated as shown in equation (3.73) and equation (3.75).

$$P_s = \frac{3}{2} \cdot \text{Re} \{ \underline{u}_s \cdot \underline{i}_s^* \} = \frac{3}{2} \cdot \text{Re} \{ (u_{s\alpha} + j u_{s\beta}) \cdot (i_{s\alpha} - j i_{s\beta}) \} = \frac{3}{2} (u_{s\alpha} i_{s\alpha} + u_{s\beta} i_{s\beta}) \quad (3.73)$$

$$P_0 = 3 \cdot u_0 \cdot i_0 \quad (3.74)$$

$$Q_s = \frac{3}{2} \cdot \text{Im} \{ \underline{u}_s \cdot \underline{i}_s^* \} = \frac{3}{2} \cdot \text{Im} \{ (u_{s\alpha} + j u_{s\beta}) \cdot (i_{s\alpha} - j i_{s\beta}) \} = \frac{3}{2} (u_{s\beta} i_{s\alpha} - u_{s\alpha} i_{s\beta}) \quad (3.75)$$

### 3.1.3. The Park Transformation (d, q, 0 equivalent frame)

In the same way as in the  $\alpha$ ,  $\beta$  - components, shown in the sub-chapter 3.1.2, the d, q - components are a separation of the complex space vector in real and imaginary part.

$$\underline{i} = i_d + j \cdot i_q = \frac{2}{3} (i_a + \underline{a} i_b + \underline{a}^2 i_c) \cdot e^{-j\gamma} \quad (3.76)$$

The opposite to referring the space vector to a stationary reference frame as done in the Clark's components, in the so called Park's transformation the complex space vector is expressed in the rotating orthogonal system linked with the rotor of the machine.

The method is however used to express the complex space vector in any rotating reference frame. The advantage by doing so rotating space vectors change to appear stationary in a rotating reference frame, which means alternating traces of the space vector are steady and the changes in absolute value of the vector is depicted clearly. This is beneficially used for fast control of electrical machines.

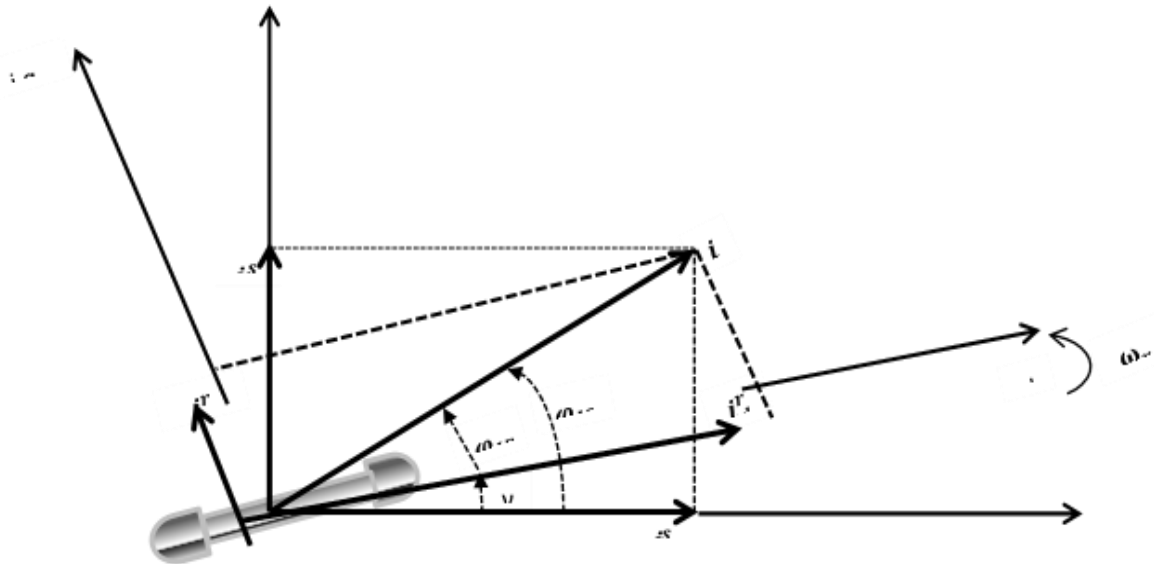


Figure 3.8. Park's – transformation

In Figure 3.8 the Park's transformation in relation to the  $\alpha$ ,  $\beta$  - components are shown. The transformation between these components and an arbitrary rotating frame is:

$$i_d + j \cdot i_q = (i_\alpha + j \cdot i_\beta) \cdot e^{-j \cdot \varphi} \quad (3.77)$$

and for return to the  $\alpha$ ,  $\beta$  – components

$$i_\alpha + j \cdot i_\beta = (i_d + j \cdot i_q) \cdot e^{j \cdot \varphi} \quad (3.78)$$

The zero – component is equal for both transformations, hence it formed during expressing the 3-phase machine into a 2-ph equivalent machine.

$$i_{0dq} = i_{0\alpha\beta} \quad (3.79)$$

Expressing the transformation in Matrices, the following Matrices for forward and back transformation can be written.

$$\begin{pmatrix} i_\alpha \\ i_\beta \\ i_{0\alpha\beta} \end{pmatrix} = \begin{pmatrix} \cos(\varphi) & -\sin(\varphi) & 0 \\ \sin(\varphi) & \cos(\varphi) & 0 \\ 0 & 0 & 1 \end{pmatrix} \cdot \begin{pmatrix} i_d \\ i_q \\ i_{0dq} \end{pmatrix} \quad (3.80)$$

$$\begin{pmatrix} i_d \\ i_q \\ i_{0dq} \end{pmatrix} = \begin{pmatrix} \cos(\varphi) & \sin(\varphi) & 0 \\ -\sin(\varphi) & \cos(\varphi) & 0 \\ 0 & 0 & 1 \end{pmatrix} \cdot \begin{pmatrix} i_\alpha \\ i_\beta \\ i_{0\alpha\beta} \end{pmatrix} \quad (3.81)$$

Transformation from a 3-ph system direct to an arbitrary rotating system can be done in the following way:

$$\begin{pmatrix} i_d \\ i_q \\ i_0 \end{pmatrix} = \frac{2}{3} \cdot \begin{pmatrix} \cos(\gamma) & \cos(\gamma - \frac{2}{3}\pi) & \cos(\gamma + \frac{2}{3}\pi) \\ \sin(\gamma) & \sin(\gamma - \frac{2}{3}\pi) & \sin(\gamma + \frac{2}{3}\pi) \\ \frac{1}{2} & \frac{1}{2} & \frac{1}{2} \end{pmatrix} \cdot \begin{pmatrix} i_a \\ i_b \\ i_c \end{pmatrix} \quad (3.82)$$

$$\begin{pmatrix} i_a \\ i_b \\ i_c \end{pmatrix} = \begin{pmatrix} \cos(\gamma) & \sin(\gamma) & 1 \\ \cos(\gamma - \frac{2}{3}\pi) & \sin(\gamma - \frac{2}{3}\pi) & 1 \\ \cos(\gamma + \frac{2}{3}\pi) & \sin(\gamma + \frac{2}{3}\pi) & 1 \end{pmatrix} \cdot \begin{pmatrix} i_d \\ i_q \\ i_0 \end{pmatrix} \quad (3.83)$$

The equivalent diagram for a machine in Park's transformation is shown in Figure 3.6. The equivalent for the zero components is equal as shown in Figure 3.7 in sub-chapter 3.1.2. Since all machine equations are nearly similar to the description of the machine in Clark components it is not necessary to show them again. Just the torque and power equations are shown in equation (3.84), (3.85) and (3.86).

$$T_e = \frac{3}{2} \cdot p_p \cdot \text{Im}\{\underline{\Psi}_s^* \cdot \underline{i}_s\} = \frac{3}{2} \cdot p_p \cdot (i_{qs} \Psi_{ds} - \Psi_{qs} i_{ds}) \quad ; \quad \Psi_{qs} i_{ds} \approx 0 \quad (3.84)$$

$$P_s = \frac{3}{2} \cdot \text{Re}\{\underline{u}_s \cdot \underline{i}_s^*\} = \frac{3}{2} (u_d i_d + u_q i_q) \quad (3.85)$$

$$Q_s = \frac{3}{2} \cdot \text{Im}\{\underline{u}_s \cdot \underline{i}_s^*\} = \frac{3}{2} (u_d i_d - u_q i_q) \quad (3.86)$$

The equivalent diagram for the d, q – components is shown in Figure 3.9. The equivalent diagram for the zero component is identical to the diagram shown in Figure 3.7.

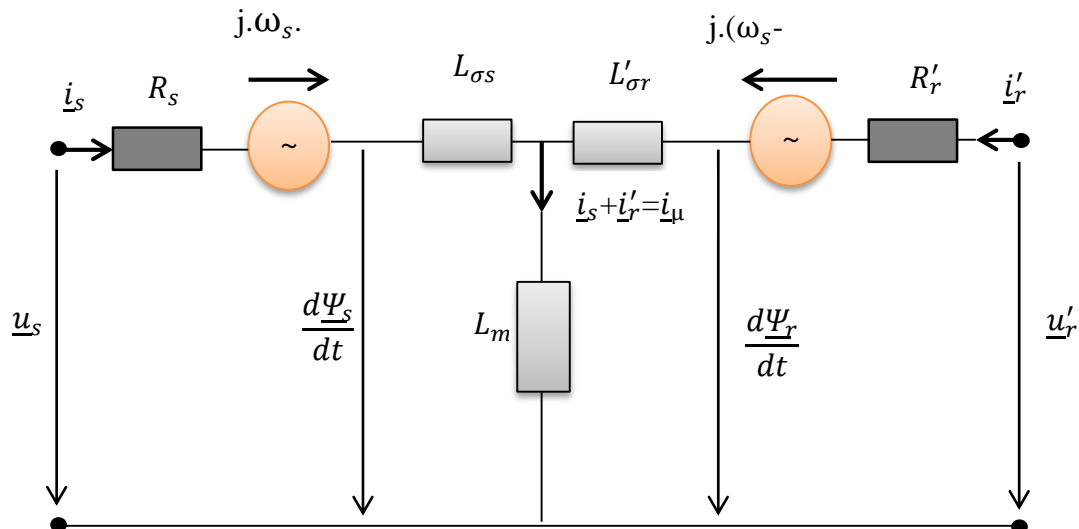


Figure 3.9. Equivalent circuit diagram for d, q – components

### 3.1.4. Saturation effects

The assumption in the ideal machine is that the leakage reactance and magnetizing reactance are independent of the current and the voltage. In a real machine the magnetic voltage through the iron is not directly proportional to the current and therefore this assumption is not valid. For taking a closer look at the phenomena, the influence of saturation of the leakage reactances and the magnetizing reactance should be taken into account [51].

#### 3.1.4.1. Saturation of main reactance

The main reactance or magnetizing reactance  $X_m$  is mainly defined through the stator induced electromotive force (EMF/ EMK). The reactance wouldn't be changing, if the characteristic of  $E_s(I_\mu)$  would be a straight line. In reality the curve is bending in the upper part as shown in Figure 3.10.

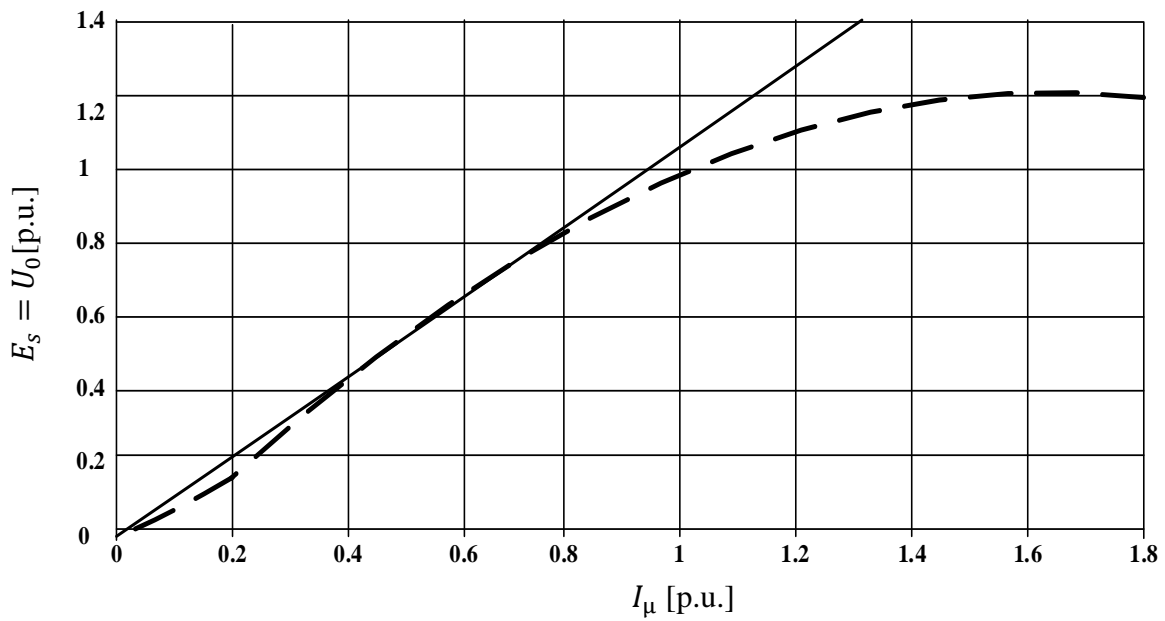


Figure 3.10. Example of a measured no load (magnetizing) curve – dashed line and the theoretical not saturating curve – solid line of an asynchronous generator

By increasing the induced voltage ( $E_s$ ) the magnetizing reactance slightly decreases. The consequence is a faster decrease of the magnetizing current as the decrease of the induced rotor EMF. The effect of main reactance saturation on the stator currents is most noticeable during no load operation. In Figure 3.11 this influence of magnetizing reactance is visualized.

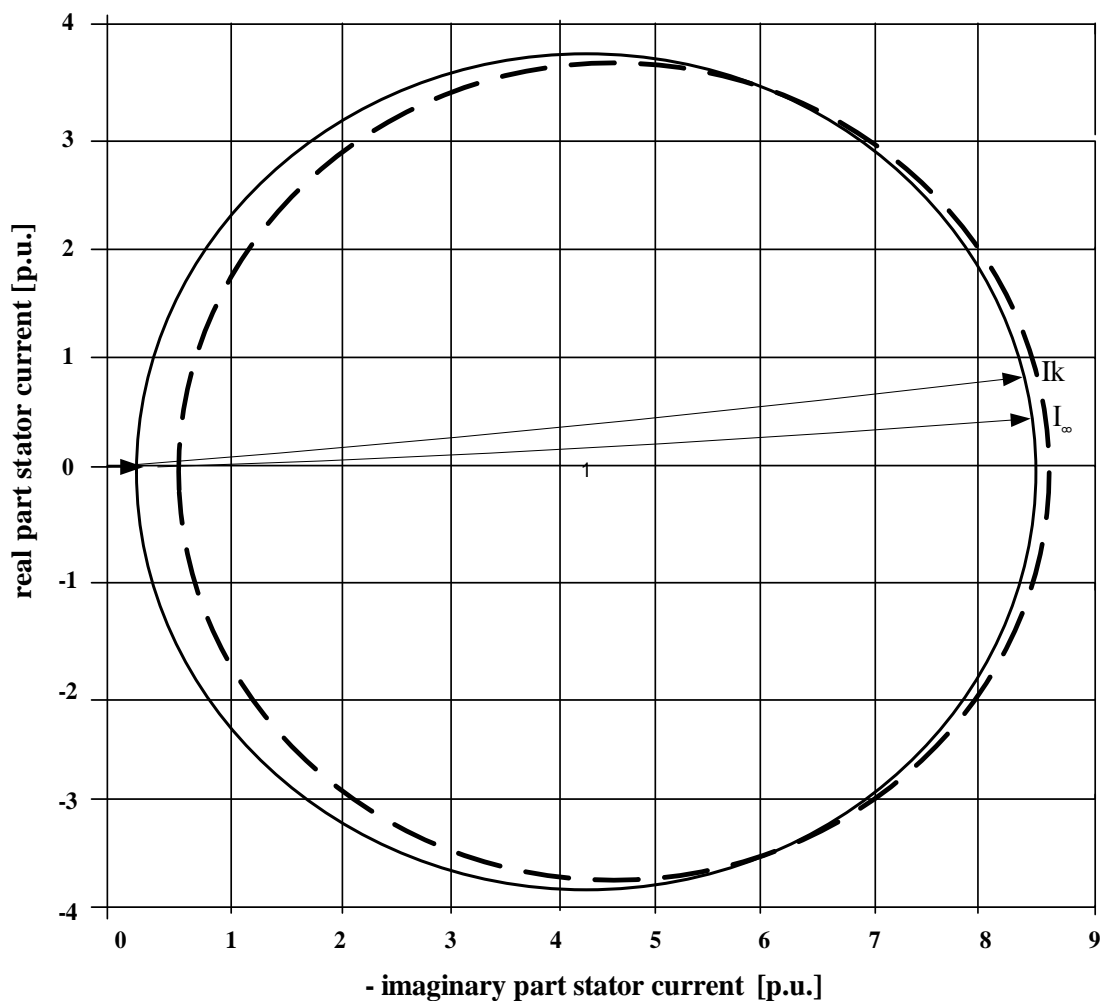


Figure 3.11. Current circle diagram showing the effect of main inductance saturation; rated-solid line, halve  $X_m$  (saturated) – dashed line,  $I_k$ -short circuit current at slip=1 and  $I_\infty$ - current at infinite slip

To find the dependency it is therefore best to measure the no load curve. There are two possibilities of measuring the curve. If a slip-ring machine is used it is possible to measure directly the rotor current and stator currents. This simplifies the machines complexity, the machine is at stand still and the rotor windings are open and voltage and currents on both terminals can be measured (direct measurement of magnetizing curve). However more common is the measurement at nearly synchronous speed (used for squirrel cage motors), the so called no load curve.

In no load operation at synchronous speed or at standstill the rotor current can be assumed to zero. Therefore it can be assumed that the current of the stator windings and

the magnetizing current are equal. The voltage drop is now only over the stator resistance, stator leakage reactance, iron loss resistance and the magnetizing reactance. The magnetizing inductance dependent at the current can be achieved with the following equations. It is assumed that the resistances and the stator leakage inductance are not changing with the current. The so deduced function of the main inductance from the magnetizing current is a common way to include saturation effects into a machine model.

$$X_m(I_\mu) = L_m(I_\mu) \cdot \omega_0 = \sqrt{\frac{U_0^2}{3 \cdot I_\mu^2} - (R_s + R_m)^2} \cdot L_{\sigma s} \cdot \omega_0 \quad (3.87)$$

In Figure 3.12 the main inductance dependency from the magnetizing current, which was achieved through the no load curve measurements and then calculated with equation (3.88) is shown. Very often rated inductance is assumed at low currents. In reality there is not enough flux in the machine because of the low voltage and the inductance is decreasing again towards low currents.

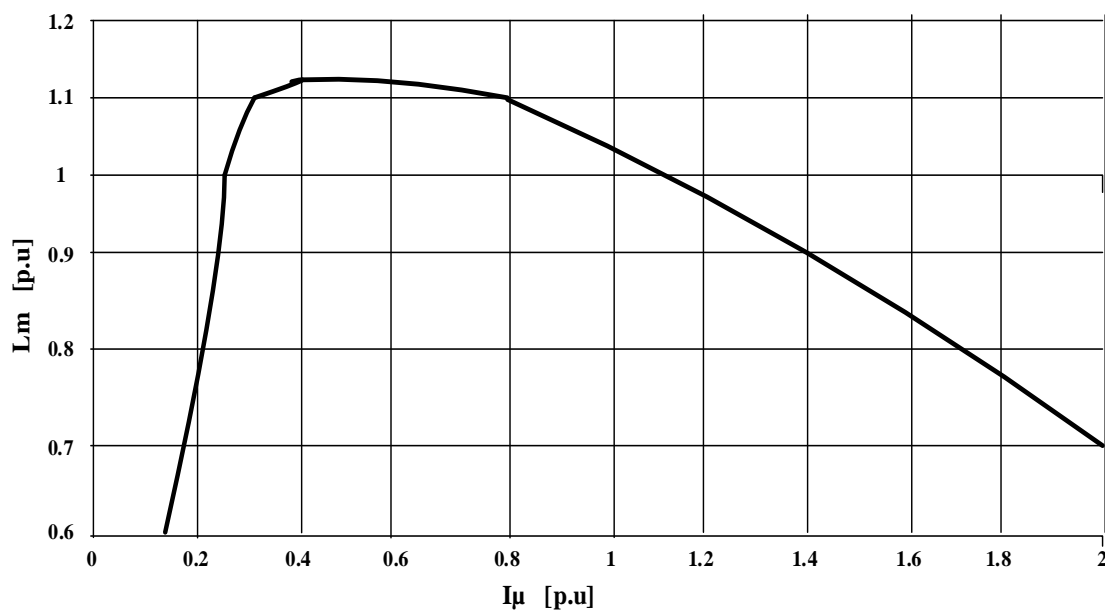


Figure 3.12. Main inductance dependency of the magnetizing current  $L_m(I_\mu) \cdot \omega_0$

### 3.1.4.2. Saturation of leakage reactance

Deep research in fault situations like short circuit the operation with high currents is far more important than no load operation. Therefore a larger importance is the consideration of the dependency of leakage reactances  $X_{\sigma S}$  and  $X'_{\sigma r}$  on the current. With increasing current the leakage reactances will decrease as well as the magnetizing reactance. In Figure 3.11 and Figure 3.12 the current circle diagram is calculated for a machine with half of the rated magnetizing reactance or leakage reactances and compared to a machine with rated values. While in rated operation range, which is around 1p.u., the influence of the magnetizing inductance is dominating, the changes during fault operations with high currents are clearly dominated by the leakage reactances. The current considering a change of leakage reactances is essentially larger than without this consideration.



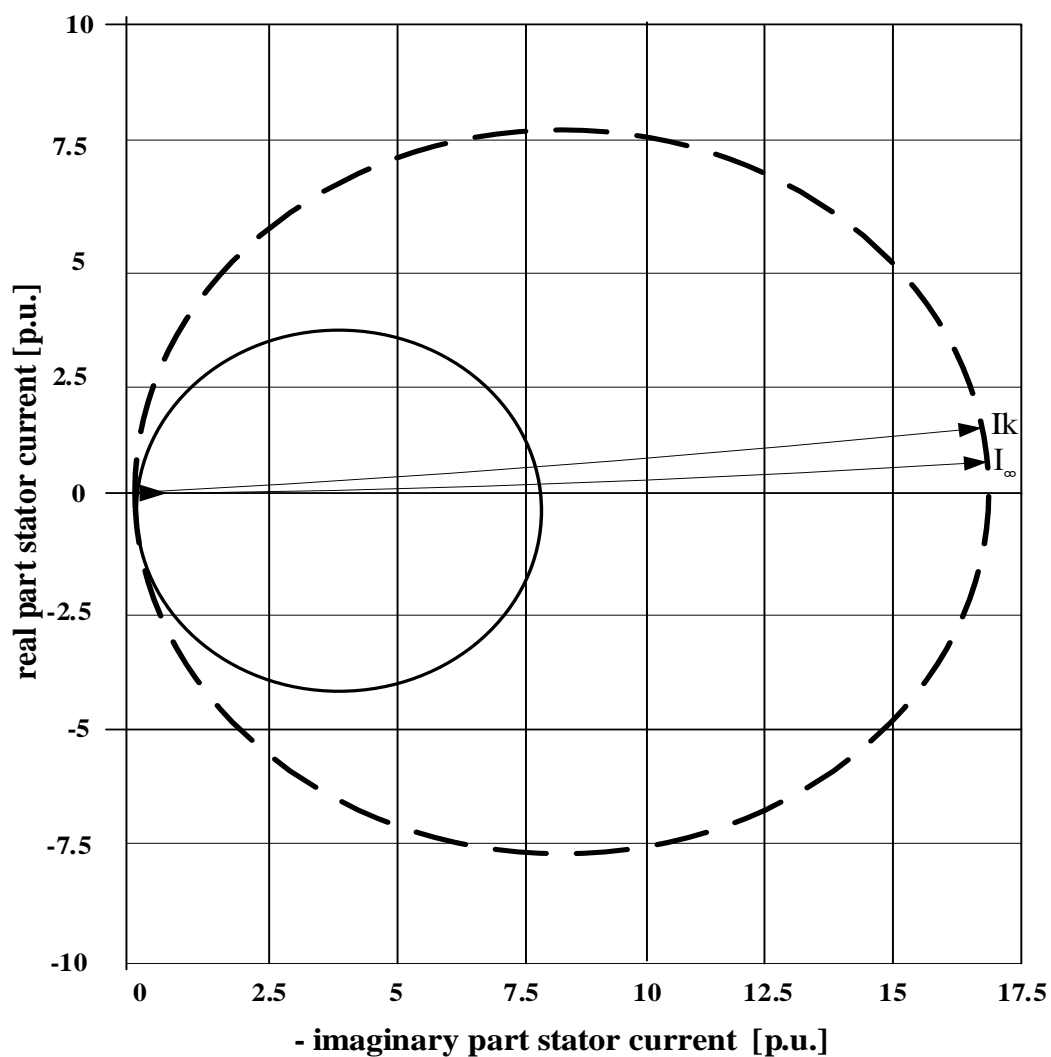


Figure 3.13. Current circle diagram showing the effect of leakage reactance saturation; rated value-solid line, halve  $X_{\sigma S}$  and  $X'_{\sigma r}$  (saturated) – dashed line

The leakage reactances will be achieved from the blocked rotor test. In this test with short circuit rotor coils the magnetizing current is very small and has been neglected. With measurement of the voltage and current and the power factor  $\cos \varphi$  the total leakage reactance will be calculated as:

$$X_{\sigma} = \frac{U \cdot \sin \varphi_k}{I} \quad (3.88)$$

To separate the leakage reactance  $X_\sigma$  into the stator leakage reactance  $X_{\sigma S}$  and the rotor leakage reactance  $X'_{\sigma r}$  the no load measurement will be used again. In the no load measurement the reactances  $X_m + X_{\sigma S}$  are measured and therewith the part of the rotor leakage reactance will be estimated. Another factor helping the more exact separation between the stator and rotor leakage reactances is the measurement of the leakage factor  $\sigma$ .

$$\sigma = 1 - \frac{X_m^2}{X_S \cdot X'_r} \quad (3.89)$$

Where  $X_S = X_{mS} + X_{\sigma S}$  and  $X'_r = X_{mr} + X'_{\sigma r}$

However, the methods are detailed, discussed in many machine books[51] and therefore will not further deepened in this thesis.

### 3.1.5. Windage losses and friction losses

Windage and frictional losses of a machine can be divided into two parts, which are having a different proportion to the rotational speed  $\omega$ .

-Ventilation losses are proportional to  $\omega^3$ . This includes all ventilation losses (end winding ventilation loss, rotor cooling ducts ventilation loss etc.)

-Frictional losses are proportional to less than  $\omega^3$  ( $P \sim \omega^{7/3}$ ). These losses include frictional losses in bearings.

The correct proportional ratio is quite hard to estimate, since it may fluctuate. e.g. temperature of the grease has some influence into frictional losses. This means that in different service conditions the proportional ratio may be different. Combining the above components total windage and frictional losses are achieved. Total losses are approximated to a proportion between  $\omega^{2.5}$  ...  $\omega^{2.7}$ . Unfortunately it is very hard to include such non integer potential dependency into the model. Since the difference between the different potential dependencies is very small in the operating area it is a good choice to use a dependency in the second order. A second order dependency due

to power losses leads to a simple dependency of the torque, which can be found in various books.

The damping factor from the no load losses is:

$$D = \frac{P_{0fw}}{\omega_0^2} \quad (3.90)$$

The windage and friction losses depending on the speed, will be calculated using the constant damping factor achieved above.

$$P_{fw}(\omega) = D\omega^2 \quad (3.91)$$

Although the damping factor is only an equivalent, there are a range of possible methods considering the leakage and windage losses. In Figure 3.13 and Figure 3.14 the influence of the different exponential dependencies is shown. The damping factor  $D$  is determined by measuring the rotational losses at synchronous speed and dividing it by the exponents chosen.

$$D = \frac{P_{0fw}}{\omega^{2 \dots 2.5 \dots 2.7 \dots 3}} \quad (3.92)$$

The windage and friction losses in the model would accordingly be calculated in the following way.

$$P_{fw}(\omega) = D \cdot \omega^{2 \dots 2.5 \dots 2.7 \dots 3} \quad (3.93)$$

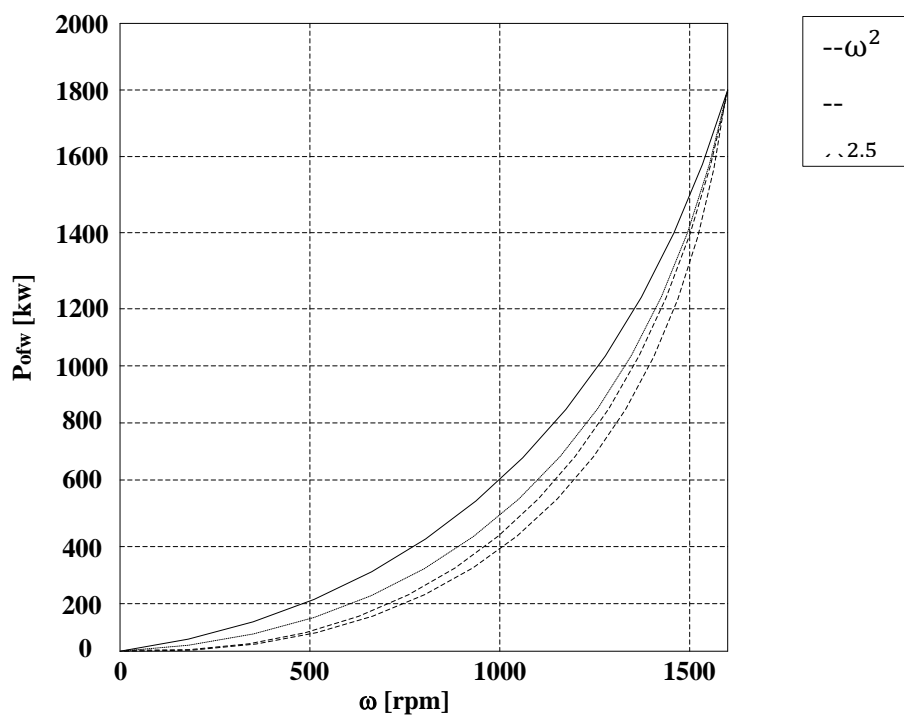


Figure 3.14. Different exponential dependencies of D between 0...1500 rpm

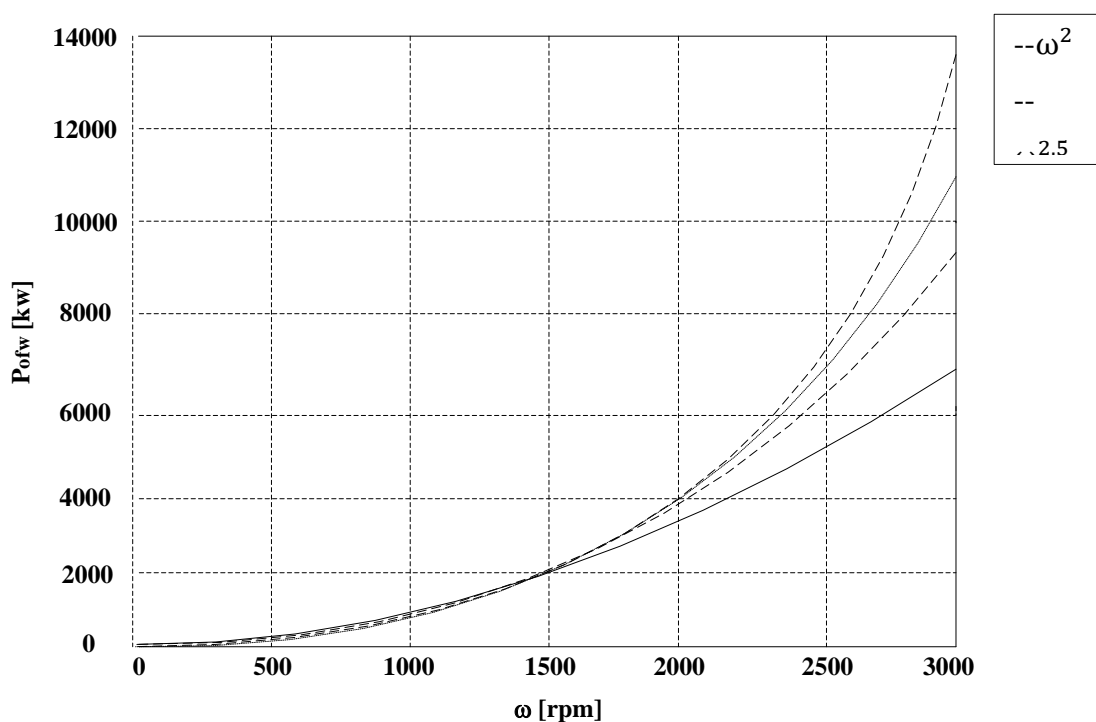


Figure 3.15. Different exponential dependencies of D at over speed

In the operation range from approx. 500 rpm up to 1700 rpm the difference in the calculation of the potential dependencies is very small. If used for the purpose of modeling at over speed situations, a change from the chosen dependency of second order

might be re-considered, and instead the use of a model with a dependency of third order is more appropriate.

### 3.1.6. The 3-ph – model in matlab/ simulink

The machine model is based on the equations (6), (7), (27), (39), (59) and implemented in Matlab/ Simulink as shown in Figure 3.16

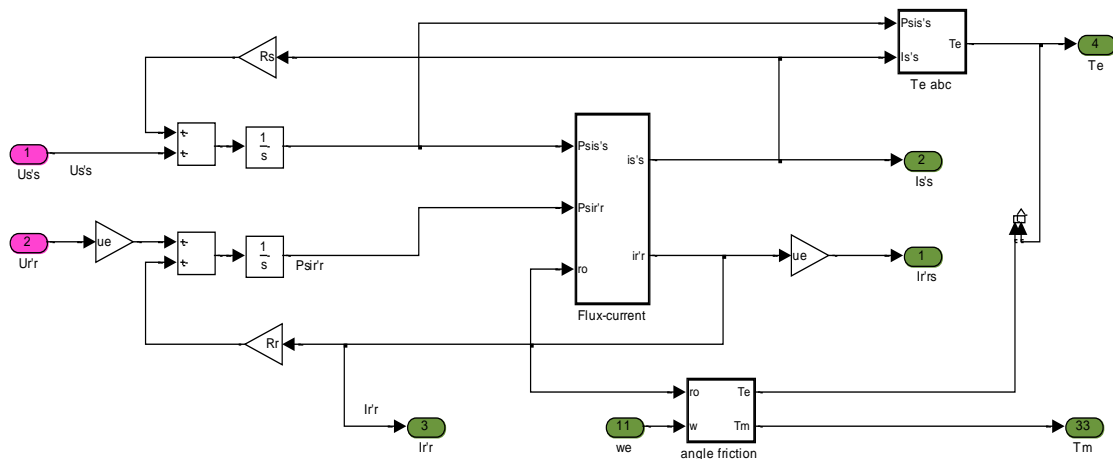


Figure 3.16. The unmasked Machine model in Matlab/ Simulink

The inputs of the machine model are the 3-ph voltages of stator and rotor and the mechanical load torque  $T_m$  of the generator axis/shaft. Outputs are the 3-ph stator and rotor currents, the speed of the machine expressed as electrical angular speed of the rotor or mechanical speed and the electric magnetic air gap torque  $T_e$  of the machine. The power of the machine is calculated from the voltages and currents of stator and rotor as described in the sub-chapter above. The model is independent of the usage as generator or motor. The mechanical load torque is defined negative for generator operation. The power is negative for power production and positive for power consumption. For rotor power calculation as already for the stator deduced equations (3.35), (3.33) are equivalently used.

$$P_r = u_{ar}i_{ar} + u_{br}i_{br} + u_{cr}i_{cr} \quad (3.94)$$

$$Q_r = \frac{1}{\sqrt{3}} \cdot (i_{ar} \cdot (u_{br} - u_{cr}) + i_{br} \cdot (u_{ar} - u_{cr}) + i_{cr} \cdot (u_{br} - u_{ar})) \quad (3.95)$$

The block called “angle – friction” expresses the equations of motion. With this equation the generator speed and the necessary rotor displacement angle  $\rho$  is achieved.

In addition, the friction losses are implemented with using the damping factor  $D$  as shown in Figure 3.14.

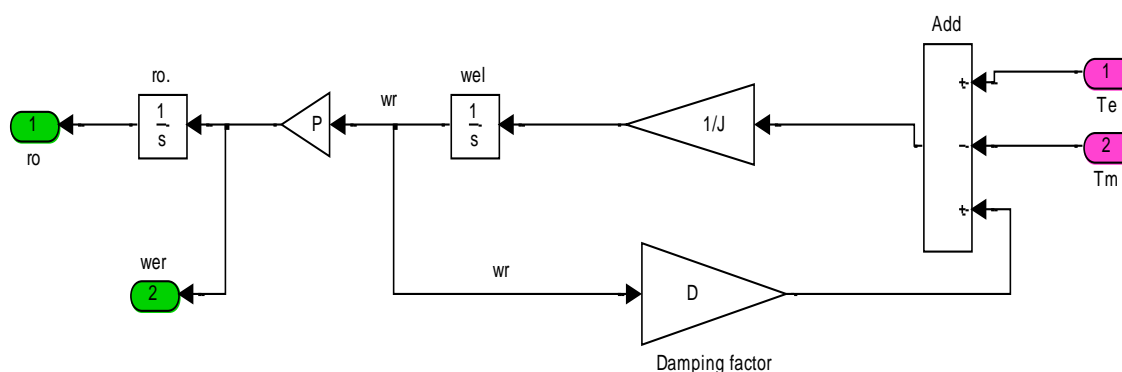


Figure 3.17. Block angle – friction

The machine block called “flux – current” is expressing the flux equations to calculate the currents with help of the inductance matrix. The saturation effect is taken into account as variable inductances in the inductance matrix.

$$L = \begin{pmatrix} L_{\sigma s} + L_{msA} & -0.5L_{mA} & -0.5L_{mA} & L_{msrAa} \cdot f_1 & L_{msrAb} \cdot f_2 & L_{msrAc} \cdot f_3 \\ -0.5L_{mB} & L_{\sigma s} + L_{msB} & -0.5L_{mB} & L_{msrBa} \cdot f_3 & L_{msrBb} \cdot f_1 & L_{msrBc} \cdot f_2 \\ -0.5L_{mC} & -0.5L_{mC} & L_{\sigma s} + L_{msC} & L_{msrCa} \cdot f_2 & L_{msrCb} \cdot f_3 & L_{msrCc} \cdot f_1 \\ L_{msraA} \cdot f_1 & L_{msraB} \cdot f_3 & L_{msraC} \cdot f_2 & L'_{\sigma r} + L_{mra} & -0.5L_{mra} & -0.5L_{mra} \\ L_{msrba} \cdot f_2 & L_{msrbB} \cdot f_1 & L_{msrbc} \cdot f_3 & -0.5L_{mrb} & L'_{\sigma r} + L_{mrb} & -0.5L_{mrb} \\ L_{msrcA} \cdot f_3 & L_{msrcB} \cdot f_2 & L_{msrcC} \cdot f_1 & -0.5L_{mrc} & -0.5L_{mrc} & L'_{\sigma r} + L_{mrc} \end{pmatrix} \quad (3.96)$$

In sub-chapter 3.1.4 the influence of the saturation on the machine is described. For the variable main inductance the magnetizing current is determined in the following way.

$$\vec{i}_{\mu} = \vec{i}_s + \vec{i}_r \quad (3.97)$$

Using (3.97) in the stator flux equation (3.98):

$$\vec{\Psi}_s^s = (L_{\sigma s} + L_m) \cdot \vec{i}_s^s + L_m \cdot \vec{i}_r^s \quad (3.98)$$

$$\vec{\Psi}_s^s = (L_{\sigma s} + L_m) \cdot \vec{i}_s^s + L_m \cdot (\vec{i}_\mu - \vec{i}_s^s) \quad (3.99)$$

the magnetizing current can be calculated with the stator flux and stator current to:

$$\vec{i}_\mu = \frac{\vec{\Psi}_s^s - L_{\sigma s} \cdot \vec{i}_s^s}{L_m} \quad (3.100)$$

Because the magnetizing curve is based on rms values, the rms value of the magnetizing current is calculated as well. This magnetizing current is used with magnetizing curve to achieve the  $L_m(I_\mu)$ . To secure a stable functioning of the model the current and therewith the main inductance are limited to the known values. Figure 3.18 show the implementation in Matlab/ Simulink.

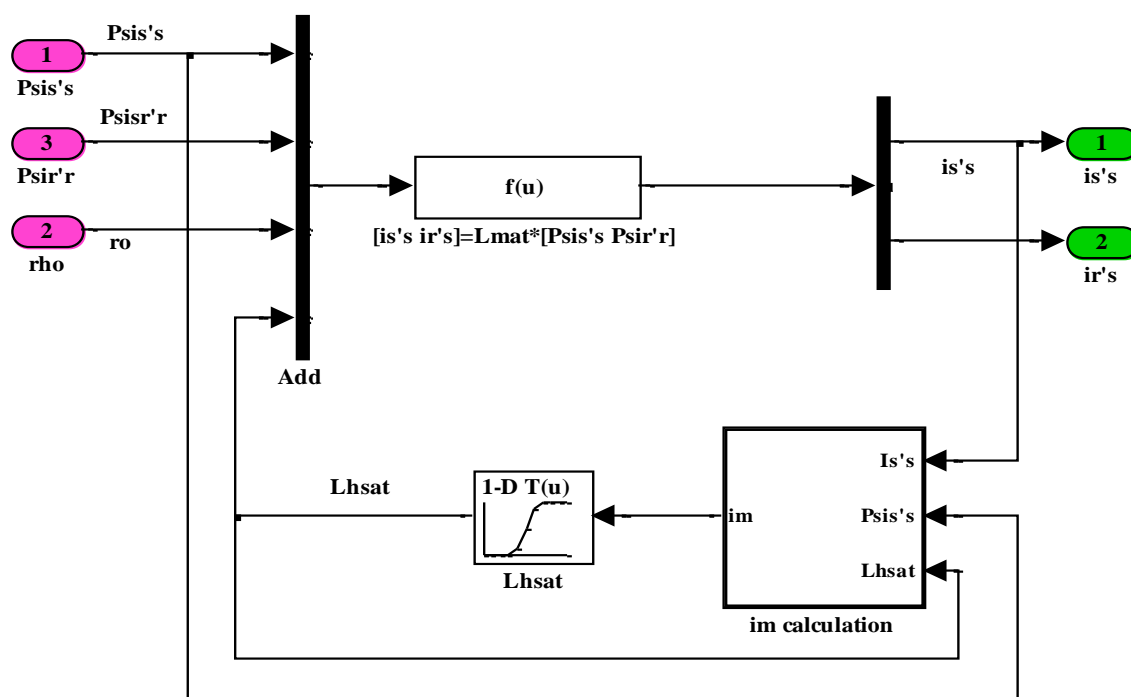


Figure 3.18. Block flux – current used in the machine model

### 3.1.6.1. Steady state validation of the different detailed ABC/abc models

In this sub-chapter a comparison between the machine models including different features are made. At first three different models during rated conditions are chosen. One

model shows the ideal machine, without friction losses or saturation effects of the reactances; the second model is a model considering friction losses and the third model is a model including friction losses and saturation of main magnetizing reactance.

The input parameters for the 3-ph model are deduced from the 1-ph equivalent supplied by the machine manufacturer, which are exemplary data of a 1.52 MW machine. During the simulation the rotor of the asynchronous generator is short circuit, which is modeled with setting the input rotor voltages to zero. The input stator voltages are rated. Therewith a start of the machine, 3 loads change and a 3-ph short circuit are simulated. The three different operation points during the load changes are then compared by the manufacturer supplied measured operation points of the machine. The machine starts up in motor mode and then settles into generator mode producing electrical power according to the load torque on the axis of the machine. The torque and the active power over the whole simulation period from the model with saturation will be shown in the future works. In Figure 3.19 and Figure 3.20 the stator current for all three models are shown in comparison to the measured rms value taken from manufacturer supplied data. The peaks of the time values should theoretically touch the line of the stator peak value ( $\text{rms} \cdot \sqrt{2}$ ). Figure 3.19 compares the ideal model and the model with implemented damping. The model with damping (friction and windage losses) shows a smaller stator current output with the same load, which is easy to explain. Since the friction losses are depending on the speed and the speed is increasing with the load, this consequently means higher losses and therewith a smaller stator current. At no load operation the friction losses are smaller than at rated load and therewith hard to notice in the simulation.



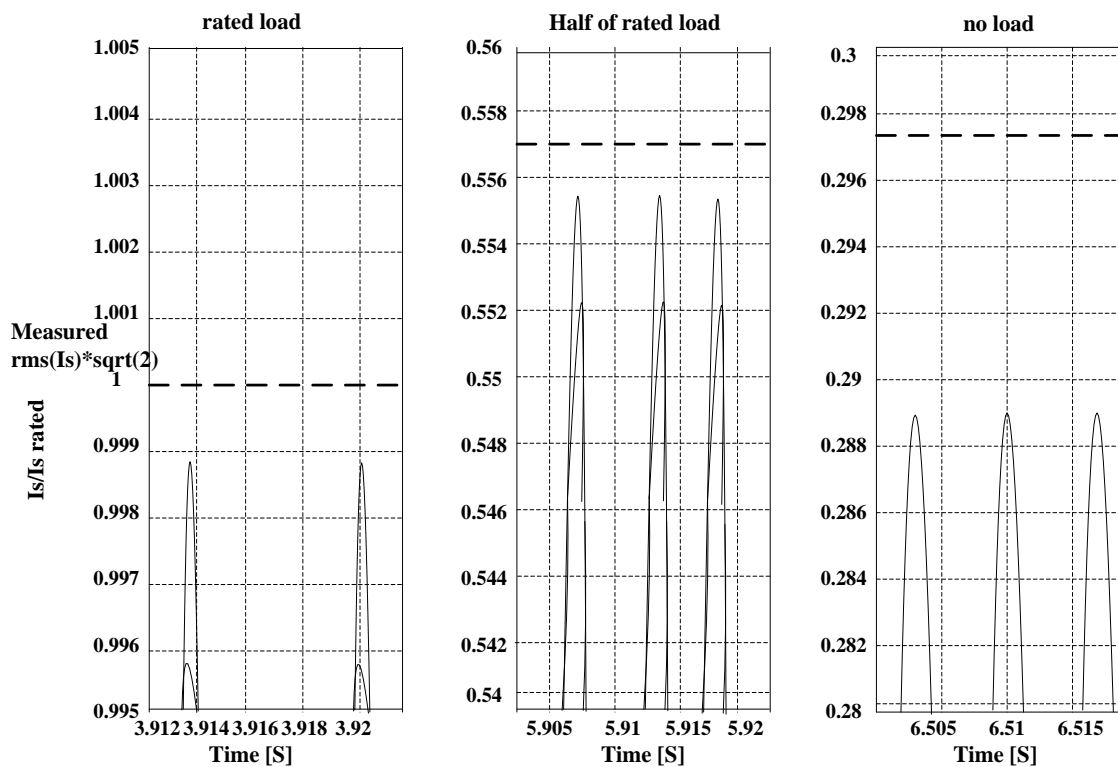


Figure 3.19. Stator current related to rated stator current; solid line – ideal model, dashed line – model with friction

Figure 3.20 compares the model with saturation and damping to the model without saturation though with included damping. During the operation with rated load it is hard to see a difference in the simulated stator currents. As it is explained in sub-chapter 3.1.4, the saturation of main inductance has only an insignificant influence in the area of rated operation up to the maximal operation point. With including leakage saturation a higher current would appear. The influence of main flux saturation is clearly seen in half of rated load operation and no load. As expected due to the theory leads the consideration of main magnetizing saturation to an improvement of the model and the simulated results.

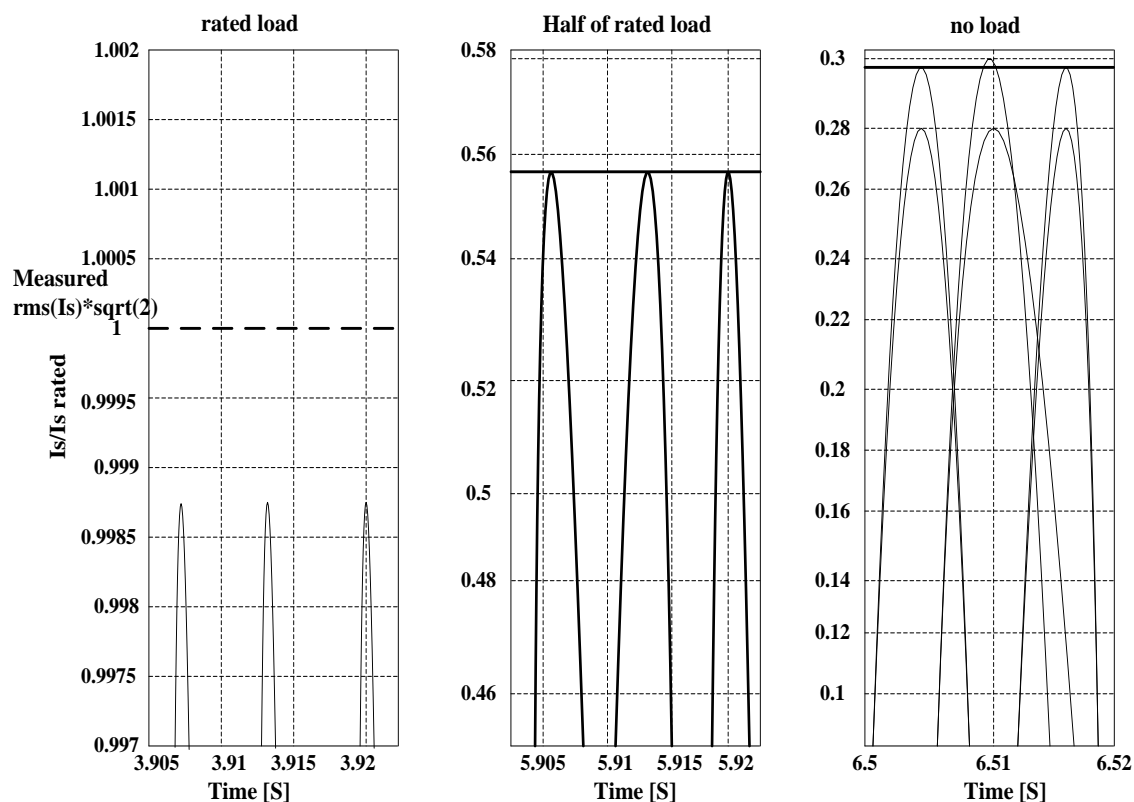


Figure 3.20. Stator current related to rated stator current; solid line – model with saturation, dashed line – model with friction and windage losses

A further criterion for improvement of the model is shown in the evaluation of the power factor or the reactive power. The power is generally more precisely measurable than the current. Here the model with included saturation and damping shows again the improvement compared to the ideal model. Calculation of the power factor also approves this result.

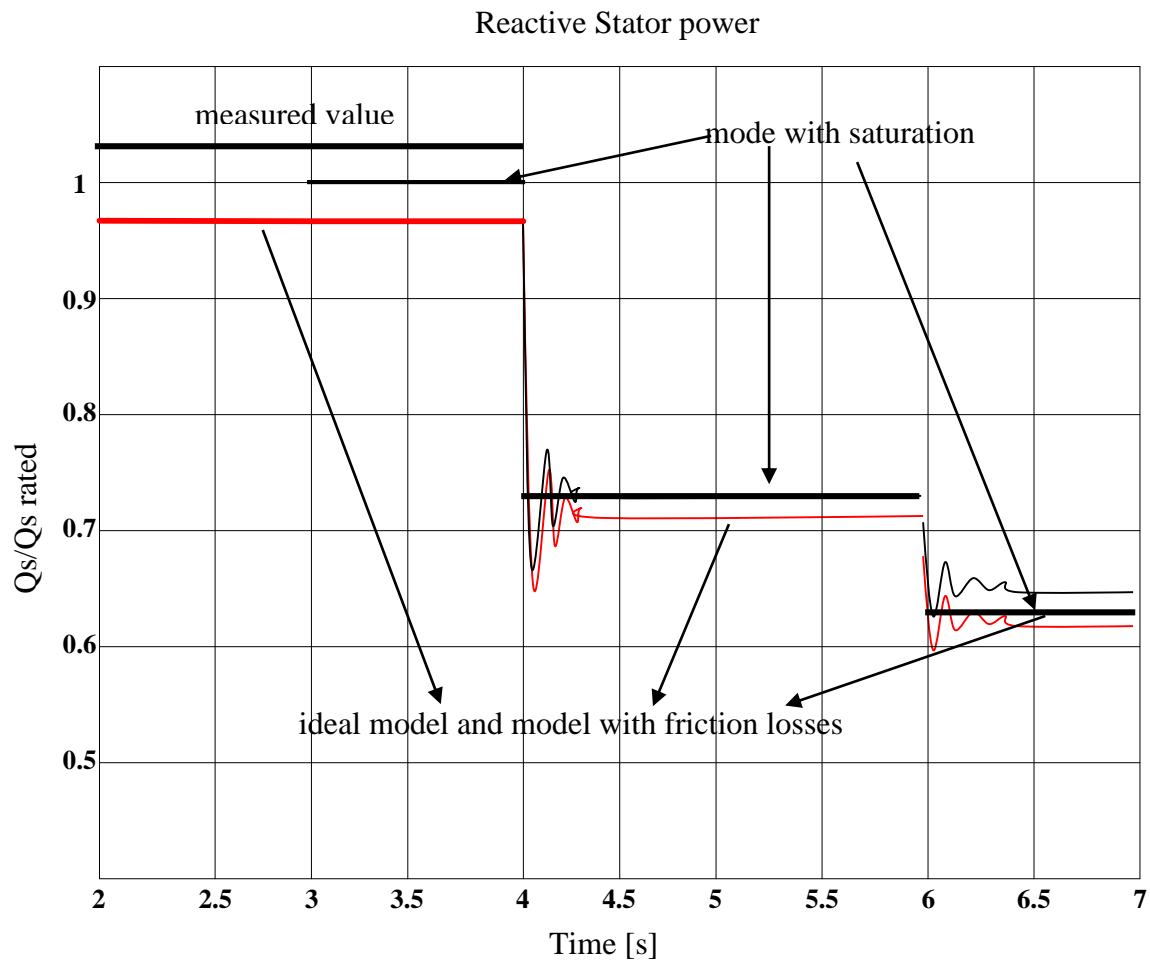


Figure 3.21. Stator reactive power related to rated reactive stator power [p.u.]; model with saturation –upper line, on top of each other –model with friction losses and ideal model –lower line

The simulation results made with the 1.52 MW machines show only small differences between the different machine models. This is due to the fact that the data used as input for the model is given to meet the expected operation area requirements. Saturation has in this area only minimal influence. Machines with stronger saturation effect will show a more significant difference. For using the model for short circuit simulations, the leakage field saturation should be included as well.

### 3.1.6.2. Dynamical validation of the abc/abc model

The aimed use of the developed model is for simulation of dynamical situations including fault situations. The above steady state validations though are not sufficient enough to verify the use for this kind of simulations. Therefore a Direct On Line (DOL) start of a 850/ 800 kW machine has to be initiated in a laboratory test set-up. The DOL

start has been chosen to produce high currents and achieve saturation effects in the machine, since real short circuits for validation of the machine model are not feasible in the researched machine size of 850kW to 3MW. During the test speed, 3-ph stator currents, 3-ph rotor currents and 3-ph stator voltages have been measured. The measured voltage is later on used as input for the machine model. At first the model considering main magnetizing reactance saturation and friction losses will be compared to the measurements. The machine has to be connected star/ star and the rotor windings are short circuited. Due to the impedance in the grid the stator voltage drops with connection the machine direct to the grid. The stator voltage keeps the decreased voltage amplitude until the machine has started up. At the end of the start up the, voltage rise to the rated value again (Figure 3.22). The experienced long starting sequence is rather unusual for asynchronous generator. The machine is designed for generator operation and not for motor operation and therefore develops very little starting torque. The long starting period gives the possibility to use it for validation. There exist an asymmetrical transient and a quasi-stationary part during the DOL start of the machine.

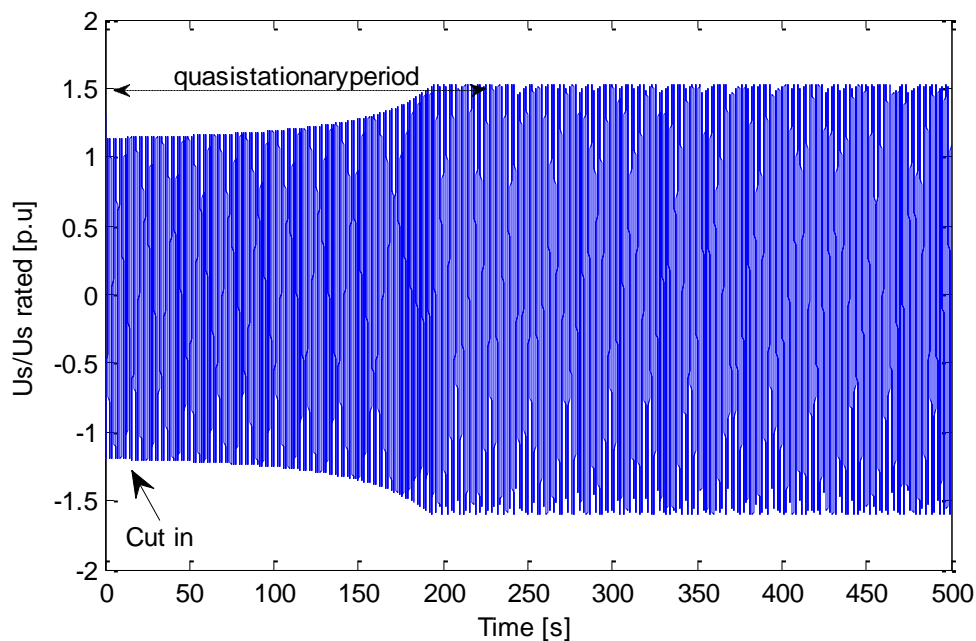


Figure 3.22. Measured Grid voltages/Stator voltages during the DOL of a 850/800 kW generator

In Figure 3.23 the speed during the DOL start is shown. There are only small differences between the simulated speed and the measured speed. In the last phase of the

start, before reaching the final steady speed the model shows a small overshoot. There are many different possibilities causing this overshoot.

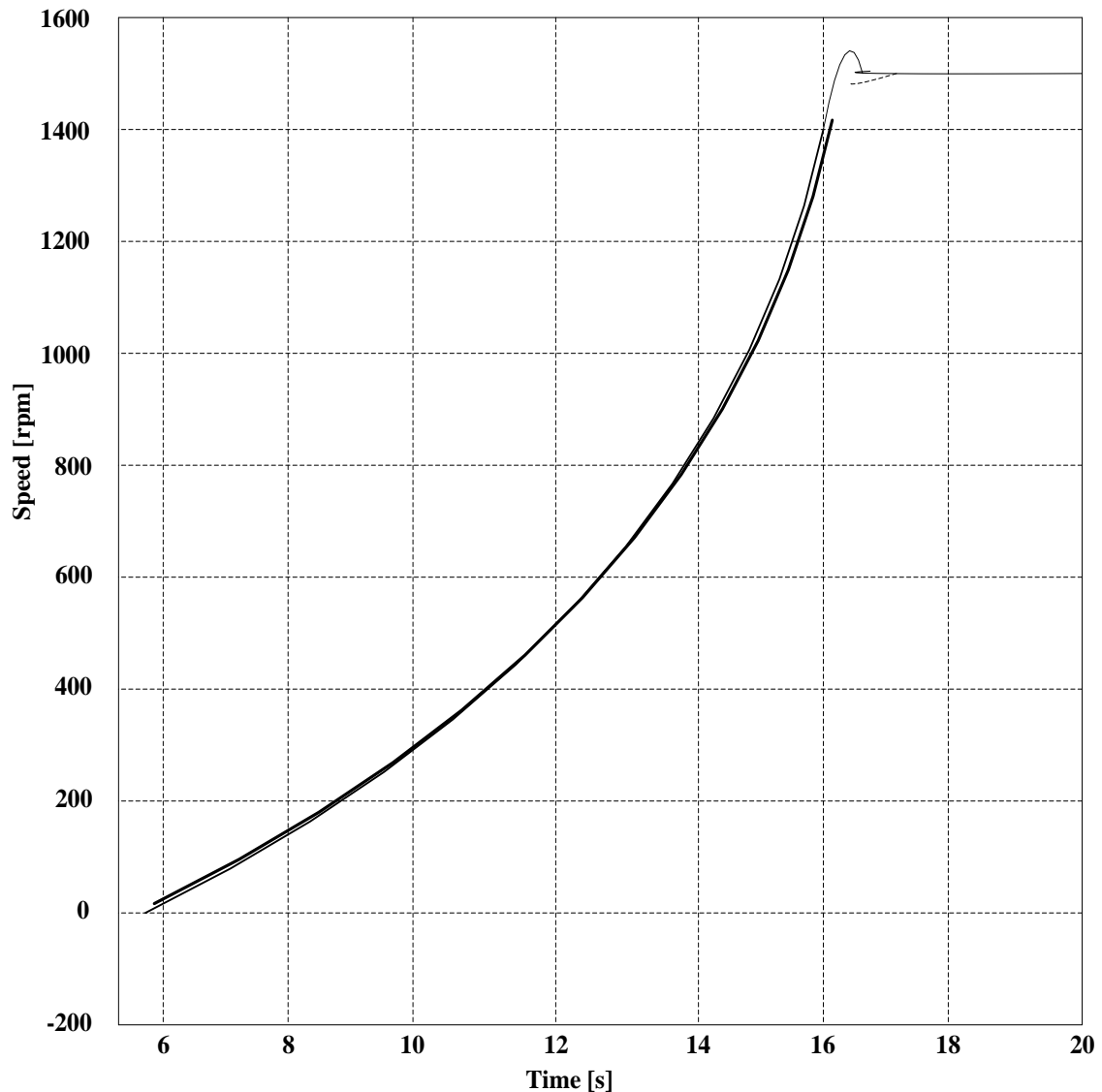


Figure 3.23. Speed during DOL start of a 850/800 kW generator; model with main saturation and friction losses – solid line, measurement speed –dashed line

Figure 3.24 and Figure 3.25 show a window of the simulated and measured stator currents. The measured stator currents are bigger than the simulated values. This is not surprising, since different effects are not included in the model for example the saturation of leakage reactances. The biggest difference though is seen in the transient situation as in Figure 3.24, during the first seconds after connecting the machine to the grid. The biggest difference between the simulated values and the measurements are

at the highest peak value, which is 38% smaller than the measured value. The smallest difference is seen at the first peak, which is the smallest of all, with 11% difference referred to the measured peak value. During the quasi-stationary period while running up of the machine, the current is quasi-stationary as well. The average difference between the peak values of the stator currents is now 10% (Figure 3.25).

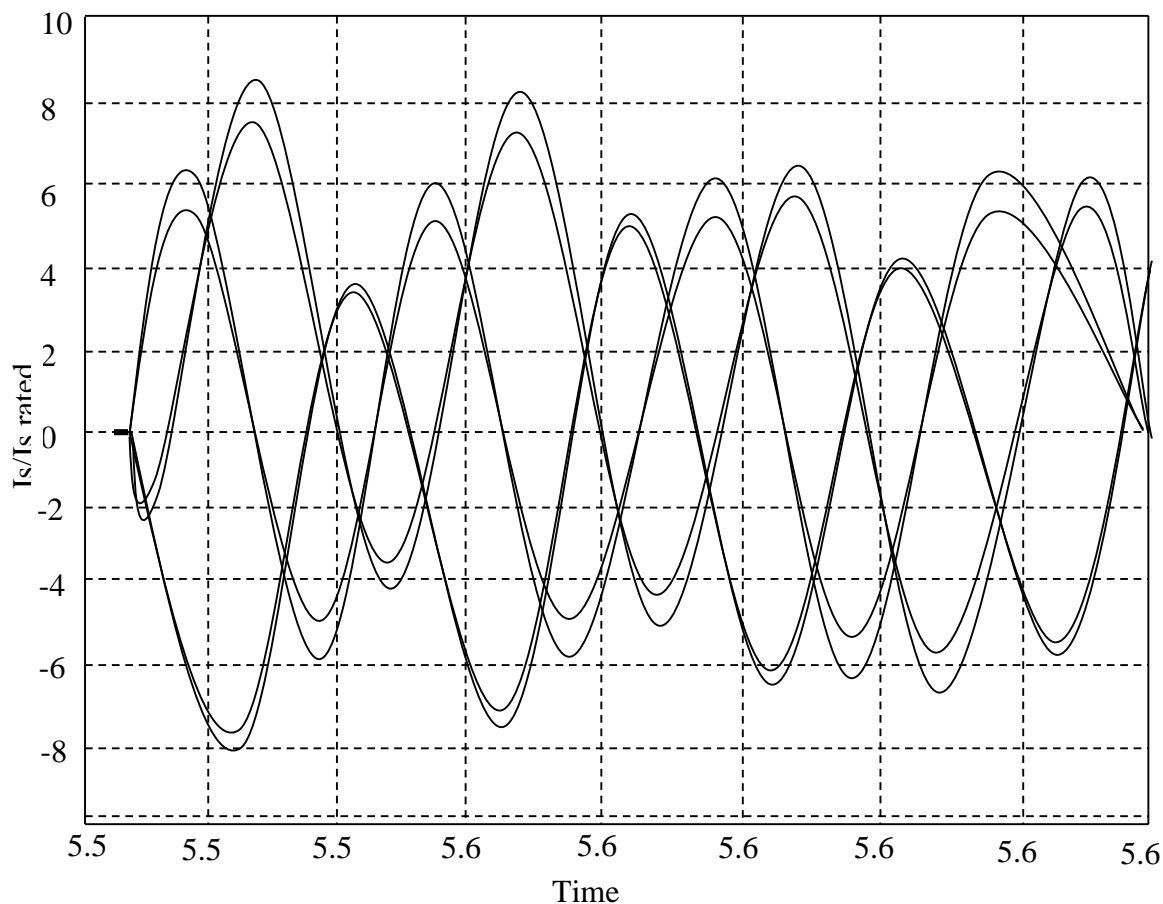


Figure 3.24. Zoom into the stator currents at start of the DOL-start (solid- model including main saturation and friction losses, dashed –measured)

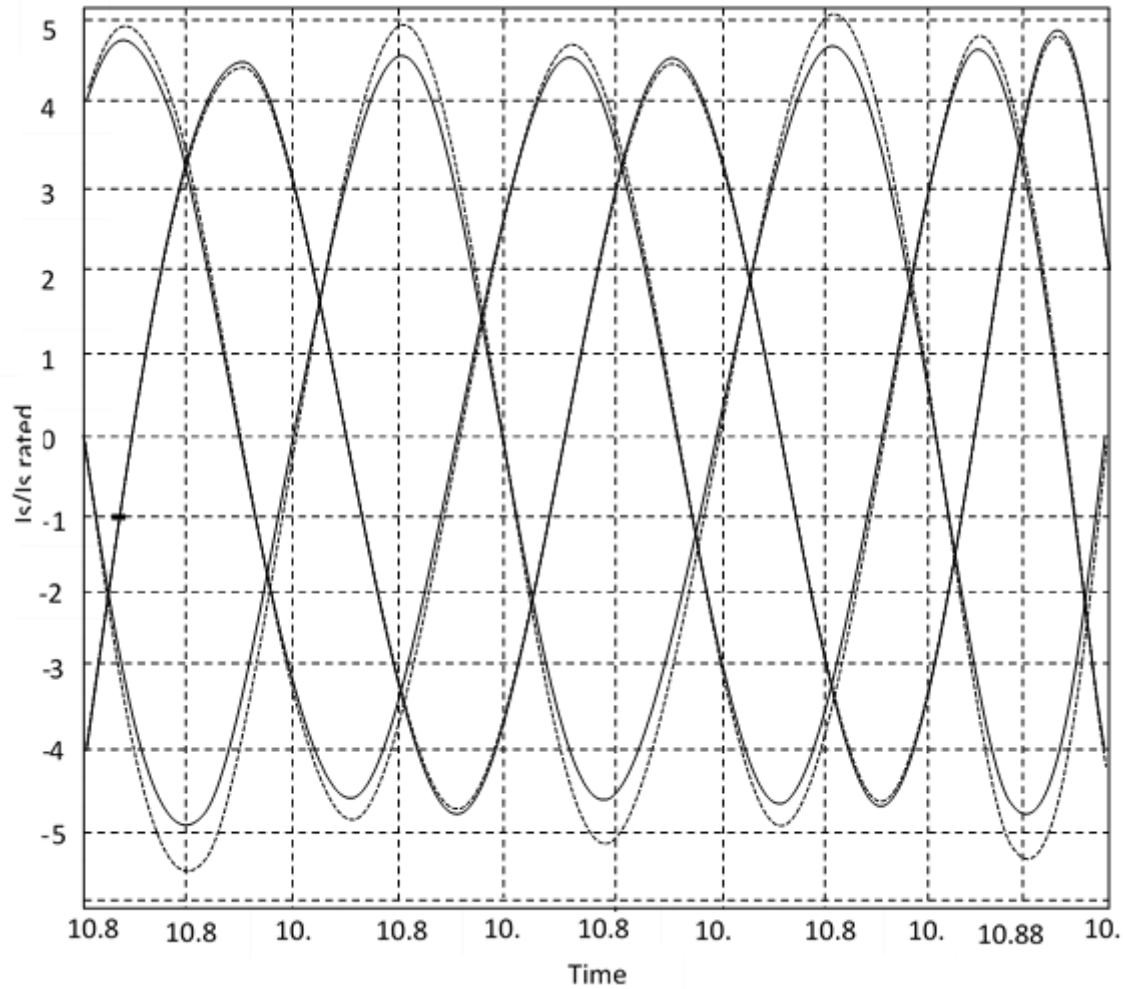


Figure 3.25. Window of the stator currents in the middle of the DOL-start (solid- model including main saturation and friction losses, dashed measured)

After the start up, the machine is running in no load operation and consumes only the power for covering the own losses. Figure 3.24 shows the current during this no load conditions. The simulated current is insignificantly bigger than the measured, which verifies the correct implementation of the main magnetizing reactance saturation. The noticeable asymmetric between the phase currents is due to the slightly asymmetrical real voltage input.

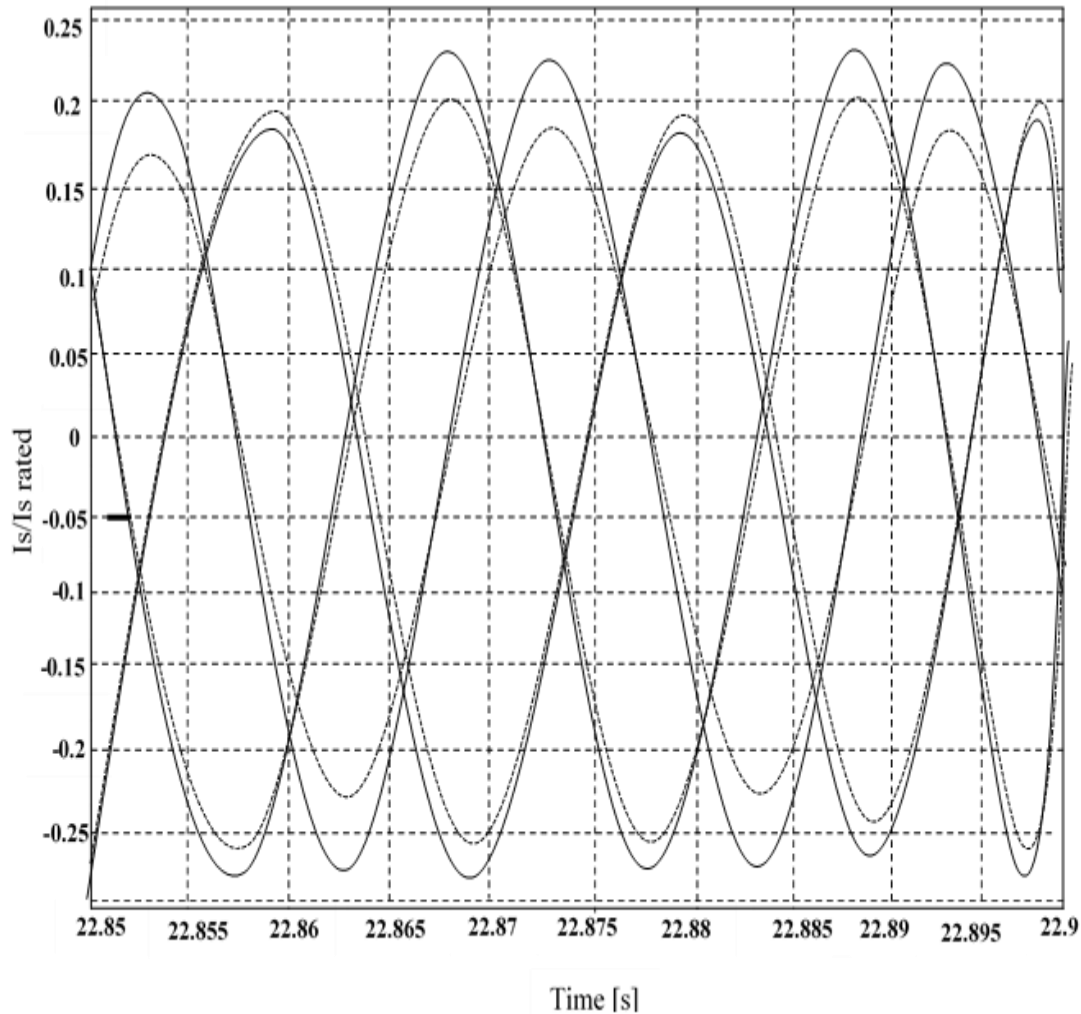


Figure 3.26. Window of stator currents at no load operation after DOL- start

### 3.1.6.3. Implementation and validation of leakage reactance saturation

It is highly desirable to minimize the differences between the simulated and experimental values in Figure 3.24 and Figure 3.26. The exact knowledge of the current peaks enables a better design of protection systems or the components withstanding the dynamical load. As already implied in the sub-chapter about saturation effects an implementation of leakage reactance saturation could improve the model especially during situations with high currents like short circuits. Unfortunately, there is a lack of data to have a detailed implementation of the nonlinearity of the leakage reactances. However the saturated leakage reactance of stator and rotor are estimated from the blocked rotor measurements with smaller voltage and available in the data sheet supplied by the manufacturer also known as the saturated stator currents or blocked rotor



stator current. Using the two described points of rated and saturated operation a linear approximation has been chosen to express change in the leakage inductances.

Table 3.1. Leakage inductance saturation reference

Stator current	Leakage inductance
0	rated
rated value	rated
Blocked rotor stator current	saturated value at slip=1
10x rated current value	saturated value at slip=1

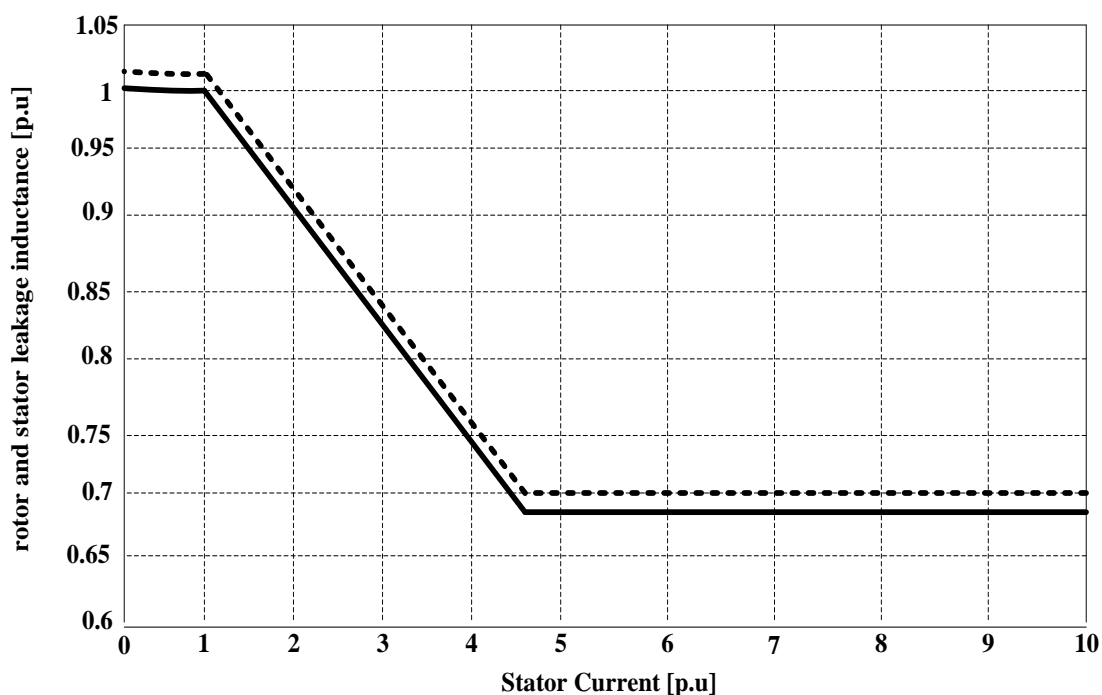


Figure 3.27. Example of stator (solid line) and rotor (dashed line) leakage inductance

Changing the leakage inductance in the presented manner might seem odd, since commonly the changes in inductances are made depending on the slip of the machine. Dependency from the slip though has the disadvantage that all 3-ph values are changed simultaneously. The dependency on the current gives the possibility of changing the phase inductances separately due to the phase instantaneous current. Figure 3.28 shows

the implementation of main and leakage saturation in the machine model in Matlab/ Simulink. The rest of the machine model is the same as already described above.

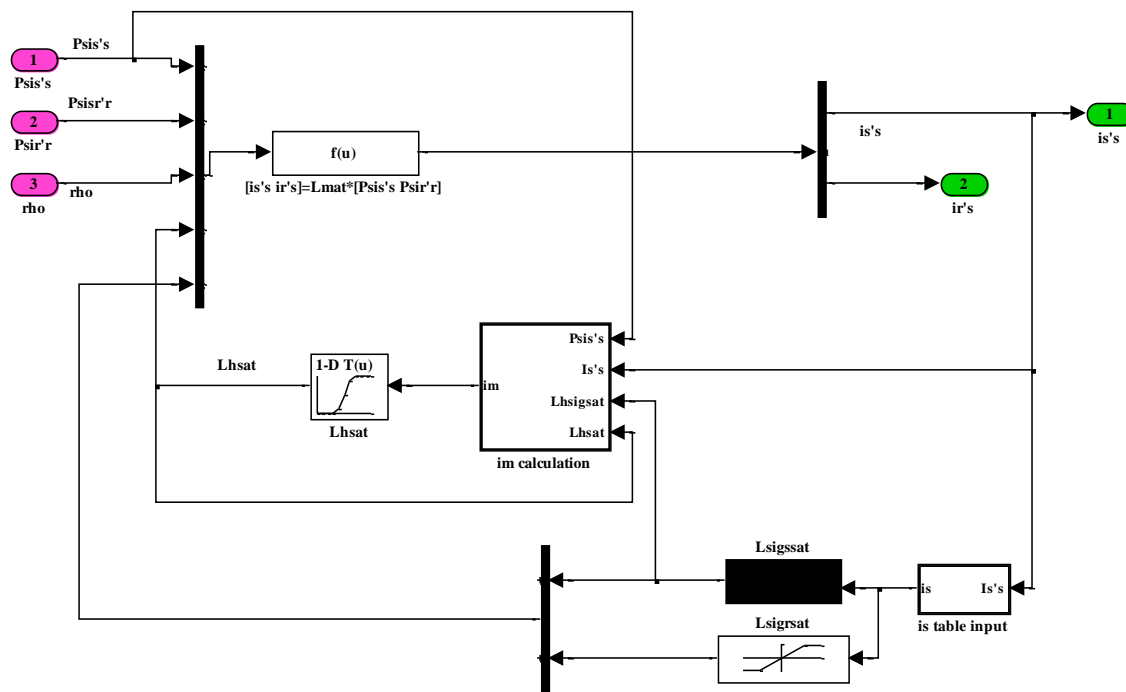


Figure 3.28. Modified Matlab/ Simulink block “flux – current” including leakage inductance saturation

The same simulation has been performed as already done with the model considering only the main magnetizing inductance saturation. There isn't a noticeable change in the speed characteristic compared to the model including only main saturation. Figure 3.29 shows the model with the implementation of the leakage inductance saturation compared to the measurement of the test bench.

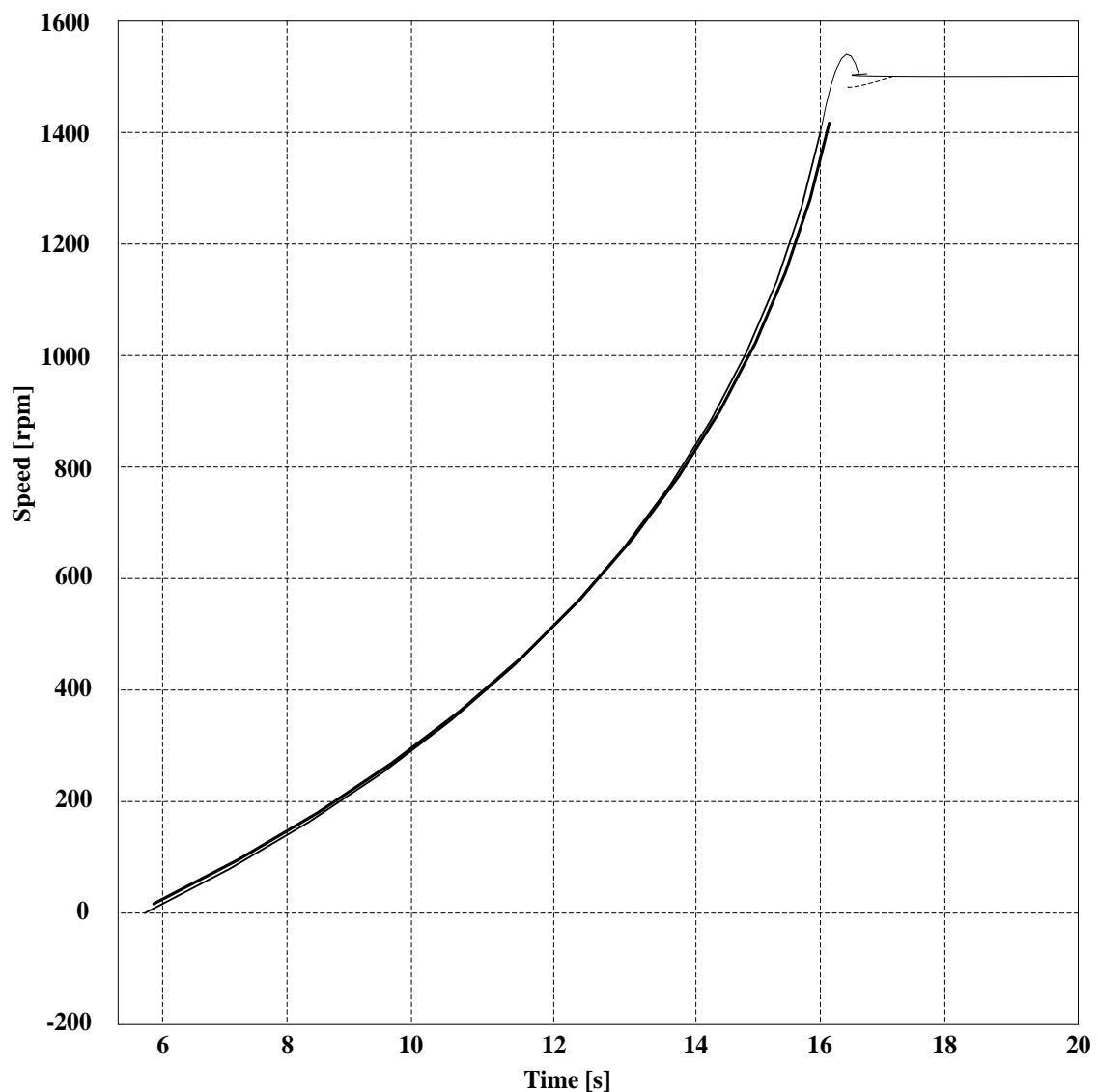


Figure 3.29. Speed during DOL start (solid line – model including main and leakage inductance saturation, dashed –measurement)

In Figure 3.30 and Figure 3.31 the stator current windows from the cut in of the machine and from the quasi stationary situation are shown. Implementation shows a large improvement in the stator current simulation compared to the simulations with the models not considering leakage saturation. The difference in the maximum peak values during the DOL start have been decreased from 38% to 21%. In the quasi stationary state after the start up the average difference between the peak values of the stator current is decreased from 10% to 2% (Figure 3.31).

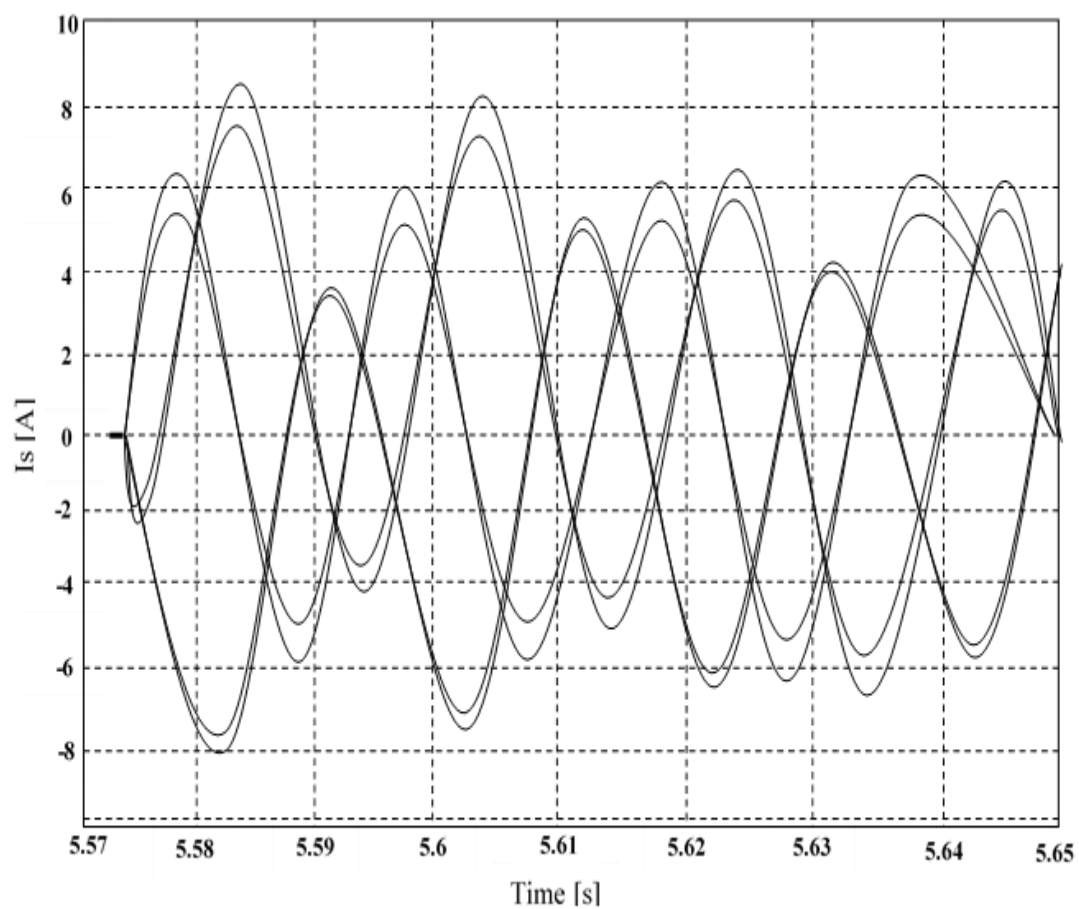


Figure 3.30. Zoom into stator currents simulation at start of the DOL start (solid- model including main and leakage saturation, dashed - measured)

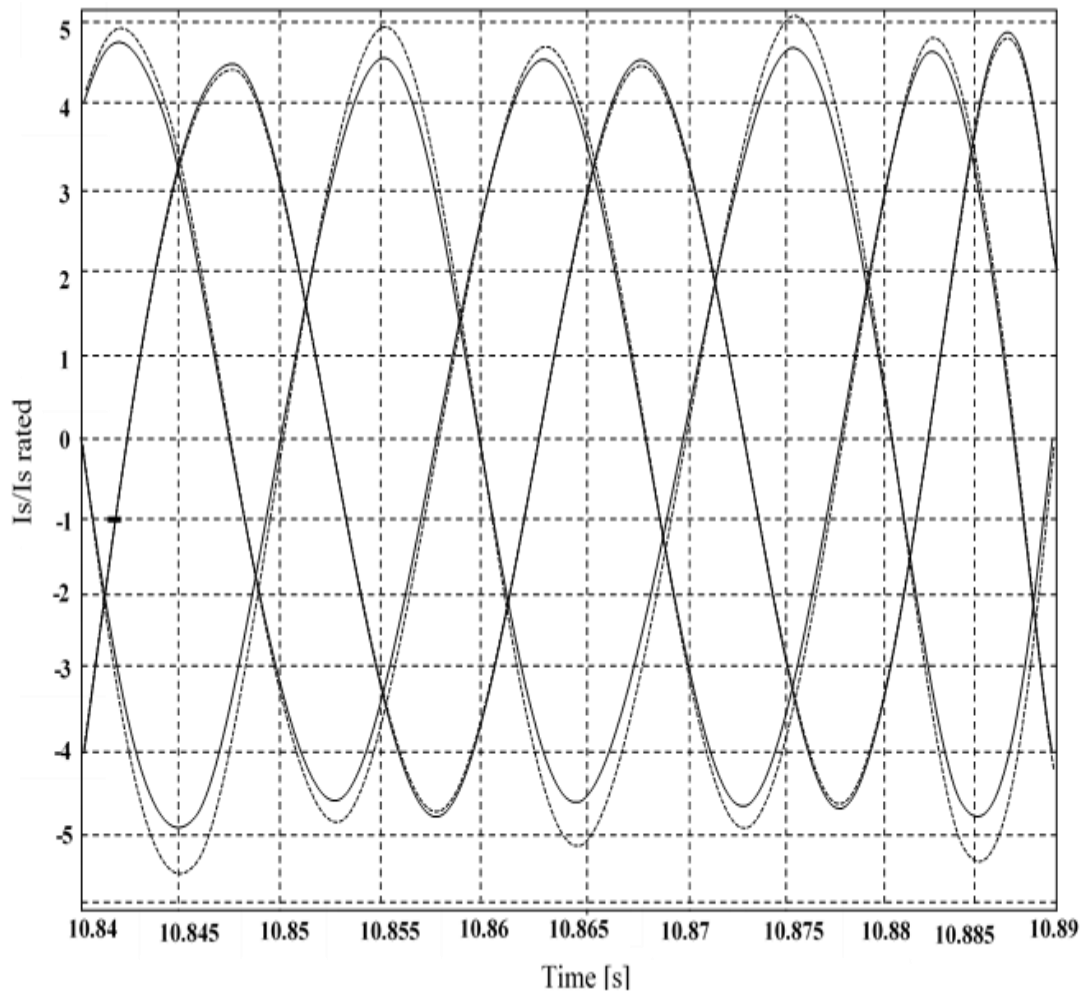


Figure 3.31. Window of Stator currents in the quasi stationary state of the DOL-start (solid-model including main and leakage saturation, dashed –measured)

Hence the influence of the saturation of main and leakage inductances could be clearly shown, the influence during no load operation is non-significant. Figure 3.32 shows the currents during the no load state after the DOL start. The missing behavior during no load operation is easily explained with the used implementation method. While the main inductance is more correctly changing accordingly the available points from the no-load curve, the leakage inductances are assumed constant to their rated values and do not change dependent from the current between zero and rated current. The Figure 3.32 gives also only information about the functionality of the model even with very small currents.

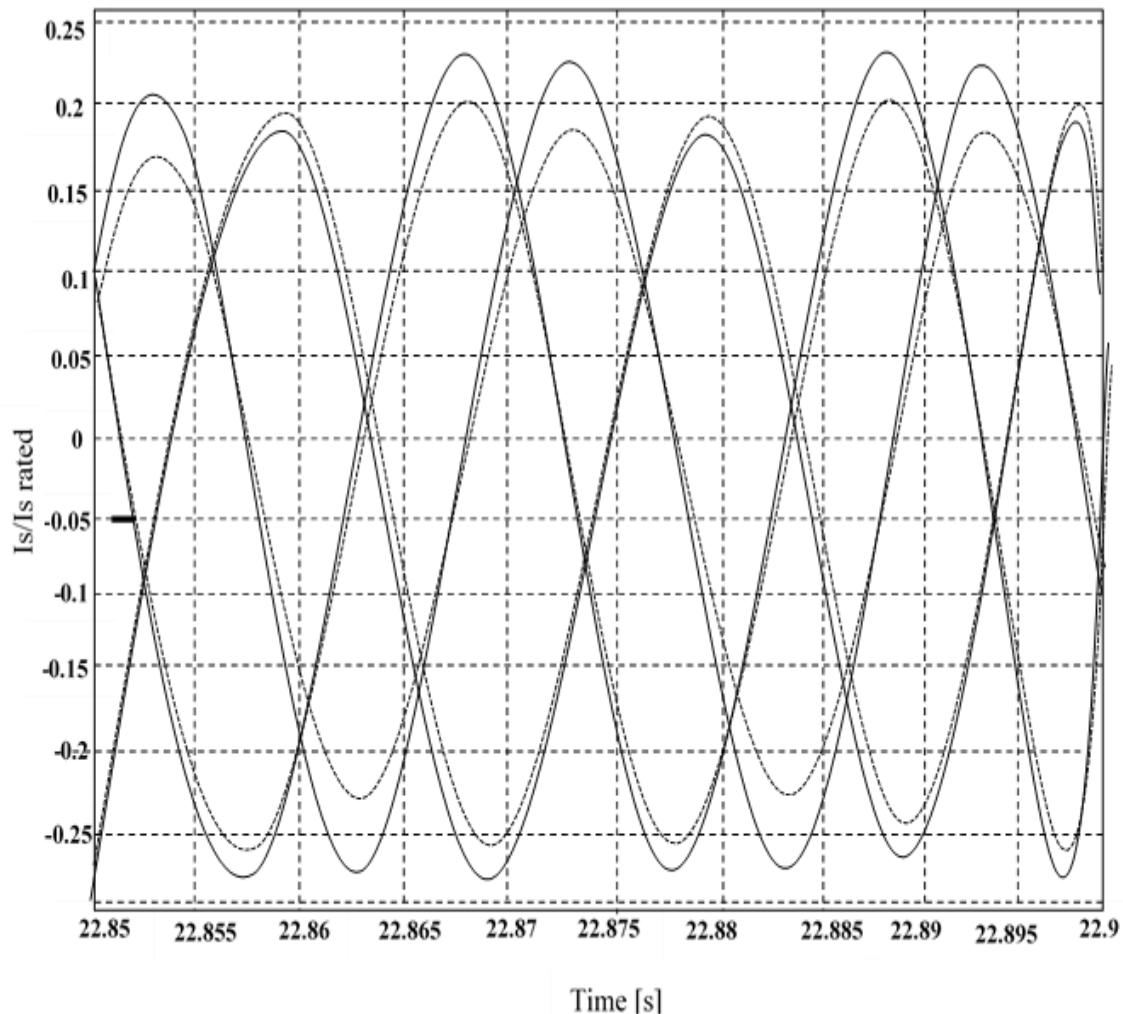


Figure 3.32. Zoom into stator currents at no load operation after DOL- start; solid line –model including main and leakage inductance saturation, dashed line –measured

#### 3.1.6.4. Influence of the Machines Coupling

In the above sub-chapters the influences of saturation effects and friction losses have been discussed. The discussed dependencies are in principle the same independence of the use of a 3-ph model or made with Clark or Park transformation. In the following the influences of the machine coupling will be discussed. Unfortunately it isn't only secondary discussed, though found important during the consideration of choosing the method of machine modeling for the purpose of simulating non rated conditions. Therefore some presumption done during developing the analytical model will be paid attention. The general ABC/abc generator modeling has been described. Gaining the input for this model is very challenging under the given circumstances. Though it is

worth the effort, since a 3-ph ABC/abc generator model gives the possibility to look at each phase separately as well as the coupling between the phases[52] thereby the ABC/abc model isn't limited by conditions of symmetry of either supply voltages or phase impedances. The 3-ph analytical model can be easily improved with accessibility of more input parameters, without complete model changes. All these advantages are improving the simulation result. Another possible presentation of the ABC/abc per phase machine model, point out the field coupling between stator and rotor and the correlation to the voltage equation is given in Figure 3.33.

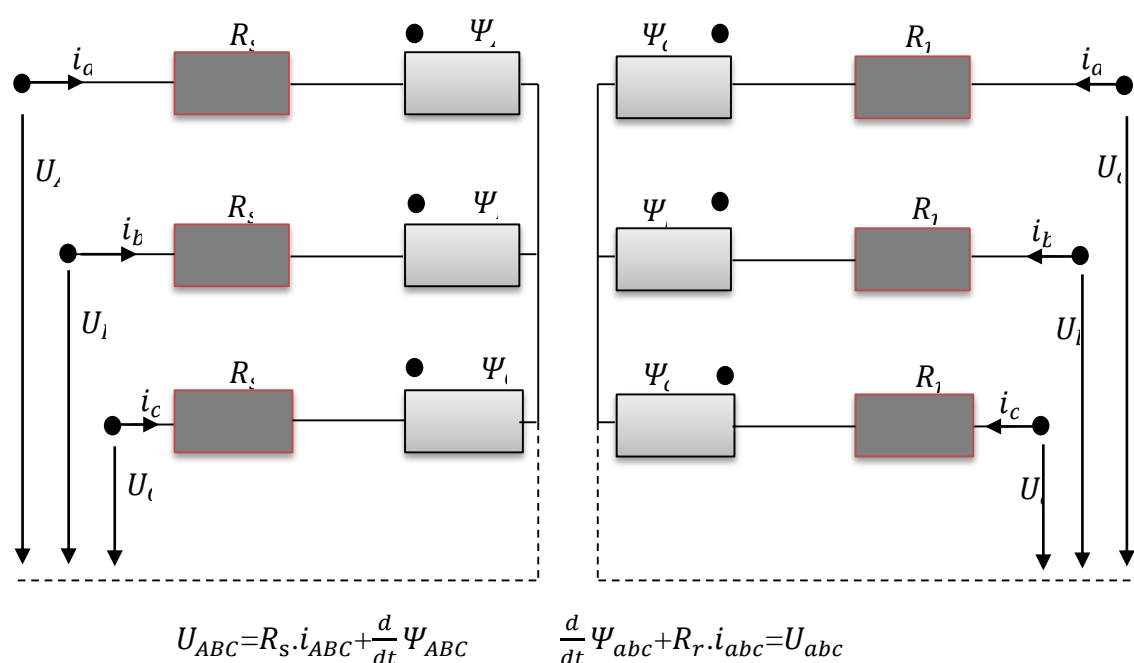


Figure 3.33. 3-ph equivalent ABC/abc circuit diagram of a doubly fed asynchronous generator

The coupling is derived to be expressed as a product of the inductance matrix  $L$ [53] and the current vector  $i$ . The inductance matrix of the machine model takes a central position. During the computing of the machine model the inverse of the inductance matrix has to be calculated. This introduces a rather difficult task and is slowing down the simulation process. Including saturation effects improves the realistic presentation of the machine but also complicates the model even more, since the inverse of the matrix has to be computed every step. Taking into account the electrical coupling, the asynchronous matrix give a possibility to make easy the complexity of the model itself and therewith simplify the computing of the inverse matrix as proposed by Pillay[53] and

Goldemberg[54]. The inductance matrix of the asynchronous generator including saturation of the inductances has been previously determined to:

$$L = \begin{pmatrix} L_{\sigma sA} + L_{msA} & -0.5L_{mSA} & -0.5L_{mSA} & L_{msrAa} \cdot f_1 & L_{msrAb} \cdot f_2 & L_{msrAc} \cdot f_3 \\ -0.5L_{mSB} & L_{\sigma sB} + L_{msB} & -0.5L_{mSB} & L_{msrBa} \cdot f_3 & L_{msrBb} \cdot f_1 & L_{msrBc} \cdot f_2 \\ -0.5L_{mSC} & -0.5L_{mSC} & L_{\sigma sC} + L_{msC} & L_{msrCa} \cdot f_2 & L_{msrCb} \cdot f_3 & L_{msrCc} \cdot f_1 \\ L_{msraA} \cdot f_1 & L_{msraB} \cdot f_3 & L_{msraC} \cdot f_2 & L'_{\sigma ra} + L_{mra} & -0.5L_{mra} & -0.5L_{mra} \\ L_{msrbA} \cdot f_2 & L_{msrbB} \cdot f_1 & L_{msrbC} \cdot f_3 & -0.5L_{mrb} & L'_{\sigma rb} + L_{mrb} & -0.5L_{mrb} \\ L_{msrcA} \cdot f_3 & L_{msrcB} \cdot f_2 & L_{msrcC} \cdot f_1 & -0.5L_{mrc} & -0.5L_{mrc} & L'_{\sigma r} + L_{mrc} \end{pmatrix} \quad (3.101)$$

Assuming a star/star (YY) connected machine with no external accessible star point, the addition of the rotor currents per phase and stator currents per phase is zero in the star point as shown in equation (3.102).

$$i_A + i_B + i_C = 0, \quad i_a + i_b + i_c = 0 \quad (3.102)$$

Taking this into account, the induction matrix takes the following form.

$$L = \begin{pmatrix} L_{\sigma sA} + 1.5L_{msA} & 0 & 0 & L_{msrAa} \cdot f_1 & L_{msrAb} \cdot f_2 & L_{msrAc} \cdot f_3 \\ 0 & L_{\sigma sB} + 1.5L_{msB} & 0 & L_{msrBa} \cdot f_3 & L_{msrBb} \cdot f_1 & L_{msrBc} \cdot f_2 \\ 0 & 0 & L_{\sigma sC} + 1.5L_{msC} & L_{msrCa} \cdot f_2 & L_{msrCb} \cdot f_3 & L_{msrCc} \cdot f_1 \\ L_{msraA} \cdot f_1 & L_{msraB} \cdot f_3 & L_{msraC} \cdot f_2 & L'_{\sigma ra} + 1.5L_{mra} & 0 & 0 \\ L_{msrbA} \cdot f_2 & L_{msrbB} \cdot f_1 & L_{msrbC} \cdot f_3 & 0 & L'_{\sigma rb} + 1.5L_{mrb} & 0 \\ L_{msrcA} \cdot f_3 & L_{msrcB} \cdot f_2 & L_{msrcC} \cdot f_1 & 0 & 0 & L'_{\sigma r} + 1.5L_{mrc} \end{pmatrix} \quad (3.103)$$

Notice, the stator and rotor mutual inductances  $L_{ms}$ ,  $L_{mr}$  are of  $2/3L_m$  the 1-ph equivalent diagram. For models represented in Clark or Park transformation the YY coupling of the machine is assumed in many cases and the experiences made with the 3-ph model are exemplary for the models made with a transformation as well. In case of a  $\Delta Y$  connected machine the coupling of the rotor phases can be simplified as shown above in the YY example, while leaving the stator phases untouched. The inductance matrix for a  $\Delta Y$  connected machine takes the form shown in (3.104).



$L=$

$$\begin{pmatrix} L_{\sigma SA} + L_{mSA} & -0.5L_{mSA} & -0.5L_{mSA} & L_{msrAa} \cdot f_1 & L_{msrAb} \cdot f_2 & L_{msrAc} \cdot f_3 \\ -0.5L_{mSB} & L_{\sigma SB} + L_{mSB} & -0.5L_{mSB} & L_{msrBa} \cdot f_3 & L_{msrBb} \cdot f_1 & L_{msrBc} \cdot f_2 \\ -0.5L_{mSC} & -0.5L_{mSC} & L_{\sigma SC} + L_{mSC} & L_{msrCa} \cdot f_2 & L_{msrCb} \cdot f_3 & L_{msrCc} \cdot f_1 \\ L_{msraA} \cdot f_1 & L_{msraB} \cdot f_3 & L_{msraC} \cdot f_2 & L'_{\sigma ra} + 1.5L_{mra} & 0 & 0 \\ L_{msrbA} \cdot f_2 & L_{msrbB} \cdot f_1 & L_{msrbC} \cdot f_3 & 0 & L'_{\sigma rb} + 1.5L_{mrb} & 0 \\ L_{msrcA} \cdot f_3 & L_{msrcB} \cdot f_2 & L_{msrcC} \cdot f_1 & 0 & 0 & L'_{\sigma r} + 1.5L_{mrc} \end{pmatrix}$$

(3.104)

The magnetic coupling of the stator phases in the original allows the stator currents to flow in a circle. This gives a more realistic result than the usually used method of assuming a magnetically YY connected machine and afterwards calculation of the electrical delta coupling of the stator windings, which is shown in the following example. A delta coupled generator experiences a 2-ph line to line short circuit at the terminals.

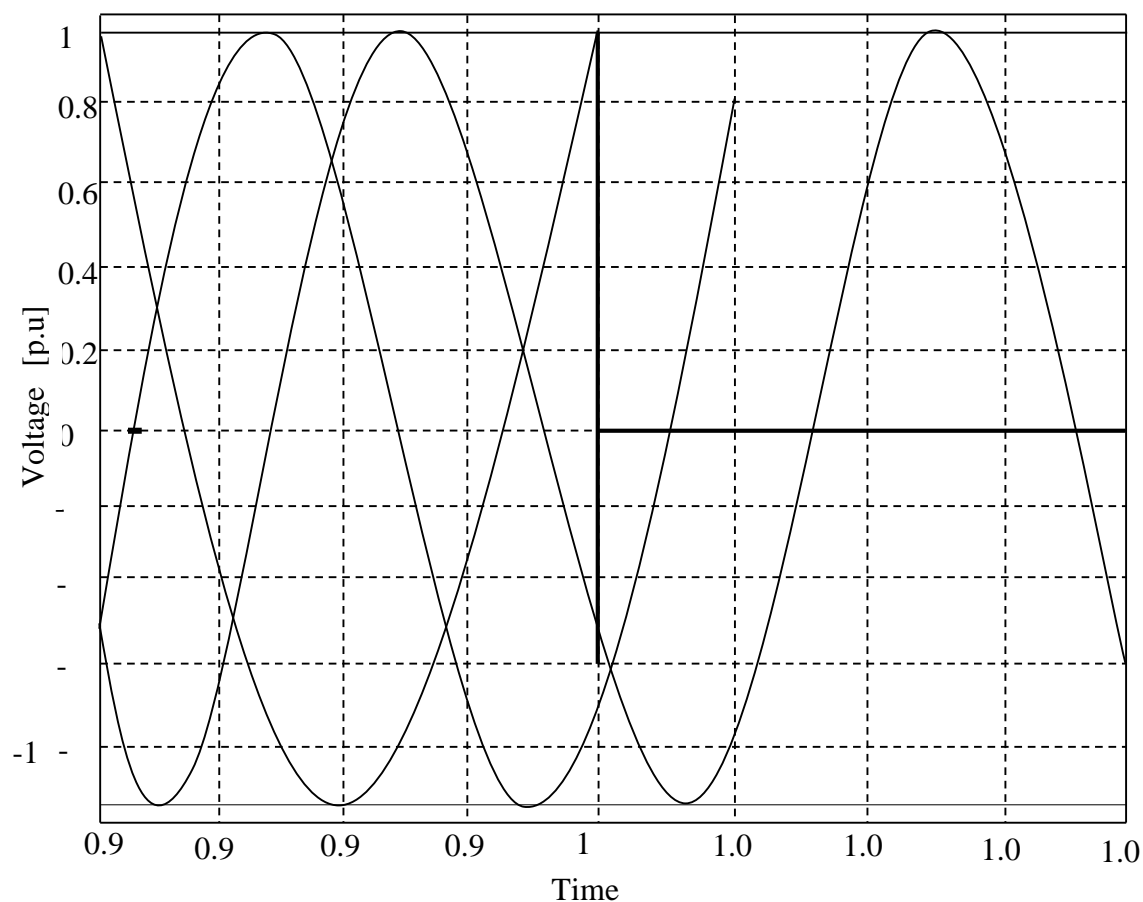


Figure 3.34. Voltage at generator stator terminal during a two-phase short circuit

While there is no difference between the simulated stator current under symmetrical conditions before the short circuit, the difference between the models can be seen in the asymmetrical condition Figure 3.34. The current modeled with the star connected machine model and a calculated delta coupling shows difference in phase and amplitude to the current simulated with the delta connected machine model.

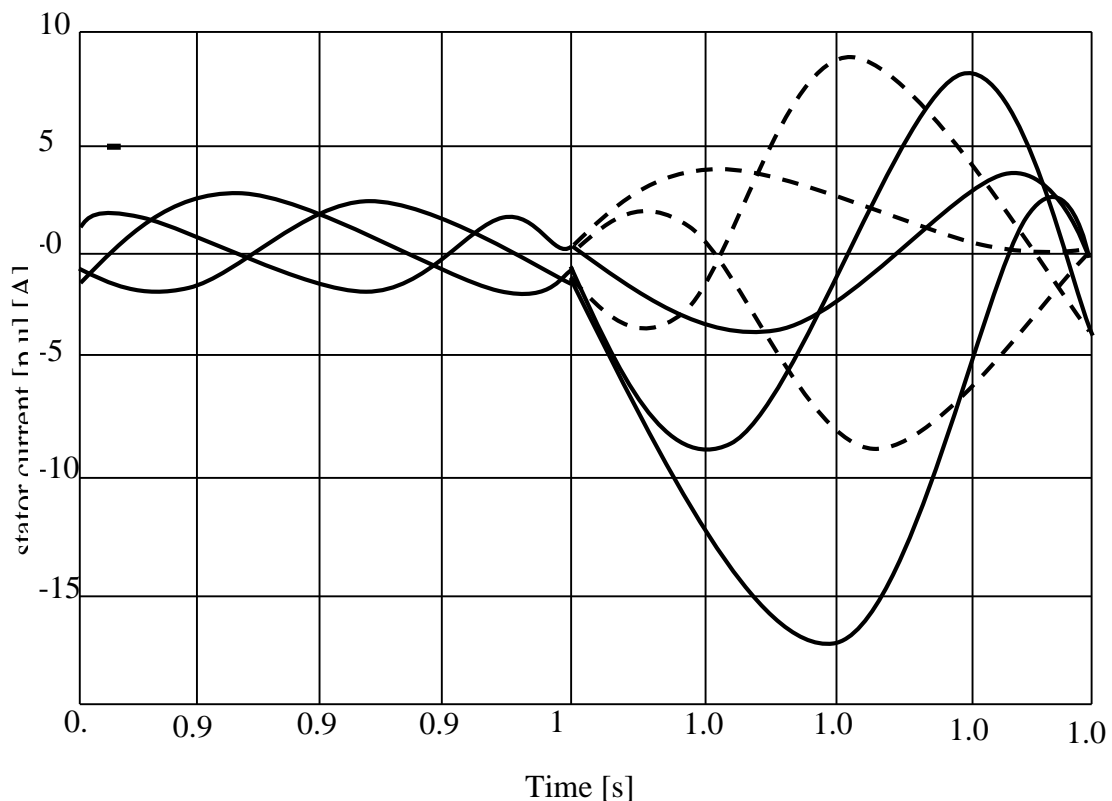


Figure 3.35. Stator currents of the generator dashed line – star modeled machine with calculated delta coupling and solid lines – delta modeled machine

There are many different ways of machine modeling, but as the machines are designed for their application, the model has to be developed for the expected use and the reality. The modeling in this thesis uses a 3-ph model because it has the purpose of accurately fault simulation for variable speed wind turbines. Thereby it has been shown, that different analytical description of the connection of the machine phases have an increased importance, while looking at asymmetrical conditions. Leakage saturation has an important influence, while looking at short circuit contribution to the grid, which plays an important role for grid connection of the turbine. Not all influences have been studied in this presented work. The influence of iron losses and skin effect as well as the changes due to temperature changes are open for future research activities. The

ABC/abc machine model is beneficial to use, because it does not only simplify the inclusion of connection condition influence and per phase variability of saturation. The 3-ph model can be easily expanded for other simulation purposes like asymmetry in the machine parameters or harmonics.

### 3.2. Modeling of Transformers

The Transformer is an important part to connect the wind turbine to the grid. However, it is very common to neglect the dynamic behavior of the transformer and only consider a very simple ideal model or the use of equivalent impedances for calculations. In this thesis it is very important to consider the dynamic behavior of the wind turbine transformer. The content of this sub-chapter are the development of the 2-windings 3-phase transformer model and the 3-winding 3-phase transformer model. In the end the 2-winding 3-phase Autotransformer model is derived.

#### 3.2.1. The 2-windings 3-phase Transformer Model

The 2-windings 3-phase transformer (2w 3ph transformer) connects a 3-ph system with two different voltage levels. The transformer consists of 2 windings, which are connected through a magnetic circuit in the core.

The two different voltage levels on the transformer are called high- and low-voltage side or commonly also known as primary and secondary side, because the high voltage side is usual connected to the 1st winding and the low voltage side is connected to the 2nd winding. Assuming there is no air gap in the core, no voltage drop in the magnetic circle (infinite core permeability), and no hysteresis losses, the resistances of the windings are negligible. The result of all assumptions together is a loss-less (ideal) transformer, which is only representing a simple relationship between the two voltages and currents. The voltage equations for the two windings of such ideal transformer are:

$$\underline{u}_1 = -\underline{e}_1 = \frac{d\Psi_1}{dt} \quad \underline{u}_2 = -\underline{e}_2 = \frac{d\Psi_2}{dt} \quad (3.105)$$

Hence the whole flux is closing inside the core the flux in winding 1 and winding 2 are identical and therewith the flux linkages can be expressed as:

$$\underline{\Psi}_1 = w_1 \cdot \underline{\Phi} \quad \underline{\Psi}_2 = w_2 \cdot \underline{\Phi} \quad (3.106)$$

In this loss-less transformer the summation of the currents considering the number of windings is  $w_1 \cdot \underline{i}_1 + \underline{i}_2 \cdot w_2 = 0$ . Using the current correlation in combination with the voltage equation the relationship between primary and secondary voltage can be easily expressed with the winding ratio  $a_{12}$ .

$$\frac{\underline{u}_1}{\underline{u}_2} = \frac{w_1}{w_2} \quad a_{12} = \frac{w_1}{w_2} \quad \underline{u}_1 = a_{12} \cdot \underline{u}_2 = \underline{u}'_2 \quad (3.107)$$

The secondary voltage transformed with the winding ratio is equivalent to the primary voltage. Similarly the currents can be expressed with the winding ratio to:

$$\underline{i}_1 = \frac{1}{a_{12}} \cdot \underline{i}_2 = \underline{i}'_2 \quad (3.108)$$

These with the ideal model achieved simple correlation are the most basic equations for transformer consideration. In a realistic transformer a part of the magnetic field will close via the air and therefore only a part of the magnetic field is linked to both windings. The part of the flux, which is not linked through the core, is called the leakage flux, which only links to either primary or secondary winding. The losses in the windings of the transformer are expressed with an electrical resistance.

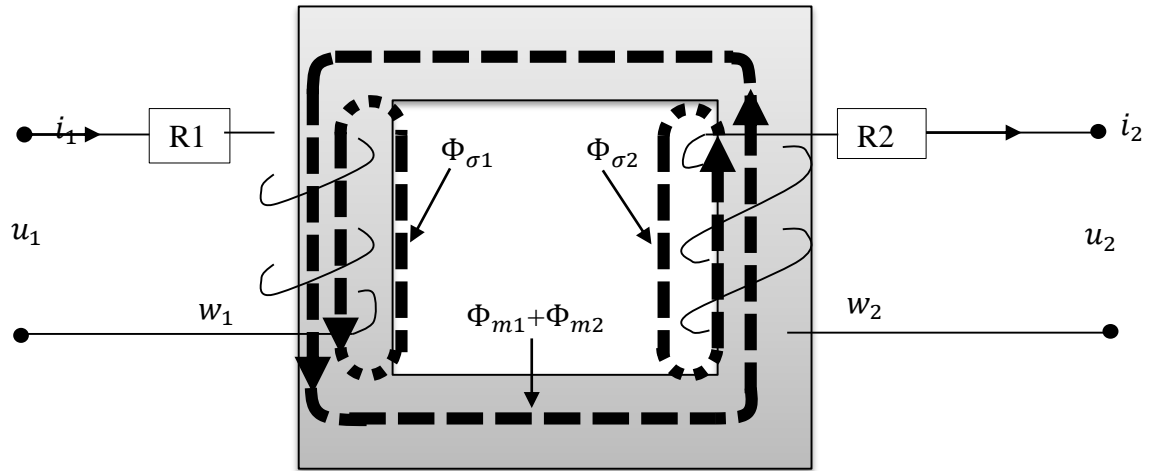


Figure 3.36. 2-windings 2-phase Transformer

The definition of the flux is very similar as in an electrical machine, divided into main flux in the core and the leakage flux.

$$\Psi_1 = w_1 \cdot \Phi_{\sigma 1} + w_1 \cdot \Phi_{m1} + w_1 \cdot \Phi_{m2} \quad (3.109)$$

$$\Psi_2 = w_2 \cdot \Phi_{\sigma 1} + w_2 \cdot \Phi_{m1} + w_2 \cdot \Phi_{m2} \quad (3.110)$$

As in the electrical machine theory the transformer is often expressed in a 1-ph equivalent. The inductances are achieved as:

$$L_{11} = L_{\sigma 1} + L_{m1} = \frac{w_1(\Phi_{\sigma 1} + \Phi_{m1})}{i_1} \quad L_{m1} = \frac{w_1 \Phi_{m1}}{i_1} \quad (3.111)$$

$$L_{22} = L_{\sigma 2} + L_{m2} = \frac{w_2(\Phi_{\sigma 2} + \Phi_{m2})}{i_2} \quad L_{m2} = \frac{w_2 \Phi_{m2}}{i_2} \quad (3.112)$$

$$L_{21} = \frac{w_2 \Phi_{m1}}{i_1} \quad L_{21} = \frac{w_1}{w_2} \cdot L_{m2} \quad (3.113)$$

$$L_{12} = L_{21} \quad L_{m1} = \left(\frac{w_1}{w_2}\right)^2 L_{m2} \quad (3.114)$$

$L_{21}$  and  $L_{12}$  describe the mutual inductances between the two windings and  $L_{11}$ ,  $L_{22}$  the self-induction of the windings. The flux coupling between winding 1 and 2 can be written as:

$$\begin{bmatrix} \Psi_1 \\ \Psi_2 \end{bmatrix} = \begin{bmatrix} L_{11} & L_{12} \\ L_{21} & L_{22} \end{bmatrix} \times \begin{bmatrix} i_1 \\ i_2 \end{bmatrix} \quad (3.115)$$

The voltage equations therewith become:

$$[u]=[R]x[i]+\frac{d}{dt}([L]x[i]) \quad (3.116)$$

$$\begin{bmatrix} u_1 \\ u_2 \end{bmatrix} = \begin{bmatrix} R_1 & R_2 \\ L_{21} & L_{22} \end{bmatrix} x \begin{bmatrix} i_1 \\ i_2 \end{bmatrix} + \frac{d}{dt} \left( \begin{bmatrix} L_{11} & L_{12} \\ L_{21} & L_{22} \end{bmatrix} x \begin{bmatrix} i_1 \\ i_2 \end{bmatrix} \right) \quad (3.117)$$

This 1-ph equivalent system can be depicted in the well-known equivalent T circuit of two magnetically coupled coils. Preferred is to relate the parameters and variables to one side of the transformer and using the ideal transformer to express the transformation. The parameters are transformed using the introduced ratio  $a_{12}$ . The transformation from all value to the primary side can be made in the following way:

$$u'_2 = a_{12} \cdot u_2 \quad i'_2 = \frac{1}{a_{12}} \cdot i_2 \quad \Psi'_2 = a_{12} \cdot \Psi_2 \quad (3.118)$$

$$L'_{12} = a_{12}^2 \cdot L_{12} \quad L'_{22} = a_{12}^2 \cdot L_{22} \quad R'_{12} = a_{12}^2 \cdot R_{12} \quad L'_{21} = a_{12}^2 \cdot L_{21} \quad (3.119)$$

The calculation of the values to the secondary side can be made in the same way. The parameters itself can be determined with a no load and a short circuit test[45][51][55][56] [57].

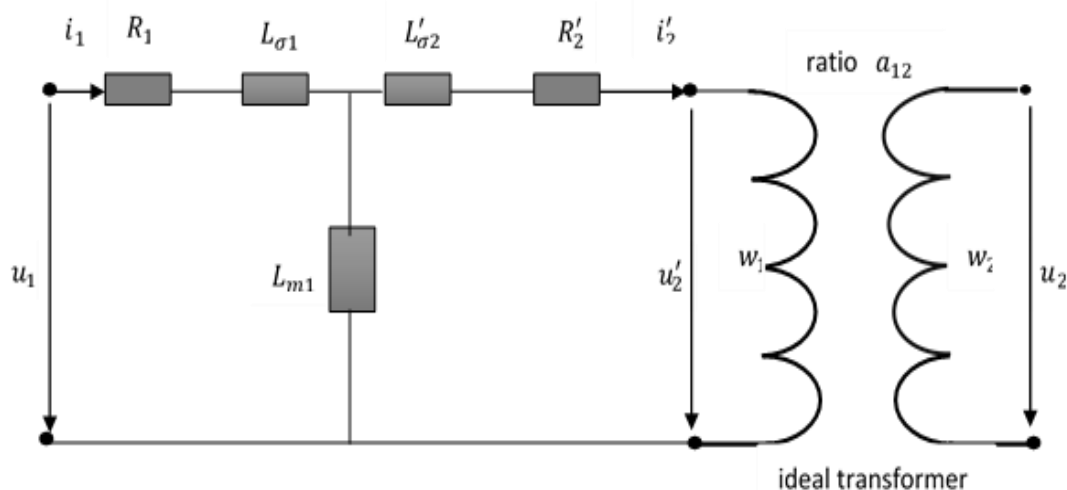


Figure 3.37. Equivalent circuit of a transformer referred to primary side

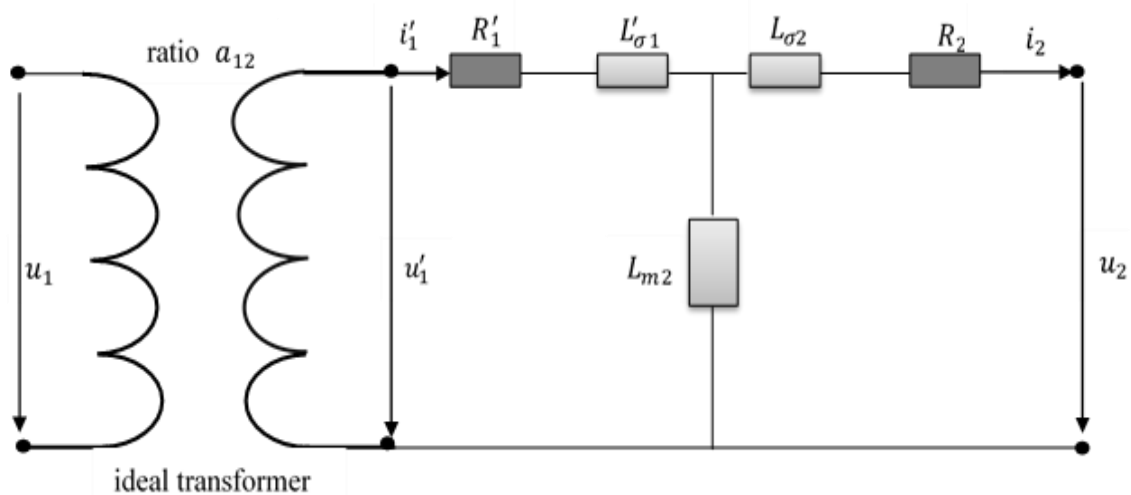


Figure 3.38. Equivalent circuit of a transformer referred to secondary side

For asymmetrical dynamic simulations of the 2w3ph transformer the equivalent 1-ph equation developed above are not sufficient enough. The coupling between the phases has to be considered as well. The general voltage equations for a two windings 2w3ph transformer considering all phases can now be written as:

$$[u] = [R] \cdot [i] + \frac{d}{dt} ([L] \cdot [i])$$

$$\begin{bmatrix} u_{1a} \\ u_{1b} \\ u_{1c} \\ u_{2a} \\ u_{2b} \\ u_{2c} \end{bmatrix} = \begin{bmatrix} R_{1a} & R_{1b} & R_{1c} & R_{2a} & R_{2b} & R_{2c} \end{bmatrix} \cdot \begin{bmatrix} i_{1a} \\ i_{1b} \\ i_{1c} \\ i_{2a} \\ i_{2b} \\ i_{2c} \end{bmatrix} + \frac{d}{dt} \left( \begin{bmatrix} L_{11a} & L_{1ab} & L_{1ac} & L_{12a} \cdot f_1 & L_{12ab} \cdot f_2 & L_{12ac} \cdot f_3 \\ L_{1ba} & L_{11b} & L_{1bc} & L_{12ba} \cdot f_3 & L_{12b} \cdot f_1 & L_{12bc} \cdot f_2 \\ L_{1ca} & L_{1cb} & L_{11c} & L_{12ca} \cdot f_2 & L_{12cb} \cdot f_3 & L_{12c} \cdot f_1 \\ L_{21a} \cdot f_1 & L_{21ab} \cdot f_3 & L_{21ac} \cdot f_2 & L_{22a} & L_{2ab} & L_{2ac} \\ L_{21ba} \cdot f_2 & L_{21b} \cdot f_1 & L_{21bc} \cdot f_3 & L_{2ba} & L_{22b} & L_{2bc} \\ L_{21ca} \cdot f_3 & L_{21cb} \cdot f_2 & L_{21c} \cdot f_1 & L_{2ca} & L_{2cb} & L_{22c} \end{bmatrix} \cdot \begin{bmatrix} i_{1a} \\ i_{1b} \\ i_{1c} \\ i_{2a} \\ i_{2b} \\ i_{2c} \end{bmatrix} \right) \quad (3.120)$$

$$f_1 = \cos(\vartheta) \quad f_2 = \cos\left(\vartheta + \frac{2}{3}\pi\right) \quad f_3 = \cos\left(\vartheta - \frac{2}{3}\pi\right) \quad (3.121)$$

In the inductance matrix equation (119) new factors  $f_1, f_2, f_3$  are introduced. The factors consider the external connection of the windings and the related turn in the phases. The factor is easily explained with an example:

A very common coupling of the windings of a three-phase transformer is DYN5. The expected phase difference between the voltage in phase a of the primary winding compared to the voltage in phase a of the secondary winding is  $5 \times 30 \text{grad} = 150 \text{grad}$ . To achieve this phase difference with the model the angle theta should be set to  $\vartheta = -2.618 \text{rad}$

### 3.2.2. The 3-windings 3-phase transformer model

The three-winding three-phase (3w3ph) transformer is modeled in the same way as the 2w3ph transformer. The general equations simply get expanded with a third system representing the additional 3-phs in the third winding:

$$[u] = [R] \times [i] + \frac{d}{dt} ([L] \times [i])$$

$$\begin{bmatrix} u_{1a} \\ u_{1b} \\ u_{1c} \\ u_{2a} \\ u_{2b} \\ u_{2c} \\ u_{3a} \\ u_{3b} \\ u_{3c} \end{bmatrix} = \begin{bmatrix} R_{1a} & R_{1b} & R_{1c} & R_{2a} & R_{2b} & R_{2c} & R_{3a} & R_{3b} & R_{3c} \end{bmatrix} \times \begin{bmatrix} i_{1a} \\ i_{1b} \\ i_{1c} \\ i_{2a} \\ i_{2b} \\ i_{2c} \\ i_{3a} \\ i_{3b} \\ i_{3c} \end{bmatrix} + \frac{d}{dt} \begin{bmatrix} \Psi_{1a} \\ \Psi_{1b} \\ \Psi_{1c} \\ \Psi_{2a} \\ \Psi_{2b} \\ \Psi_{2c} \\ \Psi_{3a} \\ \Psi_{3b} \\ \Psi_{3c} \end{bmatrix} \quad (3.122)$$



$$\begin{bmatrix} \Psi_{1a} \\ \Psi_{1b} \\ \Psi_{1c} \\ \Psi_{2a} \\ \Psi_{2b} \\ \Psi_{2c} \\ \Psi_{3a} \\ \Psi_{3b} \\ \Psi_{3c} \end{bmatrix} = \begin{bmatrix} L_{11a} & L_{1ab} & L_{1ac} & L_{12a} \cdot f_1 & L_{12ab} \cdot f_2 & L_{12ac} \cdot f_3 & L_{13a} \cdot f_1 & L_{13ab} \cdot f_2 & L_{13ac} \cdot f_3 \\ L_{1ba} & L_{11b} & L_{1bc} & L_{12ba} \cdot f_3 & L_{12b} \cdot f_1 & L_{12bc} \cdot f_2 & L_{13ba} \cdot f_3 & L_{13b} \cdot f_1 & L_{13bc} \cdot f_2 \\ L_{1ca} & L_{1cb} & L_{11c} & L_{12ca} \cdot f_2 & L_{12cb} \cdot f_3 & L_{12c} \cdot f_1 & L_{13ca} \cdot f_2 & L_{13cb} \cdot f_3 & L_{13c} \cdot f_1 \\ L_{21a} \cdot f_1 & L_{21ab} \cdot f_3 & L_{21ac} \cdot f_2 & L_{22a} & L_{2ab} & L_{2ac} & L_{23a} \cdot f_4 & L_{23ab} \cdot f_5 & L_{23ac} \cdot f_6 \\ L_{21ba} \cdot f_2 & L_{21b} \cdot f_1 & L_{21bc} \cdot f_3 & L_{2ba} & L_{22b} & L_{2bc} & L_{23ba} \cdot f_6 & L_{23b} \cdot f_4 & L_{23bc} \cdot f_5 \\ L_{21ca} \cdot f_3 & L_{21cb} \cdot f_2 & L_{21c} \cdot f_1 & L_{2ca} & L_{2cb} & L_{22c} & L_{23ca} \cdot f_5 & L_{23cb} \cdot f_6 & L_{23c} \cdot f_4 \\ L_{31a} \cdot f_1 & L_{31ab} \cdot f_3 & L_{31ac} \cdot f_2 & L_{321} \cdot f_4 & L_{32ab} \cdot f_6 & L_{32ac} \cdot f_5 & L_{33a} & L_{3ab} & L_{3ac} \\ L_{31ba} \cdot f_2 & L_{31b} \cdot f_1 & L_{31bc} \cdot f_3 & L_{32ba} \cdot f_5 & L_{32b} \cdot f_4 & L_{32bc} \cdot f_6 & L_{3ba} & L_{33b} & L_{3bc} \\ L_{31ca} \cdot f_3 & L_{31cb} \cdot f_2 & L_{31c} \cdot f_1 & L_{32ca} \cdot f_6 & L_{32cb} \cdot f_5 & L_{32c} \cdot f_4 & L_{3ca} & L_{3cb} & L_{33c} \end{bmatrix} \begin{bmatrix} i_{1a} \\ i_{1b} \\ i_{1c} \\ i_{2a} \\ i_{2b} \\ i_{2c} \\ i_{3a} \\ i_{3b} \\ i_{3c} \end{bmatrix} \quad (3.123)$$

$$f_1 = \cos(\vartheta) \quad f_2 = \cos\left(\vartheta + \frac{2}{3}\pi\right) \quad f_3 = \cos\left(\vartheta - \frac{2}{3}\pi\right) \quad (3.124)$$

$$f_4 = \cos(\vartheta 1) \quad f_5 = \cos\left(\vartheta 1 + \frac{2}{3}\pi\right) \quad f_6 = \cos\left(\vartheta 1 - \frac{2}{3}\pi\right) \quad (3.125)$$

In the same way multiphase and multi-winding systems can be modeled. One problem for modeling such a transformer is the determination of the input parameter for the model. A possible way is to determine the parameters of the 3w3ph transformer from the data sheet of the transformer, which are usually given in the following form.

Table 3.2. The parameters of the 3w3ph transformer

Typical data	Voltages	$U_{n1}, U_{n2}, U_{n3}$
	Apparent power	$S_n, S_{12}, S_{13}, S_{23}$
	Vector group	e.g DY5
	Short circuit voltages	$u_{k12}, u_{k13}, u_{k23}$
	Short circuit voltages (resistive)	$u_{r12}, u_{r13}, u_{r23}$
	No load excitation losses	$I_0$ [%]
	Iron losses	$P_0$ [MW]

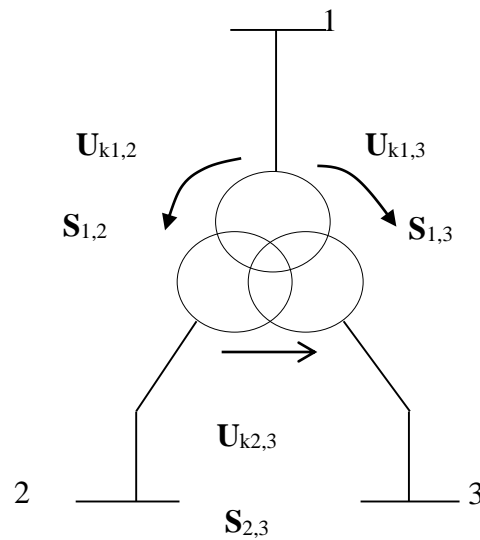


Figure 3.39. Simplification of 3w3ph transformer

The coupling between the 3 windings of the 3w3ph transformer shown in Figure 3.39 is separated into three single equivalent diagrams Figure 3.40 in order to understand the interpretation of the typical data set. The typical data describe usually the coupling between the different windings and therefore the derived parameters are always a mixture of both windings. For the 3w3ph dynamical transformer model the individual parameters per winding have to be achieved. However, it is not exactly possible, but they can be estimated with assuming a star connection of the windings. The parameters though can be used later on in the general model as described above.

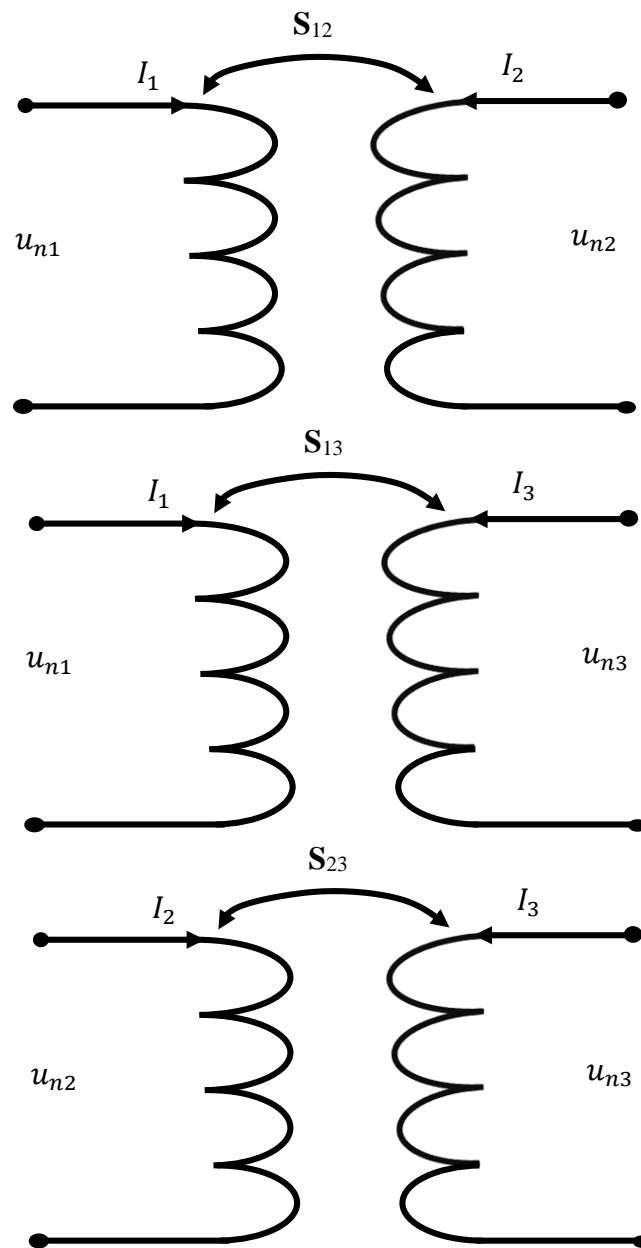


Figure 3.40. Simple equivalent circuit of a 3w3ph transformer

The parameters related to the primary side can be calculated as followed:

$$Z_{k12} = \frac{u_{k12}}{100\%} \cdot \frac{U_1^2}{S_{12}} \quad [\Omega] \quad Z_{k12} = Z_{k1} + Z_{k2} \quad (3.126)$$

$$Z_{k13} = \frac{u_{k13}}{100\%} \cdot \frac{U_1^2}{S_{13}} \quad [\Omega] \quad Z_{k13} = Z_{k1} + Z_{k3} \quad (3.127)$$

$$Z_{k23} = \frac{u_{k23}}{100\%} \cdot \frac{U_1^2}{S_{23}} \quad [\Omega] \quad Z_{k23} = Z_{k3} + Z_{k3} \quad (3.128)$$

$$R_{13} = \frac{u_{kr13}}{100\%} \cdot \frac{U_1^2}{S_{13}} \quad [\Omega] \quad R_{13} = R_1 + R_3 \quad (3.129)$$

$$R_{12} = \frac{u_{kr12}}{100\%} \cdot \frac{U_1^2}{S_{12}} \quad [\Omega] \quad R_{12} = R_1 + R_2 \quad (3.130)$$

$$R_{23} = \frac{u_{kr23}}{100\%} \cdot \frac{U_1^2}{S_{23}} \quad [\Omega] \quad R_{23} = R_2 + R_3 \quad (3.131)$$

$$X_{k12} = \sqrt{Z_{k12}^2 - R_{12}^2} \quad [\Omega] \quad X_{k12} = X_{\sigma 1} + X'_{\sigma 2} \quad (3.132)$$

$$X_{k13} = \sqrt{Z_{k13}^2 - R_{13}^2} \quad [\Omega] \quad X_{k13} = X_{\sigma 1} + X'_{\sigma 3} \quad (3.133)$$

$$X_{k23} = \sqrt{Z_{k23}^2 - R_{23}^2} \quad [\Omega] \quad X_{k23} = X_{\sigma 2} + X'_{\sigma 3} \quad (3.134)$$

$$Z_{k1} = \frac{Z_{k13} + Z_{k12} - Z_{k23}}{2} \quad [\Omega] \quad (3.135)$$

$$Z_{k2} = \frac{Z_{k12} + Z_{k23} - Z_{k13}}{2} \quad [\Omega] \quad (3.136)$$

$$Z_{k3} = \frac{Z_{k23} + Z_{k13} - Z_{k12}}{2} \quad [\Omega] \quad (3.137)$$

The resistance and the leakage reactance can be found equivalent to the impedance calculation. Notice though that resistances and impedances, which are calculated in this way, are only estimated artificial values and are not directly related to the real parameters. In some cases the calculated values become negative, especially if using the technique for an autotransformer.

The main flux inductance can be calculated from the no load measurement.

$$X_m = \frac{1}{I_0\%} \cdot \frac{U_1^2}{S_{12}} \quad [\Omega] \quad R_{fe} = \frac{U_1^2}{P_0} \quad [\Omega] \quad (3.138)$$

The Matrix parameter can now be determined for e.g. symmetrical geometry to:

$$R_1 = R_1 \quad R_2 = \frac{R'_2}{a'_{12}} \quad R_3 = \frac{R'_3}{a'_{13}} \quad (3.139)$$

$$L_{\sigma 1} = \frac{X_{\sigma 1}}{\omega} \quad L_{\sigma 2} = \frac{X'_{\sigma 2}}{\omega \cdot a_{12}^2} \quad L_{\sigma 3} = \frac{X'_{\sigma 3}}{\omega \cdot a_{13}^2} \quad (3.140)$$

$$L_{m1} = \frac{X_m}{\omega} \quad L_{m2} = \frac{X_m}{\omega \cdot a_{12}^2} \quad L_{m3} = \frac{X_m}{\omega \cdot a_{13}^2} \quad (3.141)$$

$$L_{12} = L_{21} = \frac{X_m}{\omega \cdot a_{12}} \quad L_{13} = L_{31} = \frac{X_m}{\omega \cdot a_{12}} \quad L_{23} = L_{32} = L_{m3} \cdot a_{23} \quad (3.142)$$

### 3.2.3. The 2-windings 3-phase autotransformer

Using the same approach as described in the sub-chapter 3.2.2, the three-phase autotransformer can be seen as a modification of the 3w3ph transformer; even it belongs to the group of 2w3ph transformers. While a 3w3ph transformer has three separated 3-ph windings, the Auto transformer has a galvanic connection between the second and third winding. This can be expressed in the equivalent diagram as shown in Figure 3.41.

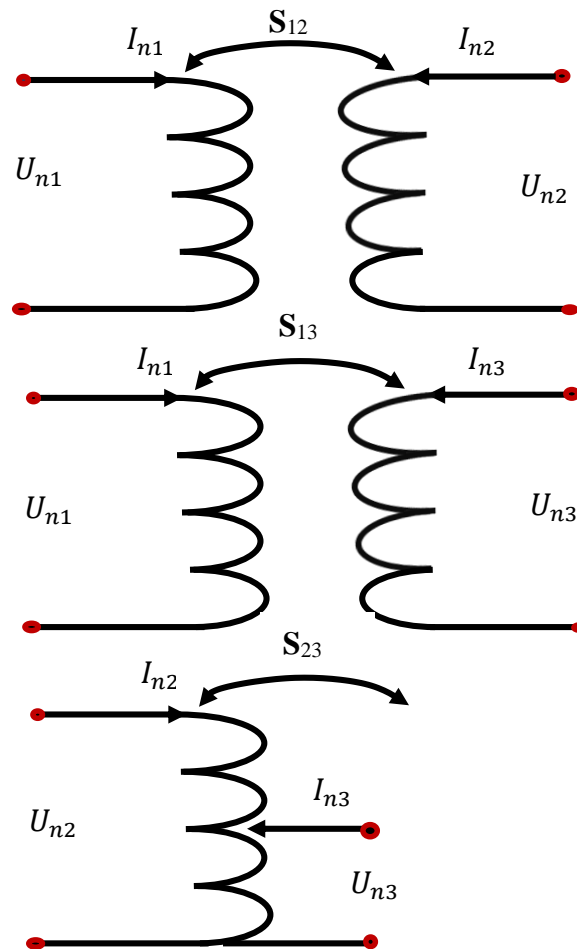


Figure 3.41. Simple equivalent diagram of the 3-ph three-windings autotransformer

The simple equivalent diagram of the 3w3ph transformer shown in Figure 3.40 has only changed the coupling between the second and third winding. In Figure 3.42 is the coupling between the second and third winding is shown separately to visualize the determination of the resistance parameters.

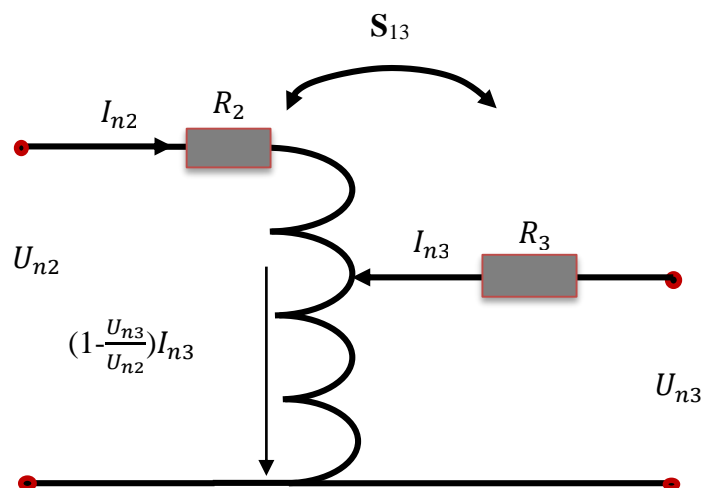


Figure 3.42. Coupling of the second and third winding in an autotransformer

$$R_{13}=R_1+R_3 \qquad R_{12}=R_1+R_2 \qquad R_{23}=R_2+R_3 \qquad (3.143)$$

If the definition of the resistances between the windings is still valid as shown in equation (125) and current between ground and the shared winding is:

$$I_{n23} = \left(\frac{U_3^2}{U_2^2} - 1\right) \cdot I_{n3} \qquad (3.144)$$

The couplings resistances between the primary and tertiary winding can be calculated to:

$$R_{13} = \left(\frac{U_3^2}{U_2^2} - 1\right) \cdot R_2 + R_{12} \qquad (3.145)$$

While the resistance of the tertiary winding is:

$$R_3 = \left(\frac{U_3}{U_2}\right)^2 \cdot R_2 \qquad (3.146)$$

Following this path the same equation set as shown for the 3w3ph transformer is deduced. The model for the 3w3ph transformer can also be used for describing the auto-transformer. The only difference is the calculation of the parameter inputs, since the parameters of winding three is dependent on the parameters from winding two.

### 3.2.4. The transformer Models Implemented in Matlab/Simulink

The 2w3ph transformer model as developed with the equation (3.114) is implemented in Matlab/ Simulink as depicted in Figure 3.43. In the block “Flux - current” is the 6x6 inductance matrix is programmed. The input values are the three-phase voltages of winding 1 and winding 2. The outputs are the three-phase currents of both windings.

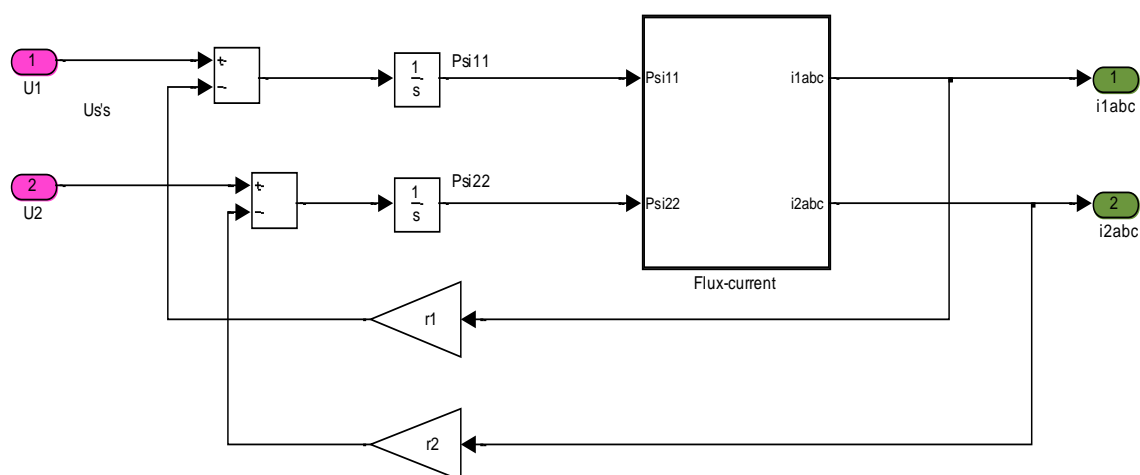


Figure 3.43. The 2w3ph transformer model in Matlab/ Simulink

Included in the model is the phase difference due to the coupling. In Figure 3.44 a simulation of a DY5 (delta-star) transformer coupling is demonstrated. The primary and secondary voltage refer to their rated values at a no load simulation is shown. The 150-degree phase difference for the 50 Hz signals is clearly visible.



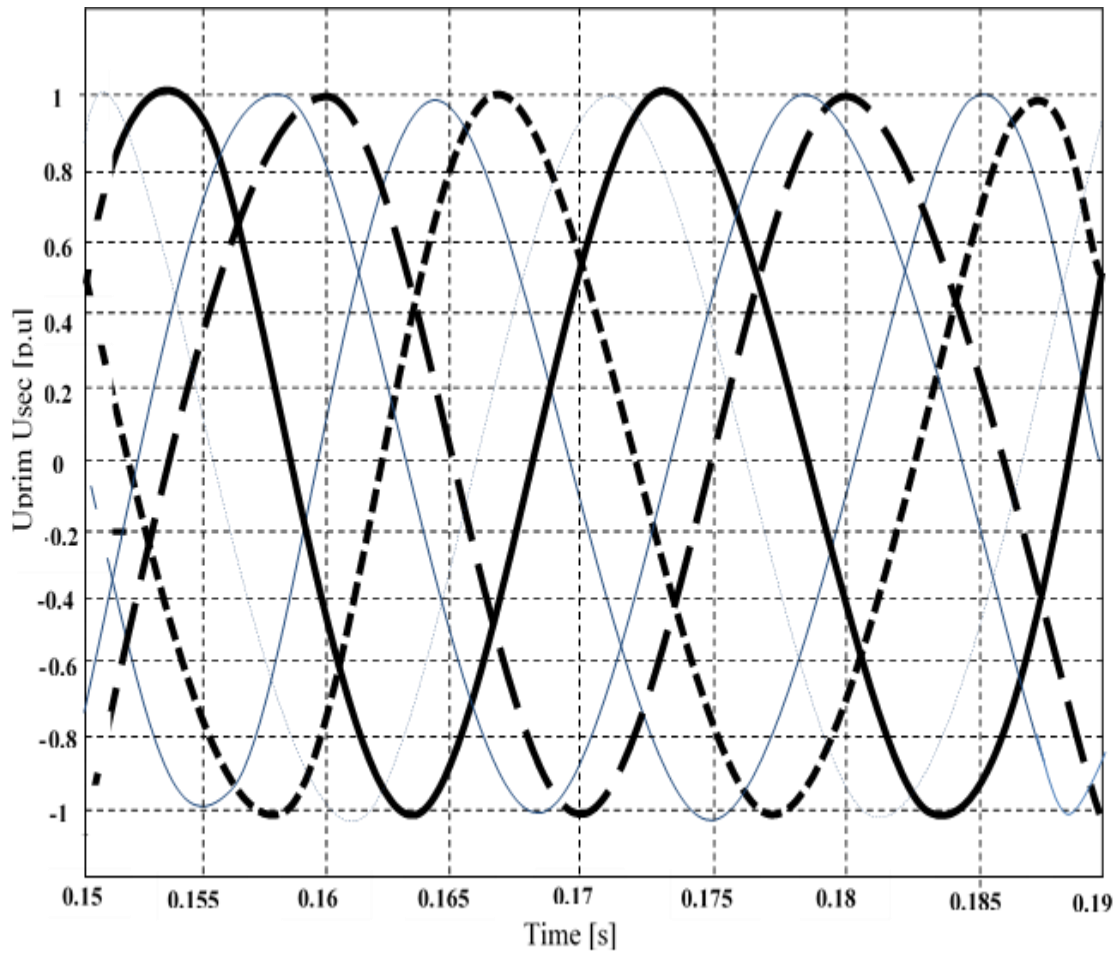


Figure 3.44. Phase difference primary (thick line) and secondary (thin line) voltage simulating a DY5 2w3ph transformer

In Figure 3.45 and Figure 3.46 the transformer is shown at no load and loaded operation. At no load there the no load losses can be measured. The voltage is not ideal and a no load current is existing. During load the transformer voltage is decreasing at the same time the current rises.

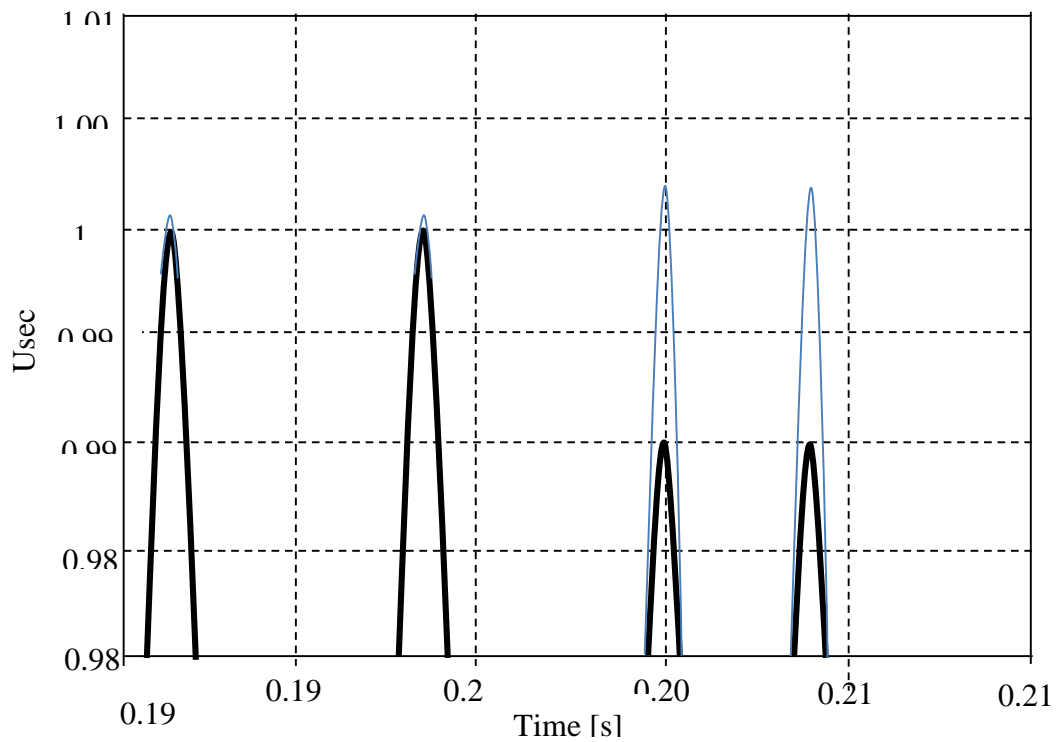


Figure 3.45. Ideal (thin line) and real secondary voltage (thick line) at no load and full loaded

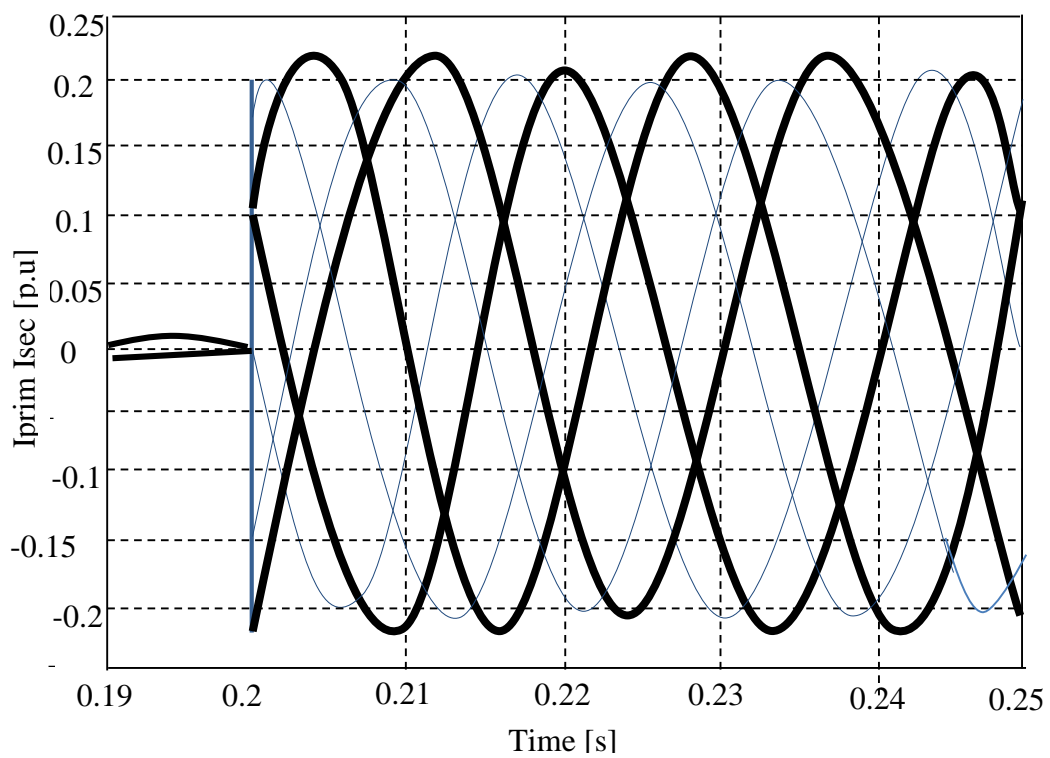


Figure 3.46. Primary (thick line) and secondary current (thin line) at no load and loaded

Typically the transformer is grounded at the star coupling of the secondary side. This grounding can be implemented in the transformer model. The ground current can be calculated as a difference between the load current and the current output of the transformer and initiate a voltage drop to ground. This potential difference is considered at the secondary voltage of the transformer. The 2w3ph transformer model inclusive with a resistive grounding is shown in Figure 3.47. The input and outputs of the model change due to the implementation. The input is now the 3-phase primary voltage and the secondary side 3-phase current. The output of the model is now the secondary 3-phase voltage and the 3-phase primary current.

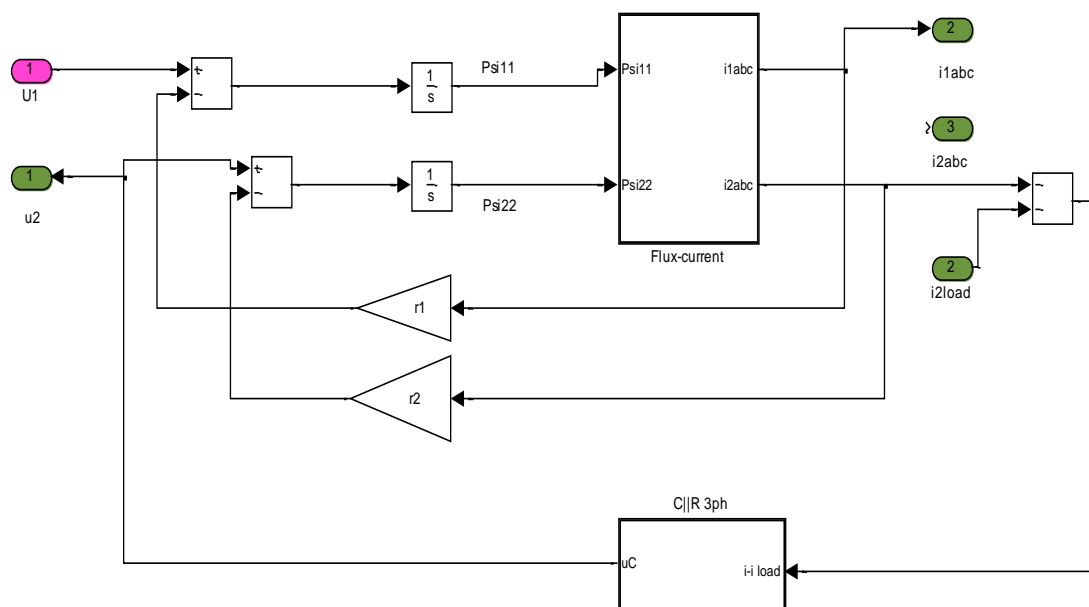


Figure 3.47. The 2w3ph transformer inclusive grounding system

The 3w3ph transformer model or the 2w3ph autotransformer model is equivalent to the 2w2ph model. The only change is the additional third input vector of the voltage and the third output representing the tertiary current. The block Flux – current now includes a 9x9 inductance matrix.

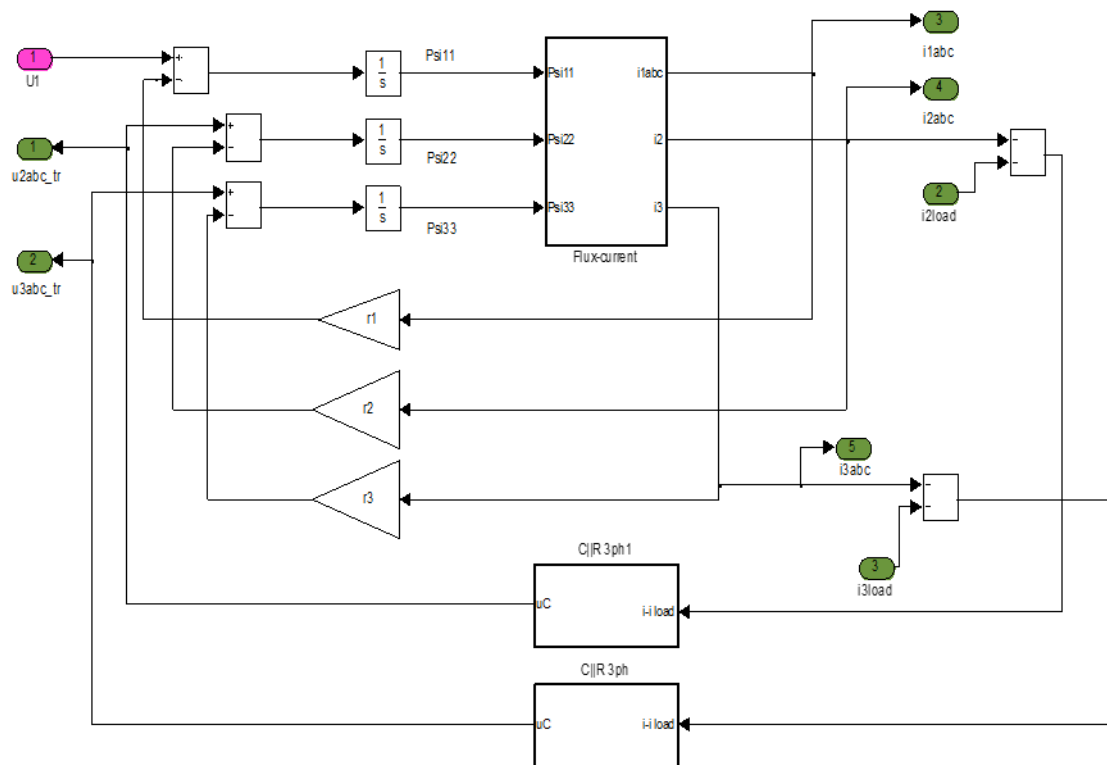


Figure 3.48. The 3w3ph transformer model in Matlab/ Simulink including star point grounding

In the same way as applied in the asynchronous generator model the main saturation can be implemented as a variable induction dependent upon from the magnetizing current. The change in the main inductance due to saturation is more than in an asynchronous generator, related to the different flux path in transformer and asynchronous generator. The beginning of the magnetizing curve characterizes the inductance of the flux through the air, while the second part of the curve characterizes the inductance influenced from the magnetizing material. Because in the transformer a huge part of the flux is coupled over the air, where contrary to the asynchronous generator which has only a minimal air gap, the curve is rising very fast in the beginning (Figure 3.49).

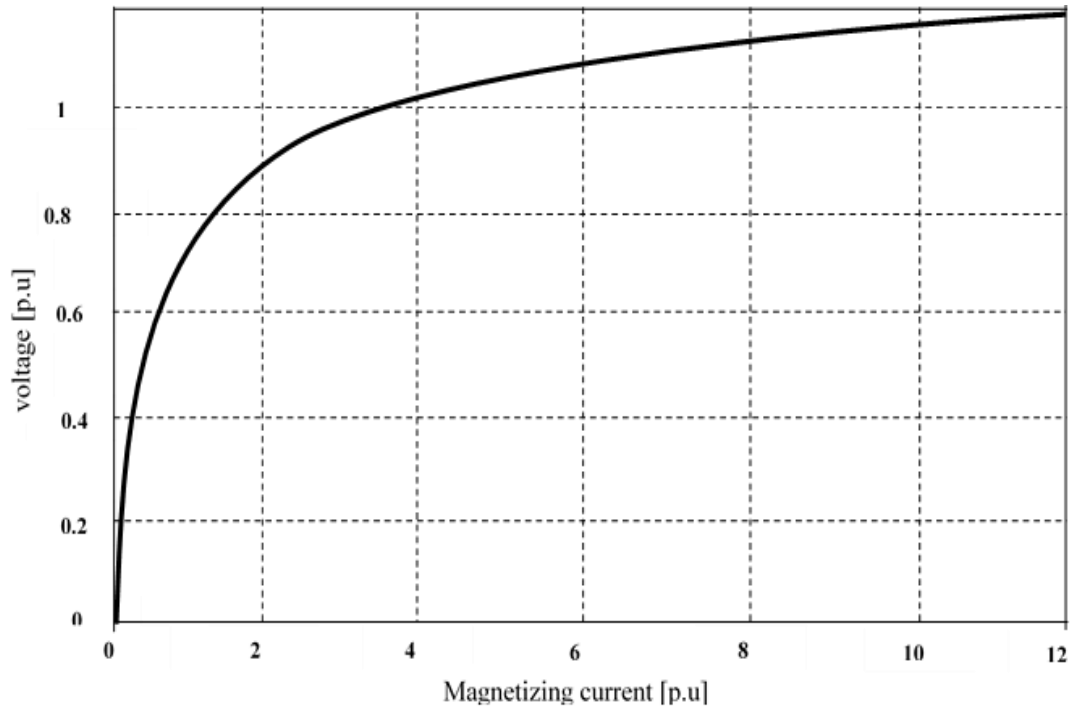


Figure 3.49. Magnetizing curve of a 2.1 MVA 3w3ph transformer related to the rated current

The magnetizing impedance can be calculated from the no load measurements. The value of the magnetizing impedance consists of an iron losses resistance in parallel to the main inductance. The magnetizing inductance can be calculated with equation (3.147).

$$Z_m = \frac{\frac{U_0}{\sqrt{3}} I_0 Z_{12}}{I_0} \quad Z_m = \frac{R_m \omega_0 L_m}{\sqrt{R_m^2 + \omega_0^2 L_m^2}} \quad L_m = \frac{1}{\omega_0} \frac{R_m Z_m}{\sqrt{R_m^2 - Z_m^2}} \quad (3.147)$$

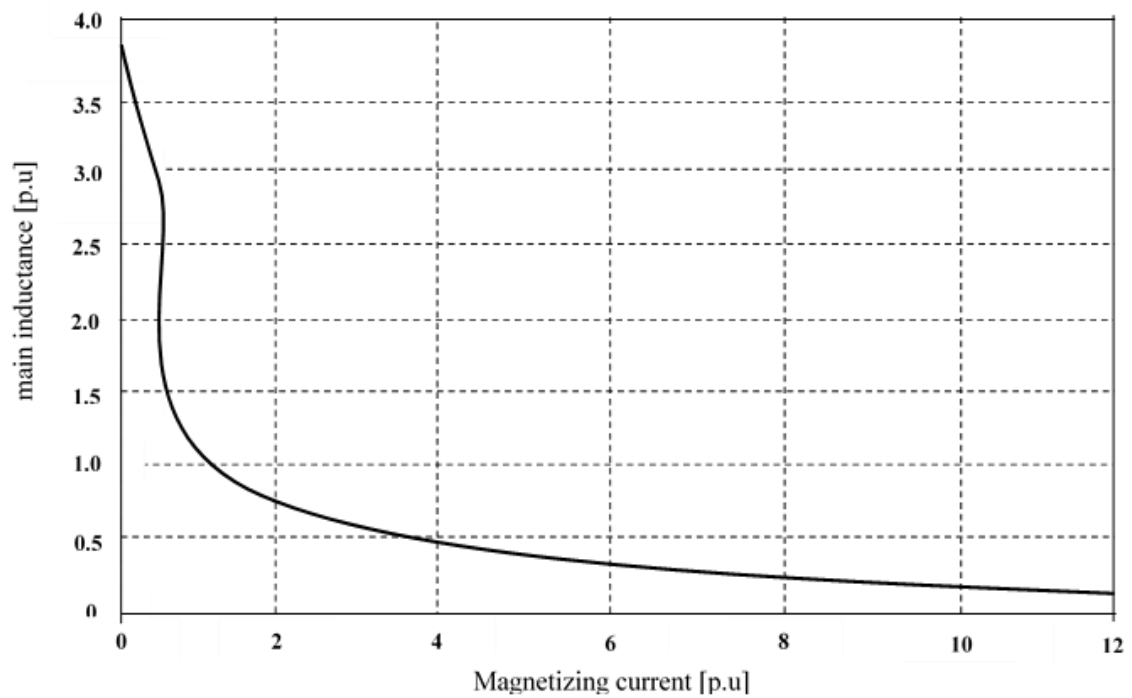


Figure 3.50. Main inductance saturation curve of a 2.1 MVA 3w3ph transformer

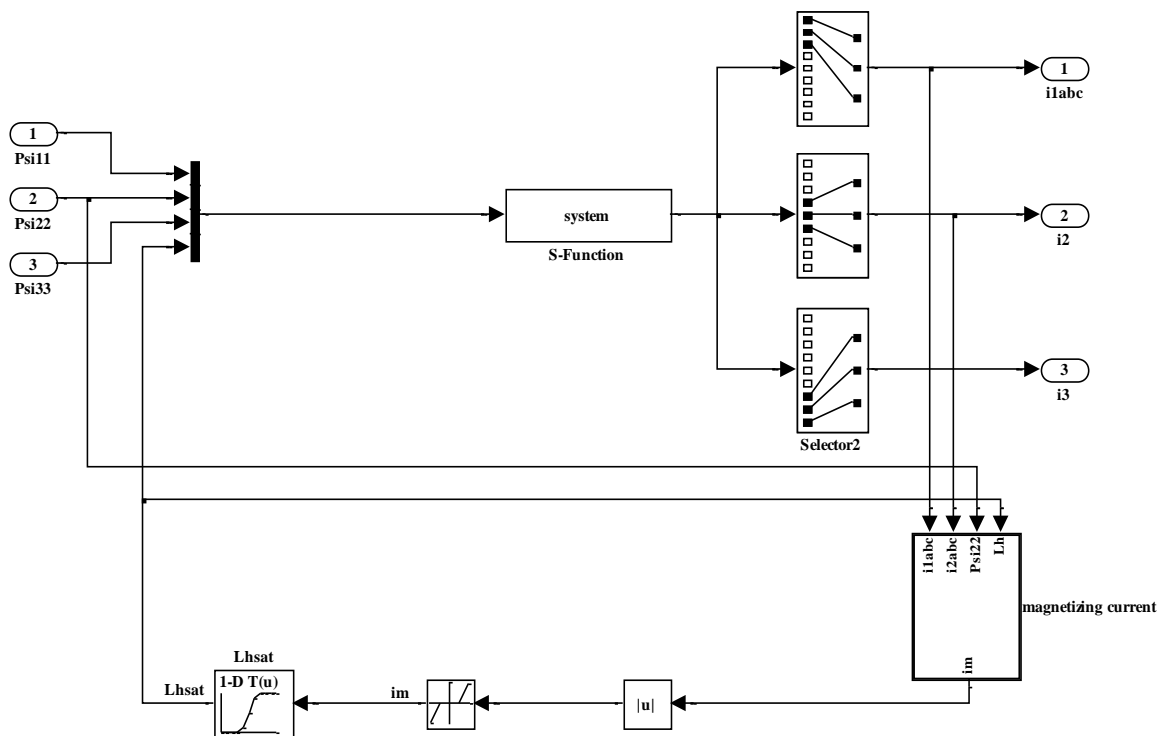


Figure 3.51. Block flux – current of a 3w3ph transformer with main saturation

The achieved generator and machine model are parts of the electrical system in wind turbine simulation. Beside these two shown components, other elements are necessary

in order to study the wind turbine's behavior during short circuits. Any small network consists of a source, line and a load. In the present case the wind turbine is the load of the network, connected to a voltage source and a transmission line or cable, which represent network dynamics. The wind turbine itself consists of different electrical elements. In the sub-chapter 3.1 developed machine model and the in sub-chapter 3.2 developed transformer model are two main parts of the wind turbine model.

### **3.3. Wind Turbine Modeling**

In the previous sub-chapters the improved models of the electrical components are described and shown. These advanced electrical models combined with the mechanical model, the aerodynamical model and control system model conclude a complete wind turbine model. In this sub-chapter the aerodynamic and the mechanic model of the wind turbine are described.

#### **3.3.1. Aerodynamic model**

The kinetic energy obtained by the blades from the wind is transformed to mechanical torque on the rotor shaft of the wind turbine. The blades are attached to the rotor shaft and rotate with the tip speed  $w_{rot} \cdot r$ , where  $r$  is the length of the blade. The blade profile experiences a relative wind velocity generated by the superposition of the tip speed and the wind velocity  $v_w$ . While wind is passing the profile it introduces lift (L) and drag (D) forces on the blade, which results in movement of the blade. From these forces the power obtained from the wind can be calculated as shown in equation (3.147).

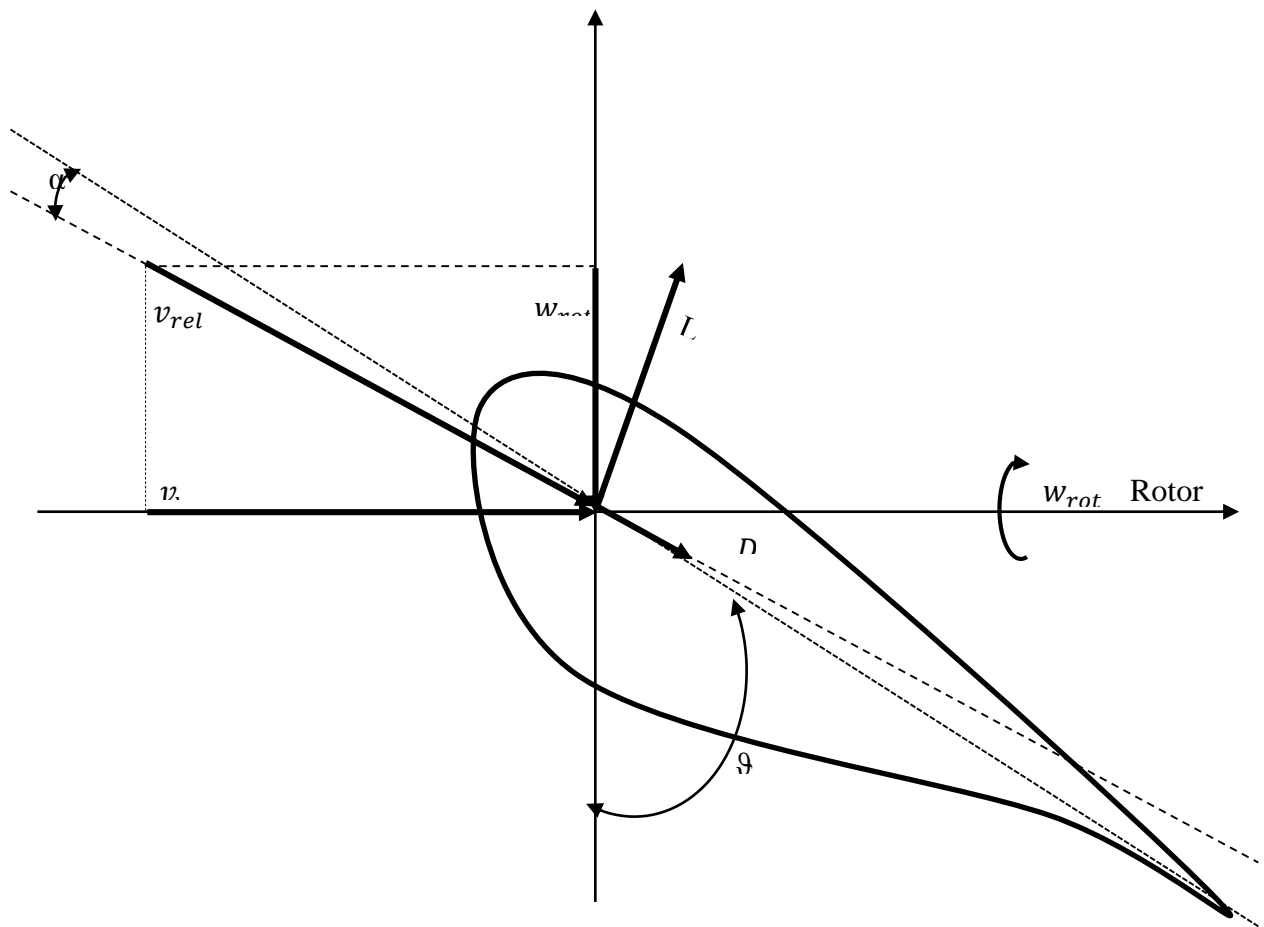


Figure 3.52. Cross section of a wind turbine blade ( $\alpha$ -angle of attack).

$$P_w = \frac{1}{2} \rho_{air} \cdot A_r \cdot c_p(\lambda, \vartheta) \cdot v_w^3 \quad (3.148)$$

Thereby  $\rho_{air}$  is the air density,  $v_w$  the free wind speed experienced by the rotor,  $A_r$  the swept rotor area and  $c_p$  the power coefficient. The power coefficient depends upon the pitch angle  $\vartheta$  (often denoted as  $\beta$ ) and the tip-speed-ratio  $\lambda$ .

$$\lambda = \frac{w_{rot} \cdot r}{v_w} \quad (3.149)$$



The tip-speed ratio is defined by the ratio of the tip speed  $w_{rot} \cdot r$  and the wind speed  $v_w$ . The power coefficient is typically given in a form of a table as shown in Figure 3.53.

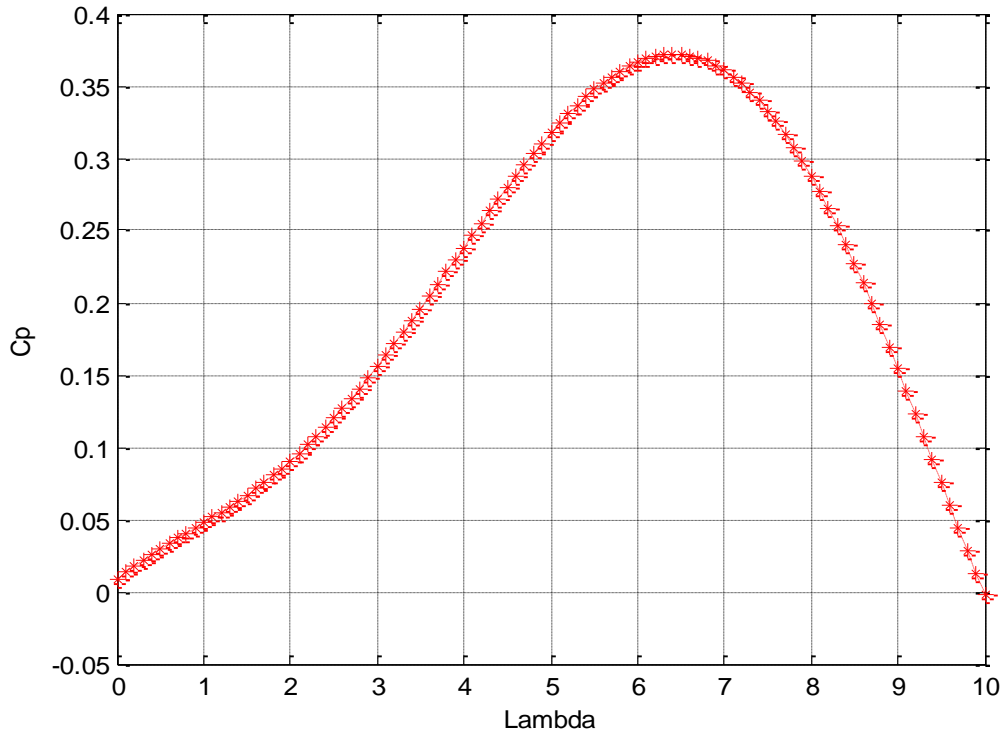


Figure 3.53. The power coefficient – tip speed ratio curve as a function of the pitch angle

The torque on the rotor shaft, which is important for the shaft model later on (Figure 3.56), therewith can be calculated from the power with help of the rotational speed.

$$T_A = \frac{P_w}{\omega_r} \quad (3.150)$$

In Figure 3.54 the implementation of the aerodynamical model is shown. Notice that the torque calculated with equation (3.150) is called  $T_{rot}$  in the picture. It is the torque which is obtained by the rotor shaft through the blades related to the low speed side of the turbine shaft.

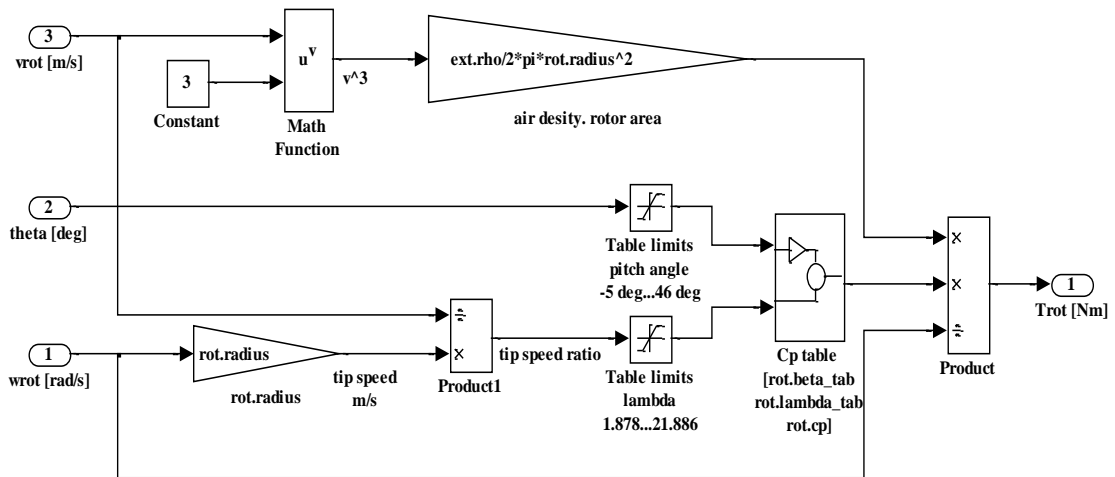


Figure 3.54. The aerodynamical model implemented in Matlab/ Simulink

### 3.3.2. Pitch model

The mechanical arrangement for pitching the blades of the turbine is later found in the Matlab/ Simulink block mechanical systems/pitch system and shown in Figure 3.55. The pitch model consists of the pitch actuator. The pitch actuator is expressed as a non-linear function between the control voltage signal and the real pitch angle. The characteristic is modeled as a non-linearity with a dead-zone.

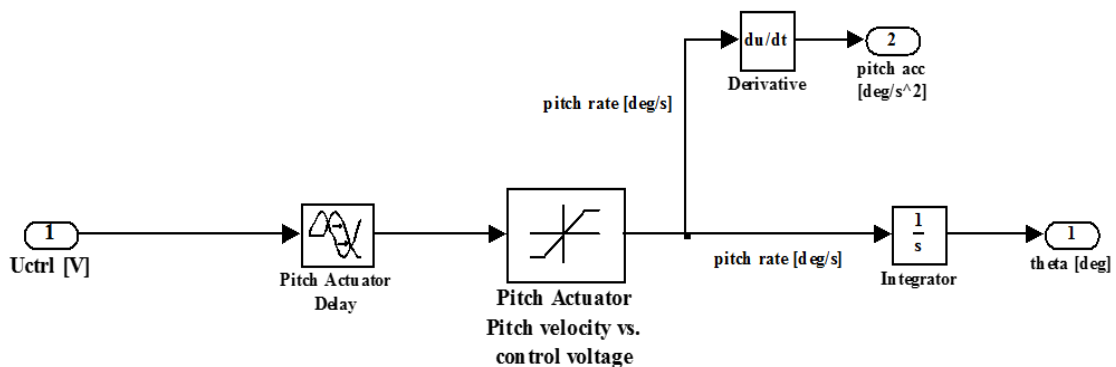


Figure 3.55. Model of the pitch system implemented in Matlab/ Simulink

### 3.3.3. Mechanical model

In this sub-chapter the simplified mechanical model of the wind turbine will be described. This dynamical model is widely accepted as expressing the dynamical behavior of the drive train for the area of research[49][57]. The simplified model of the drive train is shown in Figure 3.56. In this model all masses are lumped at the low and high speed shaft. The inertia of the low speed shaft comes mainly from the rotating blades and the inertia of the high speed shaft from the generator. Thus it is more important to include all small masses of the high speed shaft, because they have an important influence on the dynamic system due to the gear ratio transformation. The mass of the gearbox itself is insignificant and neglected. Stiffness and damping of the shaft are combined in one equivalent stiffness and damping placed at the low speed side.

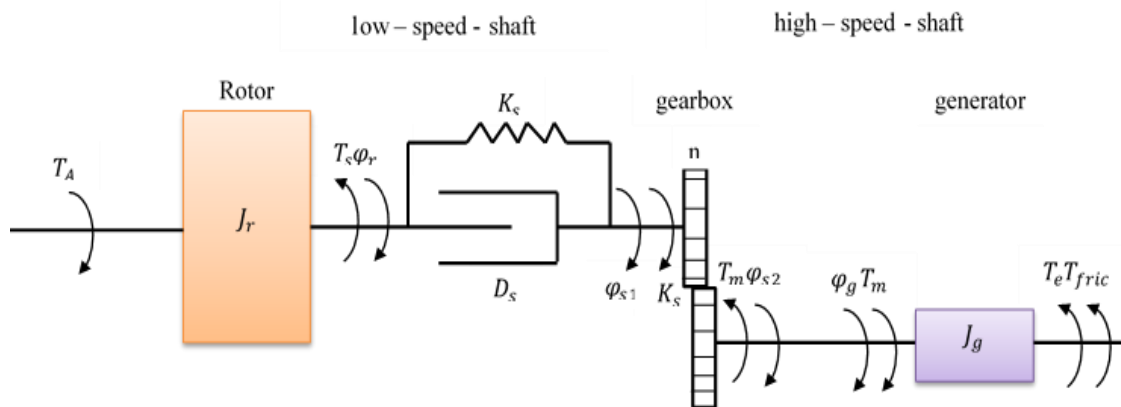


Figure 3.56. Drive train schematic for modeling of a wind turbine

Input to the model for a two mass system is the torque  $T_A$  obtained by the aerodynamic system and the generator reaction torque  $T_e$ . Output is the changes in rotor speed  $\omega_r$  and generator speed  $\omega_g$ . The high speed generator dynamics can be expressed as already shown in the description of the machine model. Please notice the sign adjustment due to generator operation. The difference of the mechanical driving torque  $T_m$ , the generator reaction torque  $T_e$  and the torque due to friction losses  $T_{fric}$  result in the change of the generator angular speed  $\dot{\omega}_g$ .

$$T_m - T_e - T_{fric} = J_g \cdot \dot{\omega}_g \quad (3.151)$$

$$\dot{\omega}_g = \ddot{\phi}_g \quad (3.152)$$

The changes of the angular rotor speed  $\dot{\omega}_r$  are caused by the difference of the aerodynamic torque  $T_A$  and the shaft torque  $T_s$  at the low speed side.

$$T_A - T_s = J_r \cdot \dot{\omega}_r \quad (3.153)$$

$$\dot{\omega}_r = \ddot{\phi}_r \quad (3.154)$$

The mechanical driving torque  $T_m$  and the shaft torque  $T_s$  are connected by the use of the gear ratio in the following way:

$$T_m = \frac{T_s}{n} \quad (3.155)$$

The dynamics of the shaft can be described with the equation (3.133)

$$T_s = K_s \cdot \Delta\phi + D_s \cdot \Delta\dot{\phi} \quad (3.156)$$

$$\Delta\dot{\phi} = \Delta\dot{\phi}_r - \frac{\dot{\phi}_g}{n} = \omega_r - \frac{\omega_g}{n} \quad (3.157)$$

Inserting the equations (133) and (134) into (3.150) and (3.150) and using the equations (3.151), (3.153) and (3.154) the equations (3.155) and (3.156) will be obtained.

The equations are used to describe the drive train dynamics.

$$\dot{\omega}_r = \frac{1}{J_r} \left( T_A - D_s \cdot \omega_r + \frac{D_s}{n} \cdot \omega_g - K_s \int \left( \omega_r - \frac{\omega_g}{n} \right) dt \right) \quad (3.158)$$

$$\dot{\omega}_g = \frac{1}{J_g} \left( -T_e - \left( D_g + \frac{D_s}{n^2} \right) \omega_g + \frac{D_s}{n} \cdot \omega_r - K_s \int \left( \omega_r - \frac{\omega_g}{n} \right) dt \right) \quad (3.159)$$

To obtain the stiffness constant  $K_s$  the eigenfrequency of the drive train has to be known. Thinking of a two mass free swinging system the eigenfrequency is defined as:

$$\omega_{0s} = 2\pi f_{0s} = \sqrt{\frac{K_s}{J_{ges}}} \quad (3.160)$$

The total inertia of the free swinging system on the low speed side can be calculated in the following way:

$$J_{ges} = \frac{J_r \cdot J_g \cdot n^2}{J_r + J_g \cdot n^2} \tag{3.161}$$

The stiffness constant of the low speed shaft is:

$$K_s = J_{ges} \cdot (2\pi f_{0s})^2 \tag{3.162}$$

The damping constant of the shaft  $D_s$  can be obtained with help of the logarithmic decrement  $\xi_s$ . A standard approximation of the logarithmic decrement is 10%. The damping constant can be obtained according to:

$$D_s = 2\xi_s \cdot \sqrt{\frac{K_s \cdot J_{ges}}{\xi_s^2 + 4\pi^2}} \tag{3.163}$$

Figure 3.54 shows the drive train as described implemented in Matlab/ Simulink

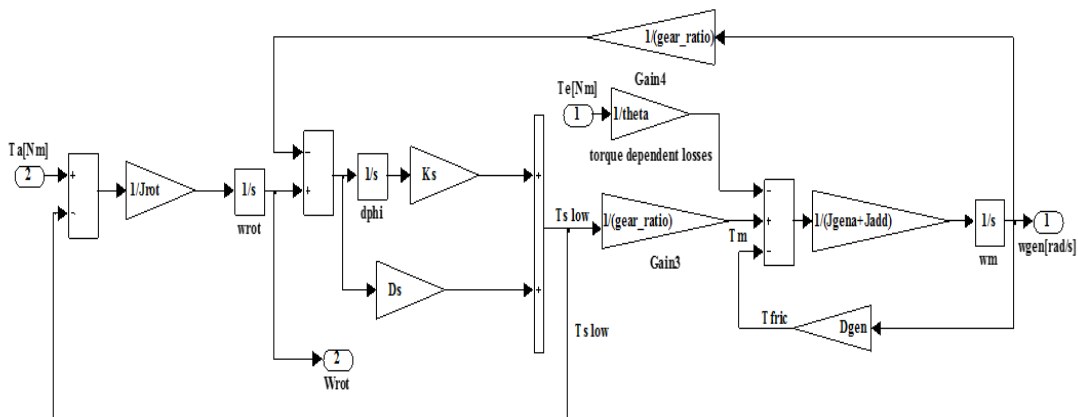


Figure 3.57. Drive train model implemented in Matlab/ Simulink

A wind energy conversion system consisting of the blades, mechanical parts, transformer and asynchronous generator was modelled. Using the presented model, the protection for wind turbine will be simulated in a simple way in Matlab/simulink. To test the performance of the proposed model, wind turbine responses both to a step increase in wind speed and blade pitch angle were investigated and simulated. In both cases, the proposed model gave valuable insight into the performance of the variable speed

wind turbine. As a normal dynamic simulation time step was adopted, this model was proven to be computationally efficient. In this thesis a detailed model of wind turbine has been developed to gain better understanding about dynamic behaviour during faults like two phase short circuits that will be discussed in the chapter 4. As a key issue, the asynchronous generator's behaviour has been investigated with a detailed three phase model. As results that will be obtained in this thesis, the present investigations contribute to the body of research in the field of wind turbine behaviour in fault situations that will be later discussed in chapter 4 and their mathematical representation. The main contributions have presented the methods for comparing different grid connection requirements, Presentation of the perspective of network operators as well as the wind turbine manufacturer has been made, emphasis of important points for the development of wind turbine grid codes has been also made, analysis of different analytical asynchronous machine representations has been made, an advanced three phase ABC/abc asynchronous machine model has been developed in Matlab/ Simulink. The model includes a representation of leakage and main inductance saturation, as well as friction and windage losses. A three phase transformer model has been developed in Matlab/ Simulink. A two-winding three-phase autotransformer has been also presented.

The results obtained during this investigation are encouraging. The potential benefits of protection for wind energy systems will be analysed; it appears that this modeling method allows for smooth wind turbine operation. Furthermore, validating the developed wind turbine model and protection with an experimental real-time implementation on an actual turbine will be very valuable. Moreover, this research is limited to the available data and further validation of the model with other wind turbines, other operating points and different disturbances will be advisable. For instance, this research will be soon improved by taking into account wind gusts and other practical problems. Since this work is a first attempt to develop an explicit protection for a wind turbine, the design of a robust explicit protection is recommended as future works.

## **CHAPTER 4. WIND TURBINE PROTECTION**

### **4.1. Overview of Electrical Faults in Wind Turbine Systems**

In order to investigate and evaluate the grid faults and grid requirements impact on wind turbine structural loads, it is necessary to perform an overview on the grid faults types, on their frequency and on the grid requirements in different countries.

### **4.2. Grid Faults**

Wind turbines connected to the grid are frequently subjected to grid faults. Various grid faults occur in the electrical networks and most of them are related with the network voltage. They are usually characterised by a change in the magnitude of the voltage and by time duration. Such a mapping of the grid faults in different countries is provided in details in [58]. In this research, statistics regarding the grid faults in the transmission system of the European countries are presented and analysed. Figure 4.1 illustrates that, in the European countries excepting Turkey, the most faults per year are located on overhead lines in the period 2010-2014. According to the investigation presented in [58], in the European countries except Norway, the most faults per year in the period 2010-2014 are located on overhead lines, while the number of faults located in cables is less than 2.5% of the total number of faults. Furthermore, in these European countries, most of the faults on overhead lines in the period 2004-2010 are located on 132kV lines, while 400kV lines are less susceptible to faults. The analysis in [58] reveals also that, in European countries, the single phase fault type has the highest probability to occur compared with other fault types, as illustrated in Figure 4.1. Nevertheless, different investigations presented in [58], indicate that three phase grid faults may however have the biggest impact on the wind turbine mechanical system.

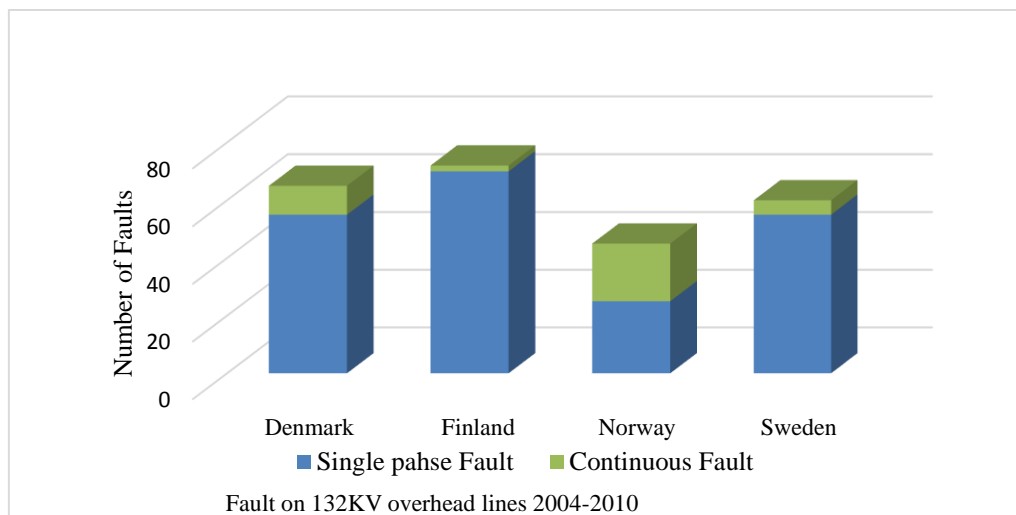


Figure 4.1. Frequency of Different fault types on 132KV overheadlines [58].

Since, the increasingly penetration of wind energy into conventional power systems, the availability of the wind turbine, and reliability of the corresponding wind energy conversion systems should be increased. This spawned active research to carry out several investigations of failure statistics in the real field since the study of wind power turbine statistics gives knowledge of reliability performance. The investigation of the statistical studies is very essential for knowledge of the most frequently failures that may aid in the system maintenance planning and reconsidered the used protection schemes.



### 4.3. Protective Design for Wind Farm

#### 4.3.1. Protection functions

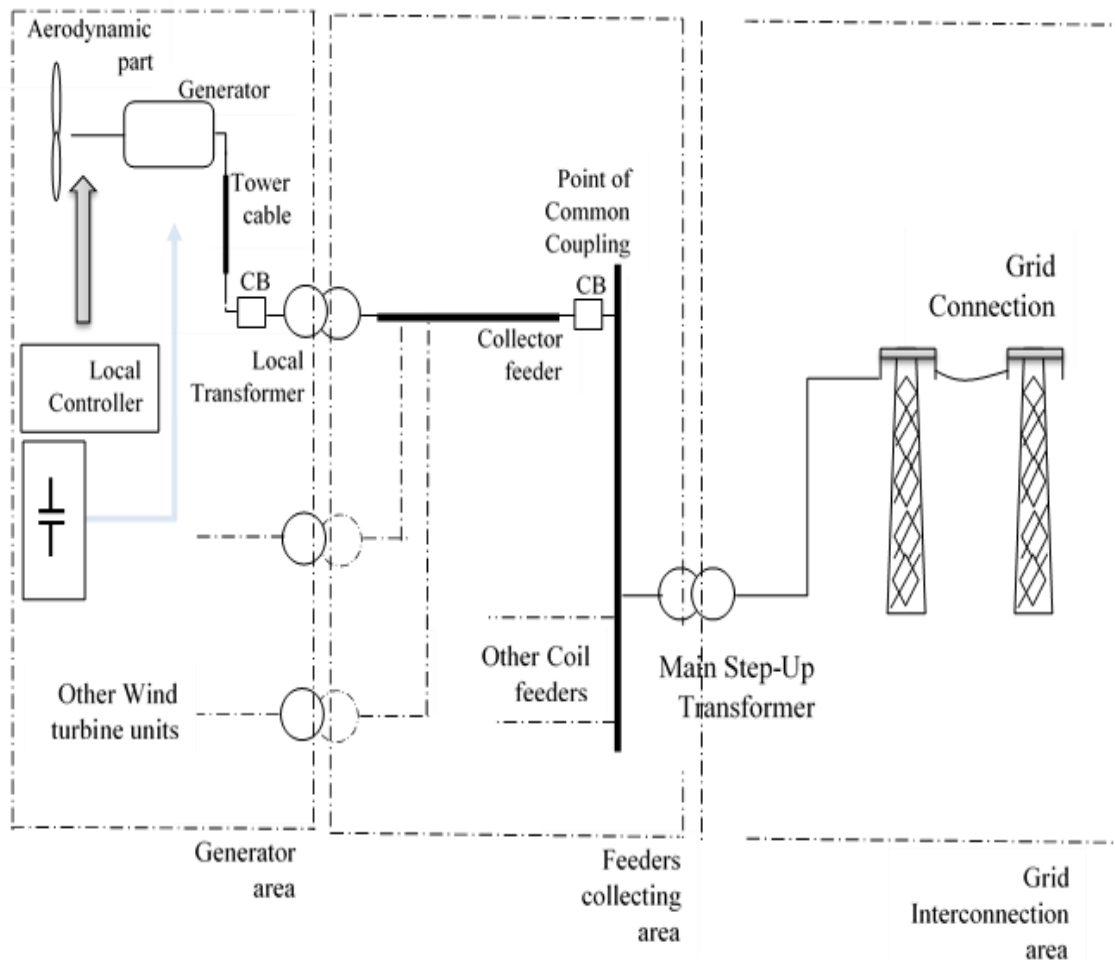


Figure 4.2. Typical wind farm construction with its protection zones.

Figure 4.2 shows a schematic diagram of a typical wind farm consisting of (n) units of wind turbines. Nowadays, modern wind farms include 20 to 150 units with typical size from 0.5 MW to 1.8 MW wind turbine generators. Larger sizes up to 3 to 5 MW are recently available in the world market, in which they were successfully installed in some European countries. The typical generator's terminal voltage which may range from 575 to 690 V with frequency of 50 Hz according to IEC standards. The generator terminal voltage is stepped up to the Collector Bus system with typical voltage of 34.5 kV. The step up transformer is an oil cooled, pad mounted located at the base of the

wind turbine unit. Sometimes, the step up transformer is mounted in the turbine nacelle. Certain considerations should be applied for avoiding the harmonic effects. The typical wind farm collector system consists of a 34.5 distribution substation collecting the output of the distributed wind turbine generators through the incoming feeders. Usually, the reactive power compensation units are provided by a collection of switched capacitors. Finally, the collected power is transferred to the utility side via an interconnection step up transformer [59], [60]. The common type of the wind turbine generators that are commercially available nowadays are asynchronous generator that are also commonly known as induction generator (IG), wound rotor synchronous generator (WRSG), and permanent magnet synchronous generator (PMSG). This research report that due to the uncontrollable natural characteristic of wind speed, the induction generators IGs are suitable for driving the wind turbines. The two basic types of wind turbines used nowadays are fixed-speed wind turbine (FSWT) that equipped with squirrel cage IGs and variable-speed wind turbines (VSWT) equipped with doubly fed IG (DFIG). Squirrel-cage induction generators work normally within a limited wind speed range, which is one of their main drawbacks in comparison with variable-speed ones. Variable-speed wind turbines are mainly equipped with a doubly-fed induction generators (DFIG) with variable frequency excitation of the rotor circuit. The stator windings are connected directly to the AC grid whereas the rotor windings are coupled through a partial scale back-to-back converter as In Figure 4.2. The main advantage of DFIG wind turbines is their ability to supply power at a constant voltage and frequency while variations of the rotor speed. The concept of DFIG for variable-speed wind turbine provides the possibility of controlling the active and reactive power, which is a significant advantage as regards grid integration. The wind farm protection system is usually divided into different protection zones including the wind farm area, wind farm collection system, wind farm interconnection system and the utility area. First, the asynchronous generator protection is typically accomplished via the generator controlling system covering some certain protection functions such as under/over voltage, under/over frequency, and generator winding temperature (RTDs). Whereas, the generator control system does not contribute for the interconnecting system or the utility zone. The generator step up transformer is usually protected with primary fuses. For those cases when the transformer is mounted in the nacelle, a circuit breaker is integrated with dedicated phase and ground time-overcurrent relays. The collector feeder

protection is simplified considering it as a radial distribution feeder using overcurrent protection (50/51). A basic challenge arises due to the distributed generators connected together to the radial feeder in determining the minimum faulty zone. That is in order to keep the remaining sound parts of the farm supplying the power. On the other hand, the protection of the wind farm substation collector bus and main power transformer consists of multi-function numerical relay system including main transformer differential relay, transformer backup overcurrent relay, collector bus differential relay and breaker failure relay. Further details are available in the literatures. Considering the utility area, different protection functions may be used according to the voltage level and the considered protection topology. Direct transfer trip scheme, line differential relay, pilot protection, zones distance relaying, over/under voltage protection, over/under frequency protection, breaker failure protection, synchronous checking and backup overcurrent protection can be used [59], [60]. Taking into consideration that, the wind farm interconnection would be applied to MV distribution network or HV system, the coordination of utility relays and the wind farm will be therefore quite different.

Communication system with dedicated SCADA system is quite important for wind farm operation. Nowadays, the data from each wind generator control is transmitted via optic cables and spread the substations for general control and monitoring purposes. This provides an ideal situation for providing them with an integrated monitoring and protection system.

#### **4.3.2. Rotor Protection System**

Historically grid codes allowed the wind turbines to be disconnected instantaneously with voltage sag below .8 per unit. In 2007, TEİAŞ (Turkish Electricity Generation Corporation-Turkey) started the studies/activities to introduce the first ENTSO-E RG CE code requirements [61]. Before, other international wind energy associations introduced their similar codes as well. Generally speaking, the grid codes required that grid connected wind turbines should withstand with voltage sags on any or all phases in the transmission system as long as the voltage measured at the high-voltage terminals of the grid-connected transformer, or in other words at the common coupling point (CCP), remains above the predetermined level of the grid code [62]-[63]. Different

benefits are expected to be gained with ENTSO-E RG CE capabilities including enhancing the system stability and fast restoration of system service if the fault is cleared during the allowable time. These capabilities will be achieved by an adapted control strategy. The core of the crowbar operation was described by UCTE members TSOs, namely RWE, TERNA, SwissGrid, HTSO, RTE, ESO, EMS, universities and manufacturers, in addition to TEIAS and EUAS (Turkish Electricity Generation Corporation), as reported in [64]. Technically, two types of crowbar systems are known including passive and active ones. For passive ones, the crowbar consists of a diode bridge that rectifies the rotor phase currents and a single thyristor in series with a resistor  $R_{crow}$ . The thyristor is turned on when the DC link voltage  $U_{dc}$  reaches its maximum value or the rotor current reaches its limit value. Simultaneously, the rotor of the DFIG is disconnected from the rotor-side frequency converter and connected to the crowbar. The rotor remains connected to the crowbar until the main circuit breaker disconnects the stator from the network. When the grid fault is cleared, the rotor-side converter is restarted, and after synchronization, the stator of the DFIG is connected to the network [64][65]. In contrast to a conventional passive crowbar, the active crowbar is fully controllable by means of a semiconductor switch. This type of crowbar is able to cut the short-circuit rotor current whenever needed and thus the DFIG wind turbine is able to ride through a network disturbance. If either the rotor current or dc link voltage levels exceed their limits, the IGBTs of the rotor-side inverter are blocked and the active crowbar is turned on. The crowbar resistor voltage and dc link voltage are monitored during the operation of the crowbar. When both these voltages are low enough, the crowbar is turned off. After a short delay for the decay of the rotor currents, the rotor-side inverter is restarted and the reactive power is ramped up in order to support the grid.

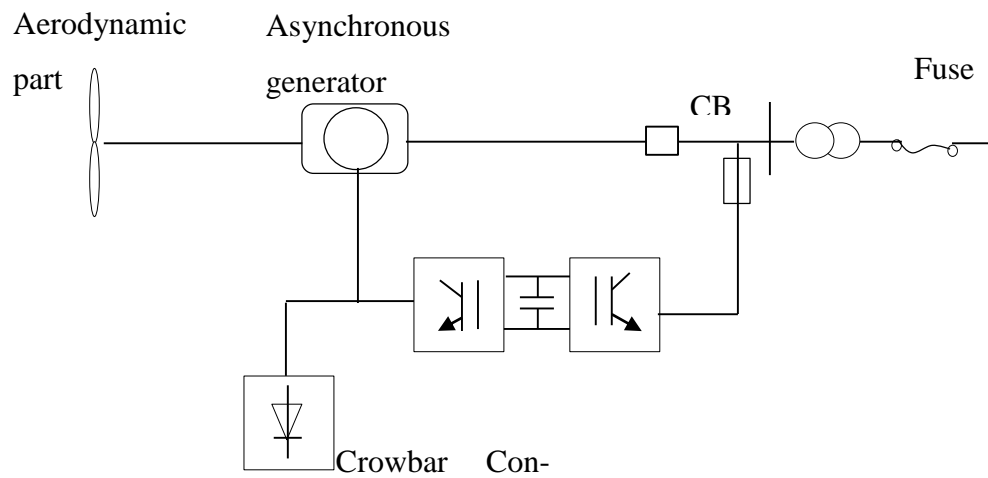


Figure 4.3. Crowbar protection system for DFIG units

Practically, crowbar mechanisms raise some problems. The crowbar ignition leads to the loss of the generator controllability through the machine side converter, since the machine rotor is short-circuited through the crowbar resistors and the machine side converter is blocked. During this time slot, the generator acts as a common single fed induction generator and consumes reactive power, which is not desirable. Hence, utilizing crowbar mechanisms has recently replaced with employing DC chopper used to limit the DC voltage by short-circuiting the DC circuit through the chopper resistors[66]. This was clearly demonstrated in Figure 4.4.

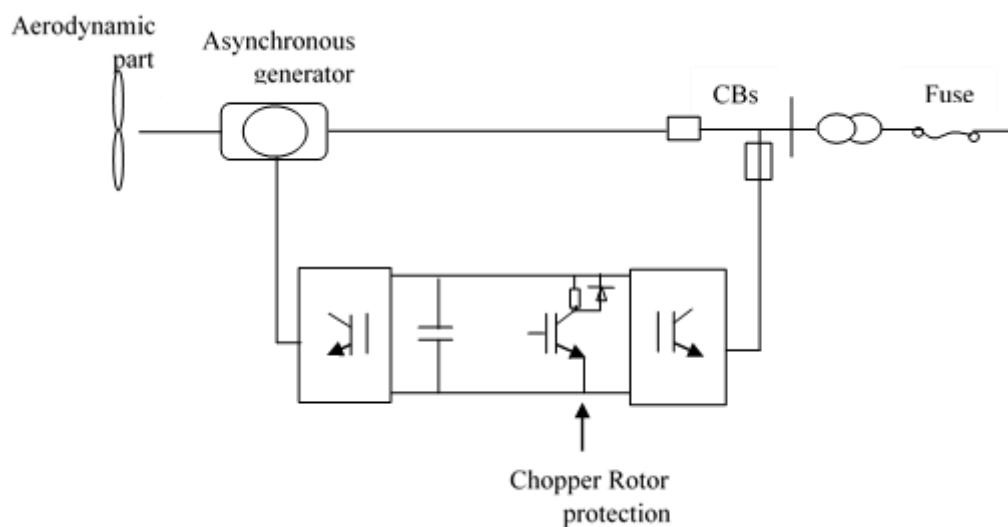


Figure 4.4. Chopper rotor protection system for DFIG units

### 4.3.3. Wind turbine controller role

Typically, each turbine set is equipped with a multi-function numerical integrated controller unit. This controller provides different control actions regarding concerning with the generator system, power factor correction, yaw operation, hydraulic system, pitch mechanism and so on. In addition to its control functions, it provides different protection

functions such as,

- a. Over/Under voltage protective relays (27/59).
- b. Over/Under frequency protective relays (81O/U).
- c. Monitoring the electrical parameters (currents, voltages, power ... etc.) and
- d. Disturbance recorders.
- e. Communication with the main control system
- f. Power flow control

The above mentioned controller unit interacts with the utilized protective elements with the generator set for providing the generator with the appropriate protection as possible. According to the manufacturer designs (or operators experience), the allowable setting for these protective elements are set. As example, some manufactures recommend to instantaneously trip the generator set for a 25% overvoltage conditions and with a 0.1 second for a 20% conditions. Also, a 0.2 second for tripping is recommended for over/under frequency conditions with  $\pm 2$  Hz frequency deviation and instantaneous tripping for  $\pm 3$  Hz frequency deviation or above.

### 4.3.4. Local step-up transformer protection

The local step-up transformer at each generator set is usually connected with DeltaGrounded Wye (or Grounded Wye-Grounded Wye) according to generator manufacturer's requirement. Current Limiting Fuses (CLFs) are commonly employed for protecting such transformer and its corresponding sub-connecting feeder for each asynchronous generator set. This is mainly due to its reliability, simplicity and low cost. This economic perspective, on the other hand, is quite essential for wind farms,

in particular, due to the massive numbers of such power system elements in large wind farms.

#### **4.3.5. Collector feeder protection**

The collector feeder is simply considered as a radial distribution. It is usually protected using overcurrent protection (50/51) element. A basic challenge arises due to the distributed generators connected together to the radial feeder in determining the minimum faulty zone. That is in order to keep the remaining sound parts of the farm supplying the power. The interconnection transformer has usually a 3-winding configuration with a grounded Wye - grounded Wye connection. The tertiary winding is connected Delta. The Delta Tertiary is used to stabilize the neutrals of the transformer and provide zero sequence current to ground fault on both sides of the main transformer bank. If a Delta-Wye transformer is used for the main interconnecting transformer, a grounding transformer may be installed on the Delta side of the transformer to provide stabilization of the transformer primary neutral. The protection for the wind farm distribution substation consists of multifunction numerical systems including a main transformer differential relay, transformer Time-Overcurrent relay for the main transformer back-up protection, collector bus differential relay, distribution Time-Overcurrent relay, and breaker failure protection. It should be considered that, the wind farm interconnection would be applied to MV distribution network, HV system and so on. Therefore, the coordination of utility relays and the wind farm will be quite different [67].

#### **4.4. Protection Challenges**

The essential benefits from the dedicated protection functions are to avoid the possible local damage resulting from incident faults and minimize the impact of these abnormal conditions on the other sound parts of the network. It enhances consequently the reliability and dependability of the overall grid performance. In spite of the obvious importance of the electrical protection of wind power plants, it surprisingly has not garnered a sufficient attention till present. The economic perspective plays a major role,

in which the enormous cost pressures usually coerce the wind farm designers for economic causes to remarkably reduce the utilized protection schemes. Different viewpoints arise as the causes for these problems as summarized below.

#### 4.4.1. Distribution system topology

The distribution connectivity nature, where infeed points are tapped sequentially from the same main feeder, may strongly influence the profile of the occurring fault. This is mainly due to the simultaneous feeding of the fault even with other unfaulted units

#### 4.4.2. System configuration protection

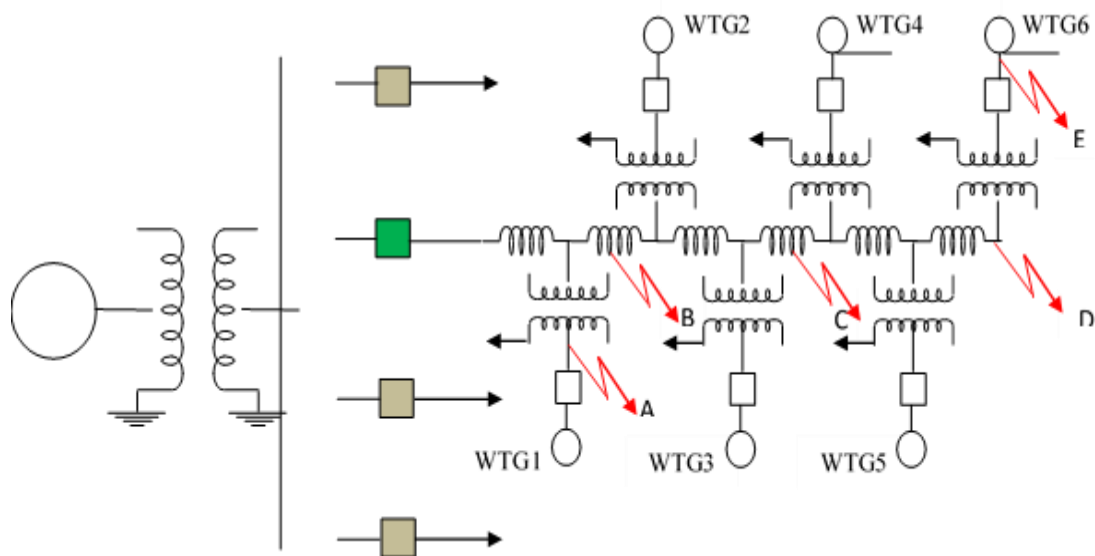


Figure 4.5. Fault location effects on the protection of the collecting feeder

The economic factor and the distribution topology of the associated electrical networks result in utilizing simple protection methodologies with the local breaker/fuse combination for each generator-transformer unit. Then discriminating and locating those faults occurring at positions A, B, C, D and E (shown in Figure 4.5) are usually lost. This results in disconnecting the whole collecting feeder for such faults.



#### **4.4.3. Distributed generation effects**

Since the collector feeder can be considered as a radial distribution feeder connecting several wind generation units, it is expected to raise those similar protection problems of common distributed generations. Relaying mis-coordination and mal-operation are the most common ones.

#### **4.4.4. Control system requirements**

Due to the impacts of the interconnection with the main power grid, some certain requirements such as "Fault Ride Through" are utilized to keep the system stability. The interaction among these operation modes and the employed relaying schemes should be considered to realize the proper and well coordinated protection performance.

#### **4.4.5. Aysnchronous generator dynamic behavior.**

This work has proved that, asynchronous machines have their own dynamic performance as compared with conventional synchronous ones. Moreover, the continuous wind speed variations and the interaction of the associated power electronics (for DFIG ones) collaborate together for providing the behavior of these machines during fault periods. More sophisticated and well coordinated relaying schemes should be provided to realize the most appropriate protection methodology for wind farm elements. Insufficient protective elements, non-integrated control scenarios and improper coordination among protective and control strategies may lead to serious problems for large grid-connected wind farms.

### **4.5. Simulated Illustrative Case Study**

#### **4.5.1. Modeling of uşak res- bereket enerji wind farm**

A 54 MW wind farm was recently established in Uşak (Aegean Region in the Western-Central Anatolia, Turkey) and connected to the 154 kV Turkish grid. This promising area (shown in Figure 4.6) is distinctive with different superior features such as an

average annual wind speed of 10 m/s, and its excellent geographical and environmental features. The farm is with fixed speed and variable pitch operation. The farm was selected for simulation purposes representing typical examples for fixed and variable speed operations respectively. Uşak RES wind farm consists of 36 wind turbines (with a 1.52MW DFIG units for each turbine) providing a total power of 1.52MW. Each wind turbine is connected to a 690V/20.3KV local step-up transformer and then integrated with the grid through 20.3/35/154KV step-up transformers.



Figure 4.6. Uşak RES- Bereket Enerji Wind Farm location

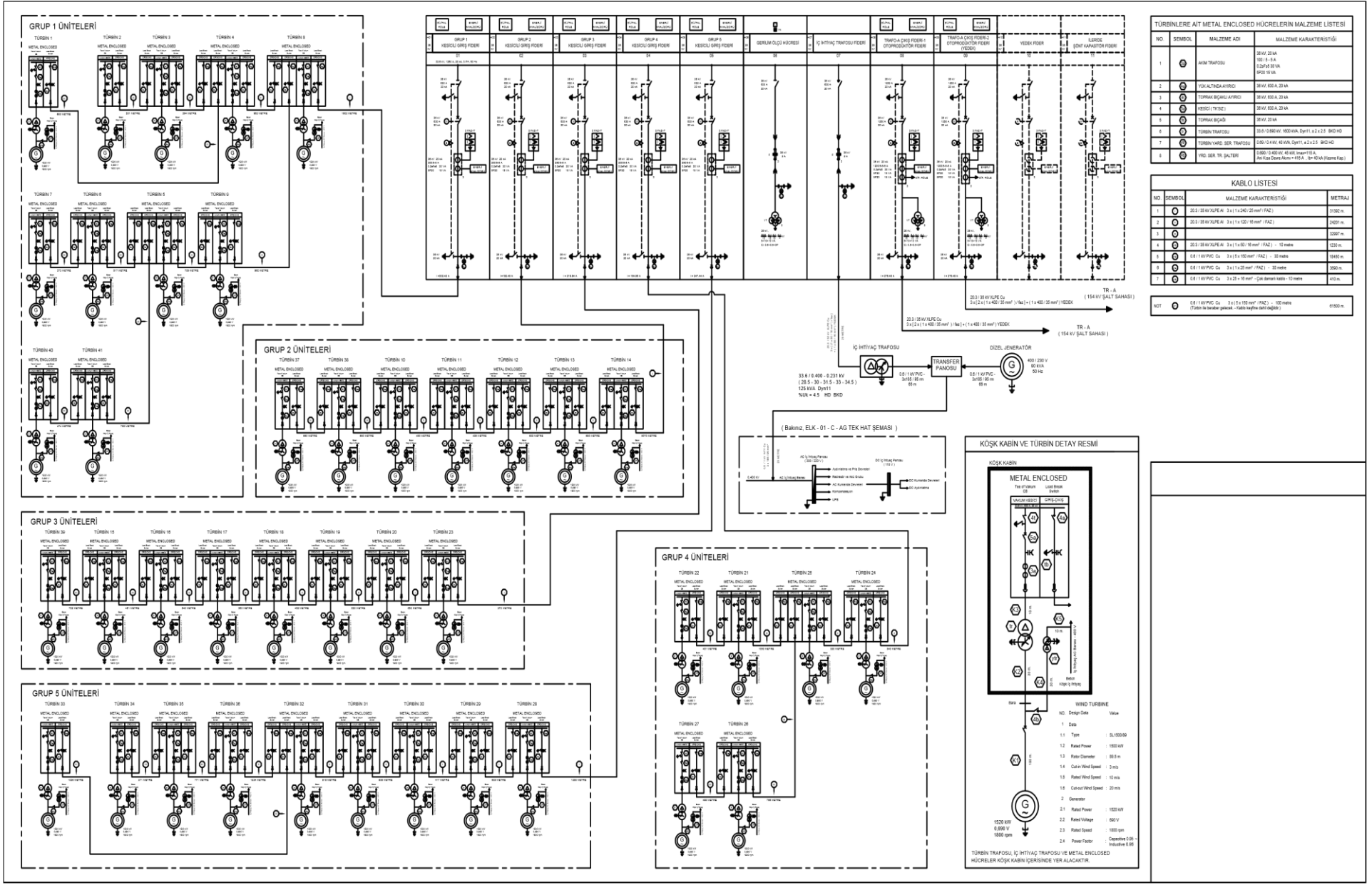


Figure 4.7. The SLD of Uşak RES- Bereket Enerji Wind Farm

The figure 4.8 show the detailed schematic of wind turbine unit constructed with the wind turbine and asynchronous machine blocks in MATLAB for DFIG. Dedicated pitch control and converter/inverter blocks are implemented as shown in the above-mentioned figures. The nominal wind speed was assigned to 10 m/s “ the annual average speed in its corresponding location”, whereas the “ cut-in wind speed was assigned to be 3 m/s”.

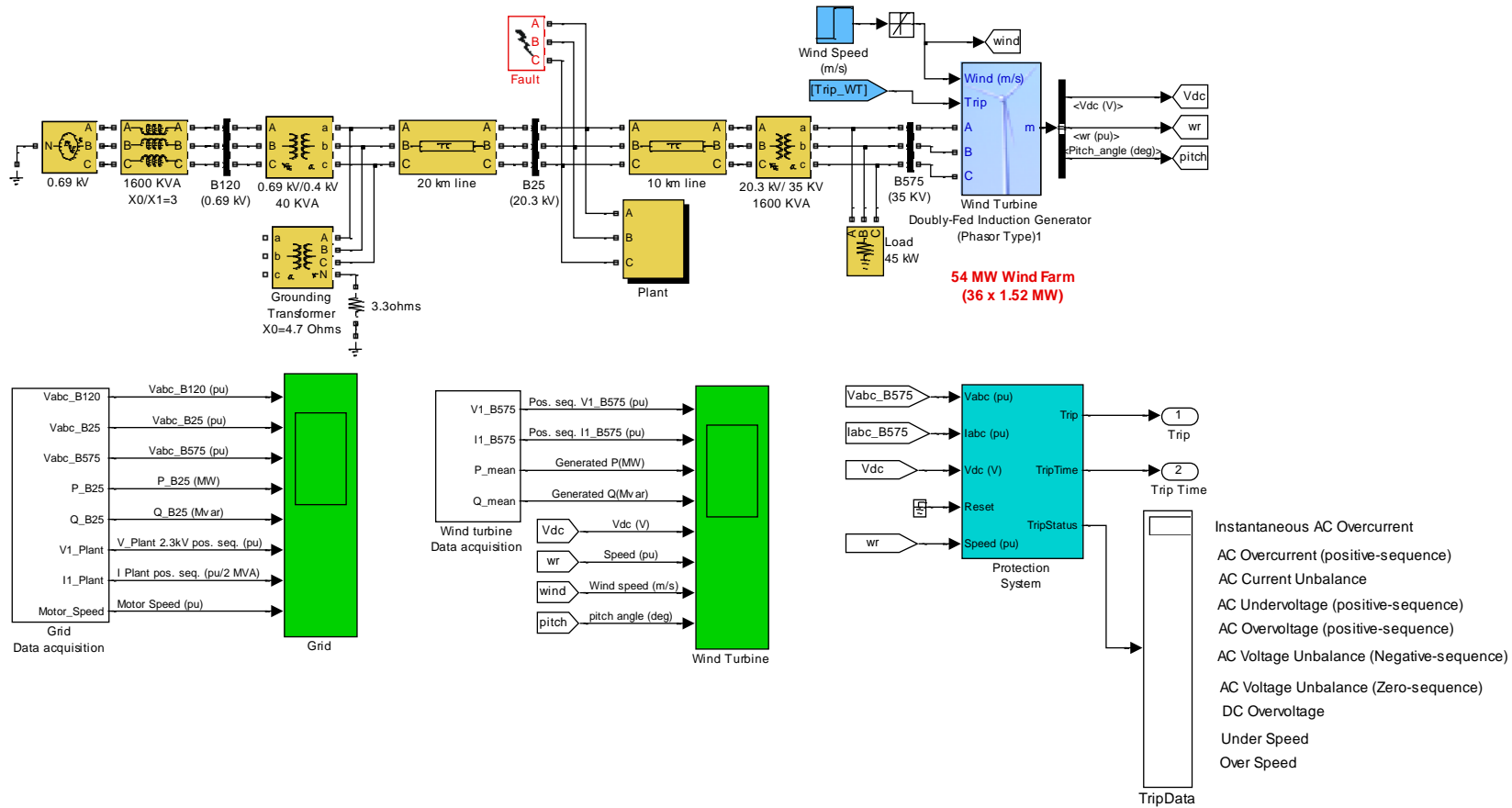


Figure 4.8. Uşak RES- Bereket Enerji Wind Farm - DFIG Detailed Model

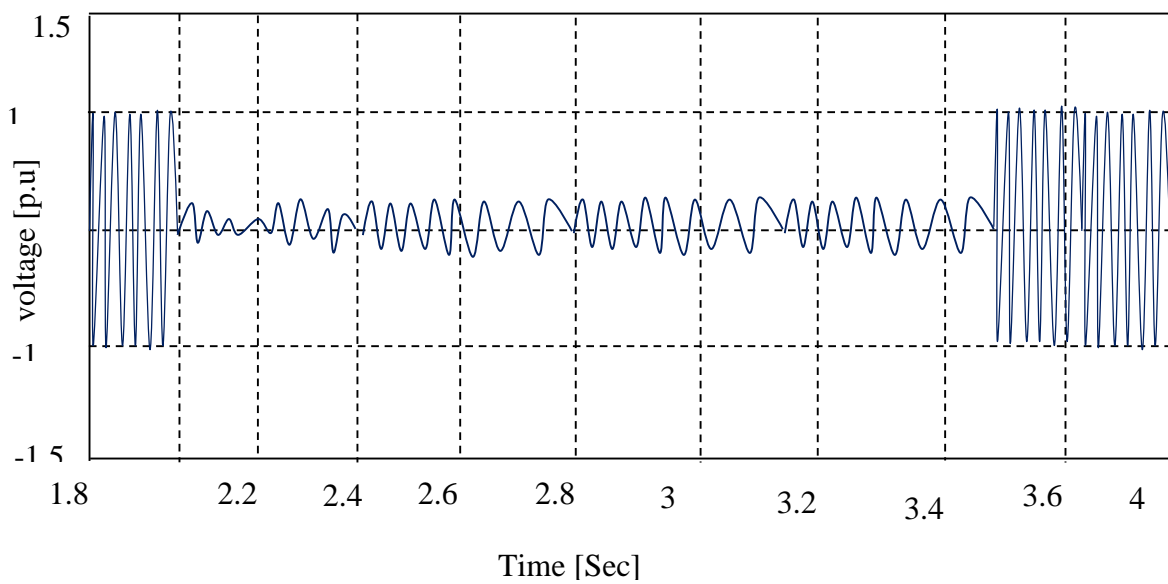
The relatively large number of Uşak RES wind turbine units, in which each of them was constructed with different individual items “Turbine, generator, local transformer, feeding cable, ...” raises the obvious need for employing a reduced modeling for the selected stages. On the other hand, reduced model should be conditioned with the following restrictions:

- a. Model Accuracy for each individual power system element should be kept in its higher level.
- b. The essential concepts for distributed generation must be satisfied.
- c. Equivalence of currents for each individual unit as well as overall farm currents for both detailed and reduced model should be realized.
- d. Equivalence of the generated power for each individual unit as well as for the overall farm for both detailed and reduced model should be realized.
- e. Total power losses (due to connecting cables) should be considered.

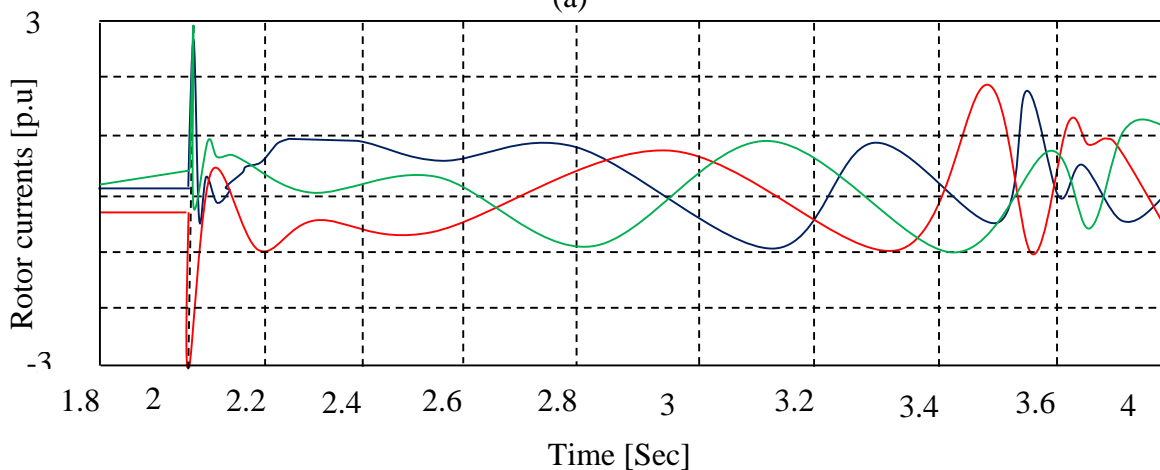
For each stage, only one collecting feeder was constructed using detailed modeling for three units (the first, second and last units), whereas other units in the same feeder were lumped by a single equivalent unit. Other collecting feeders were also represented by their total equivalent power as well. For those lumped units, cable lengths were considered for keeping the total power losses equal to those resulted with the corresponding detailed model. The response of the reduced model was validated compared with the corresponding detailed one via different simulation examples for both faulty and non-faulty operating conditions. Details for the proposed modeling methodology were fully addressed in [68]. For either simulated wind farms stages, the behavior of DFIGs were thoroughly investigated under various faulty and non-faulty operating conditions. The prepared simulation cases covered a wide variety of operating conditions including fault type, fault location, fault resistance and wind speed variations. These fault cases were prepared using the developed reduced model for both stages at different positions. For each test case, three phase voltages and currents were recorded at various locations. This facilitated to explore the overall performance of the wind farm properly.

#### 4.5.2. Performance evaluation of dfig units

Depending on the developed model of the selected Uşak RES- Bereket Enerji DFIG stage, the behavior of the modeled DFIG stage in conjunction with the related FRT mechanism was thoroughly investigated under various faulty and non-faulty operating conditions. For each case, voltage and current quantities for both stator and rotor circuitries were recorded as described in the following sub-sections.



(a)



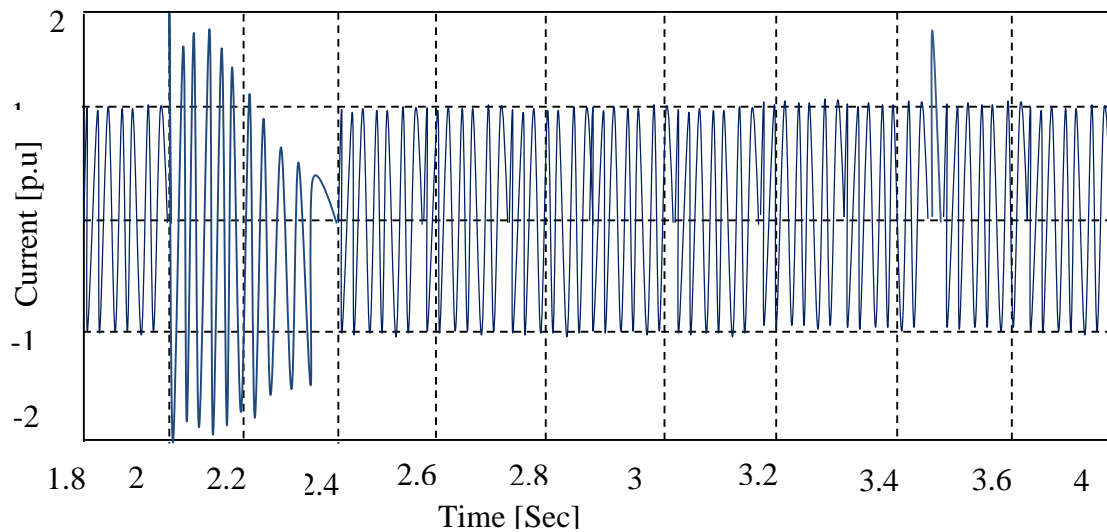


Figure 4.9. Simulation response due to a solid 3-phase grid-fault without crowbar initialization.

- (a) Stator phase voltage, pu.
- (b) Rotor phase currents, pu.
- (c) Stator phase current, pu.

#### 4.5.2.1. Grid faults

During grid faults, the occurred faults resulted in a sufficient drop of phase voltage so that the associated crowbar mechanism was initiated to protect the rotor windings from the excessive fault current. As illustrated in Figure 4.9, both rotor and stator windings suffered from the increased currents resulted from a solid three phase grid fault occurring beyond the main collecting step up transformer. The corresponding crowbar scheme was inhibited during this test case. However, the occurred current levels were not sufficient for initiating the associated fuses or local breakers at each generating unit. Utilizing the crowbar scheme resulted in rapidly decreasing the rotor currents to zero as described in Figure 4.10. As soon as the crowbar scheme was initiated as the machine reacted exactly. Hence, the stator currents we decreased to zero as remarked in Figure 4.10 (b).

Consequently the local protection at each generator set (fuses and local breakers) was blocked.



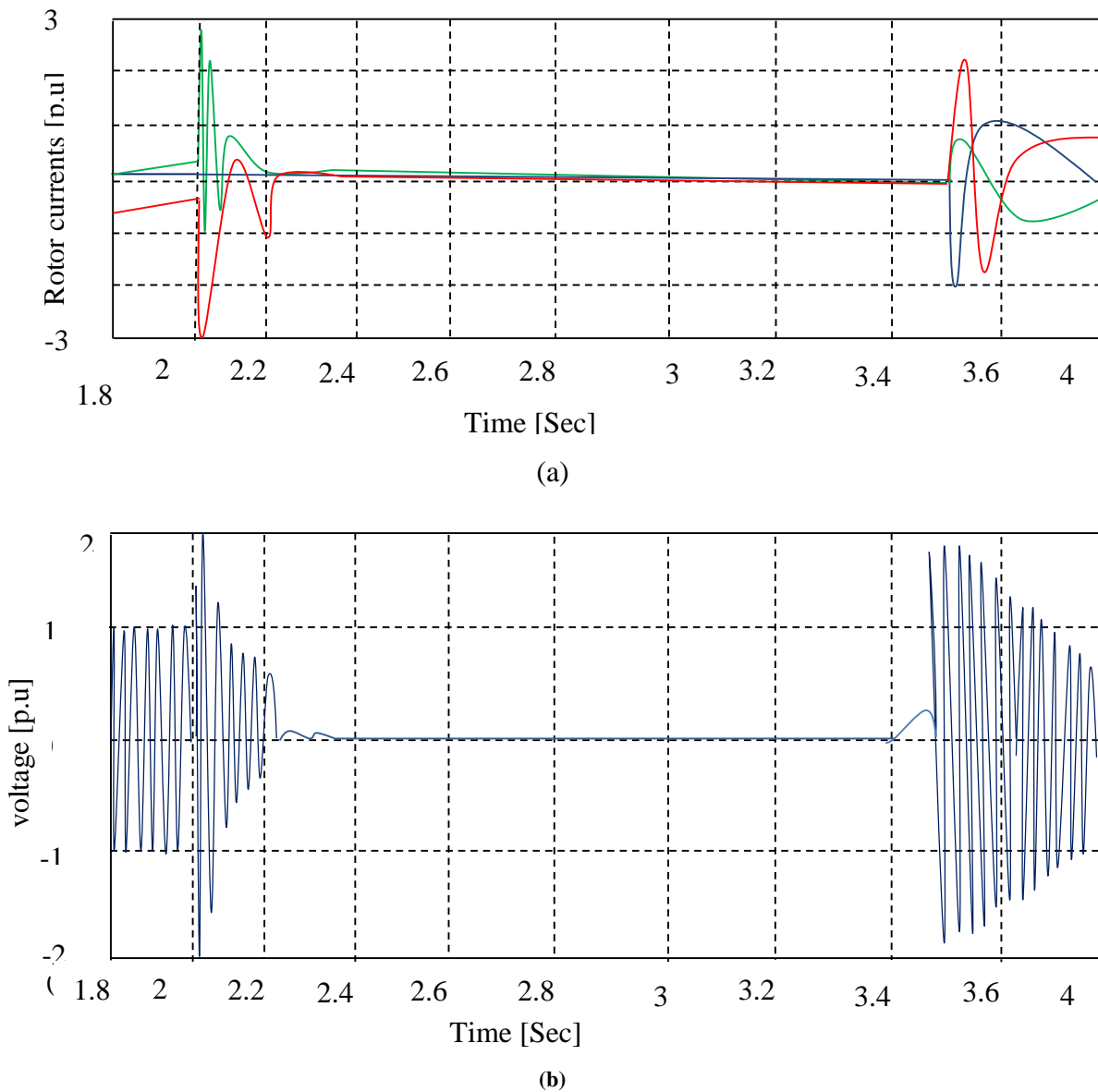


Figure 4.10. Simulation response due to a solid 3-phase grid-fault with crowbar initialization.

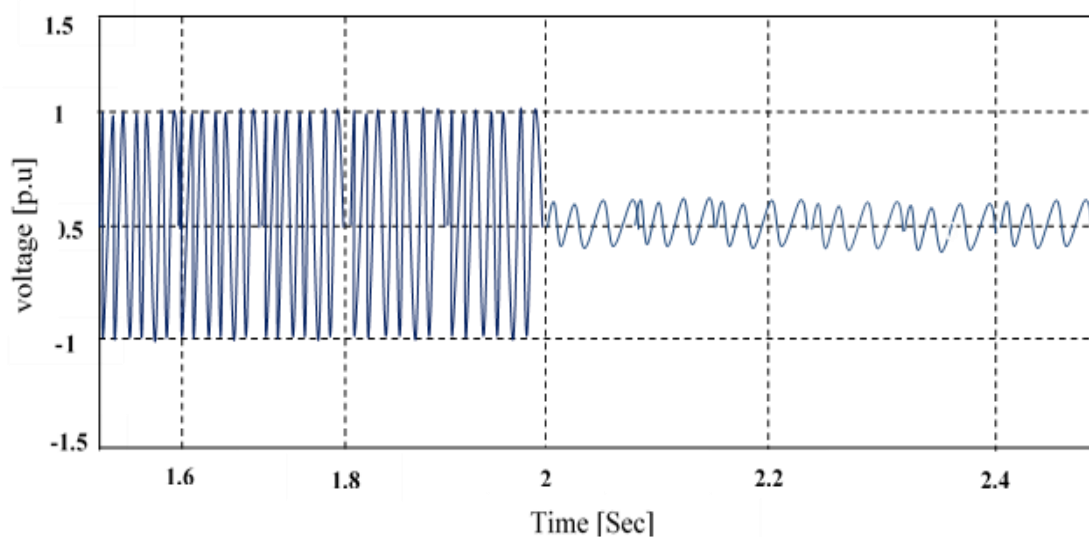
(a) Rotor phase current, pu.

(b) Stator phase current, pu.

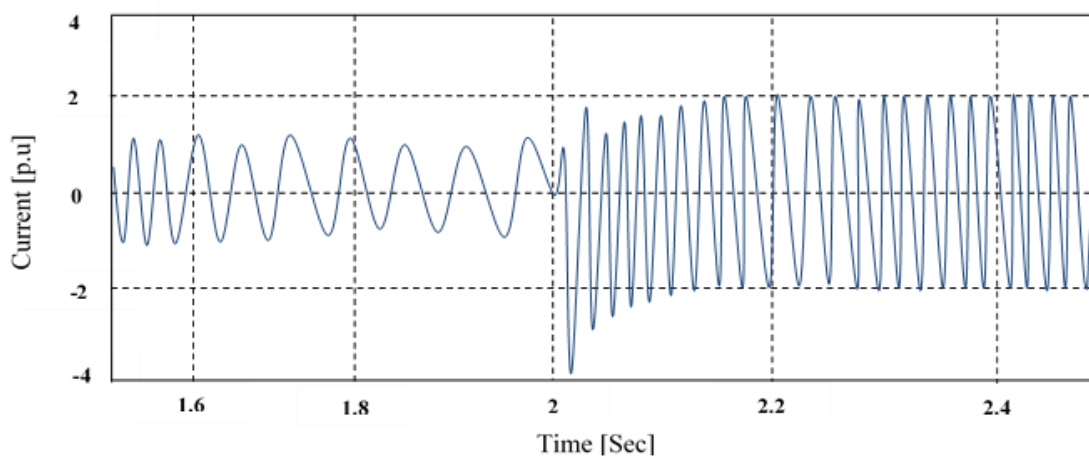
#### 4.5.2.2. Wind Farm Faults

The DFIG response for a 2-phase solid fault beyond the local step-up transformer and the fusing element was investigated in Figure 4.11. As remarked from the results, the occurred voltage drop initiated the crowbar mechanism. As noted from Figure 4.11(c), the resulted stator fault current was not enough to initialize the utilized fuse element.

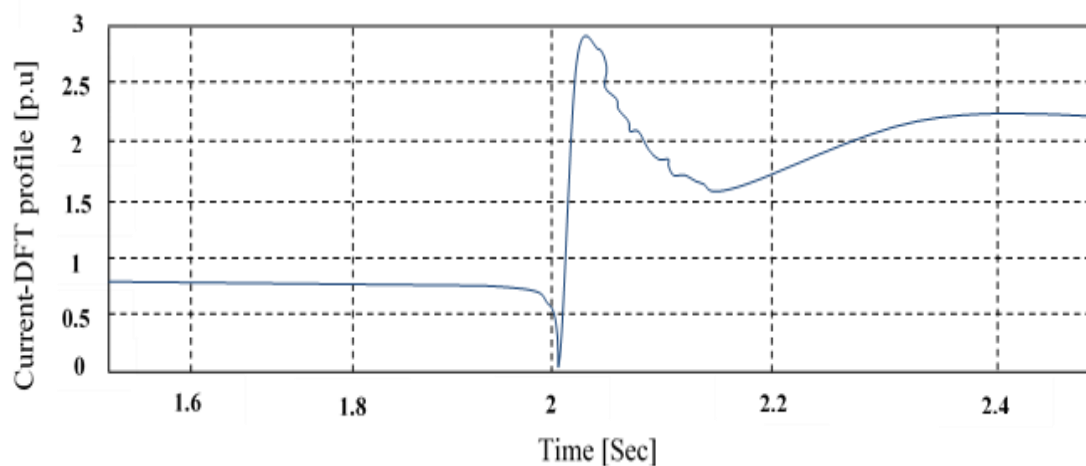
At non-solid faults usually the fault current decreases due to an increased fault resistance. These faults should be considered for evaluating the behavior of the DFIG machines equipped with FRT mechanisms. When a fault resistance is inserted into the fault current path, the decrease of the fault current is accomplished with a decrease of the occurring voltage drop at the generator terminals. Consequently, the FRT mechanism may incorrectly be initiated for faults occurring inside the wind farm. This results in inhibiting the operation of the related overcurrent protection due to the reduced fault current. This resulted in inhibiting the operation of the associated fusing element. These situations of network faults were demonstrated well in [68].



(a)



(b)



(c)

Figure 4.11. Simulation response due to a solid 2-phase fault beyond the local transformer.

- (a) Stator phase voltage, pu.
- (b) Stator phase current, pu.
- (c) Stator phase current peak profile with DFT

#### 4.6. Aims for Improving Wind Farm Protection Systems

Due to the own behavior of asynchronous generators as well as the specific topology of distributed generation concept for wind farms, employing CLFs for protecting the local transformer for each generating set was characterized with some certain shortcomings. Three different suggestions are proposed to eliminate the above-mentioned protection problems described as follows.

##### 4.6.1. Distribution network re-design

Different configurations of connecting wind turbine units were typically employed including Radial design, Single sided-ring design and double sided-ring design as described in this research. All of them are characterized with conventional distributed generation profile.

This consequently leads those un-faulty wind generators sharing the same collecting feeder to participate with the faulty unit for supplying the fault current. Larger portions

of wind turbine units may be redundantly disconnected. Redesigning this wiring connectivity may eliminate the associated problems with the conventional distribution network topology.

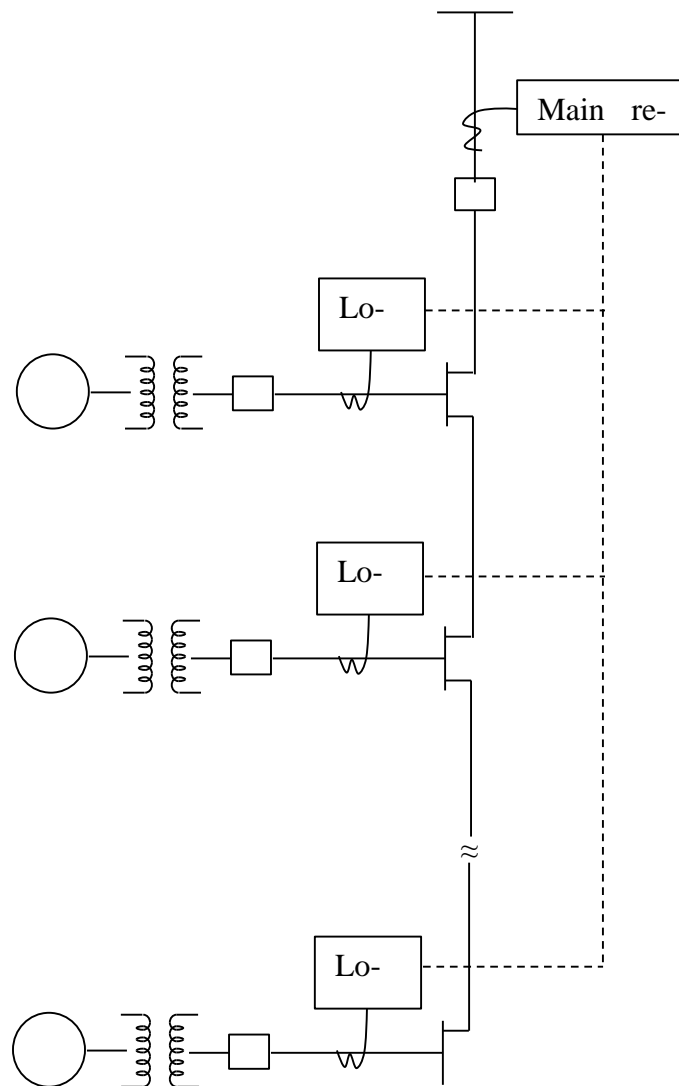


Figure 4.12. Proposed communication-based relaying employment

#### **4.6.2. Employments more protective elements**

Utilizing more protective elements may represent solutions for all highlighted problems. For instance, directional elements may eliminate the effects of distributed generator effects remarkably. Compromising between the economic prospective and the aimed performance is essential for realizing a practical and acceptable behavior.

#### **4.6.3. Integrated protection with enhanced communication employment**

The proper employment of communication facilities in conjunction with the more sophisticated and integrated protective schemes may impressively eliminate the above-mentioned problems. As described in Figure 4.12, each of the local relays at each generator unit coordinates its response simultaneously with other generating units as well as with the main protective element at the collecting bus. Fault location computation as well as the final tripping decision are then decided upon the status of these received signals. Depending on the existed communication links utilized with the used SCADA system of existed wind farms facilitates these steps.

## CHAPTER 5. CONCLUSION

In order to research and gain knowledge about wind turbine behaviour during grid faults or abnormal operations new wind turbine model has to be developed. Approximated behaviours are not sufficient for today's tasks and therefore detailed multifunctional models have to be developed. In this thesis a detailed model of the wind turbine has been developed to gain better understanding about dynamic behaviour during faults for instance two phase short circuits or voltage sags. As a key issue, the asynchronous generator's behaviour has been investigated with a detailed three phase model. This thesis emphasized also the outline of the common configuration of protective relays that are usually utilized with modern wind energy conversion systems. Electrical faults occurring into the different zones of wind farms were described. Accordingly, different problems arise with the simple and non-integrated protection schemes that are usually utilized with wind farms.

The associated challenges of those protective elements were discussed and their relevant problems were visualized. Among these problems, unwanted disconnection of wind generation units, rather than disconnecting the faulty unit only, is not acceptable. This negatively impacts the continuity and the stability of the overall system. The simulation examples were presented for demonstration purposes. These simulations were developed based on a real 54MW wind farm in Uşak RES-Turkey including DFIG configurations. For DFIGs, in particular, utilizing crowbar mechanisms may affect the behavior of conventional overcurrent protection elements against network faults occurring into the local connecting circuitry of the wind farm. The study emphasized the need for enhancing the existed protection schemes for wind farms to realize better power system performance as well as minimize the possible damages resulting from the fault occurrence. Intelligent techniques, enhancing the existed protection schemes for wind farms, redesigning the wind farm wiring topology and integrated protection schemes may play definite roles towards eliminating these problems.

## 5.1. The Work Summary

This work has focused on the development of a protected variable speed wind turbine model with an asynchronous generator to be used in normal operation as well as in fault situations. To achieve this in detail, a specific wind turbine from Bereket Energy designed by Sinovel has been implemented in Matlab/ Simulink. The models shall provide opportunities for the investigation of a wide range of wind turbine sizes and different conditions while retaining easily accessible parameters which are used as input for the model. It is important to have adequate wind turbine models for the study of grid connection conditions. In Chapter 2 a few existing grid connection requirements are discussed and compared. The basis for a realistic representation of the wind turbine and their properties is an accurate model of the generator. The third chapter introduces therefore an analytical three phase machine model and discusses the improvement achieved by considering the effects of saturation. The behaviour of the model under normal operating conditions is validated by comparison with steady state measurements, and the applicability of the machine model during dynamic fault situations is validated with a direct on line start of a machine in a test bench. It is shown, that the consideration of leakage inductance saturation of the machine is especially important during fault situations. A simulated stator current with a machine model including main and leakage inductance saturation effects shows an error of less than 2% compared to the test bench test measurements, while during high currents an error of 20 % in peak values is observed. Though a 20 % error is large it none the less represents a 10% reduction in error compared to simulations with the simple machine models neglecting any additional effects. A further reduction of the error could be achieved while including further additional affects such as proximity effect and iron losses, which are not included in this work.

In addition to the three phase generator model, the whole electrical network is depicted in a three phase system. Development of three phase models and the implementation into Matlab/Simulink turned out to be a rather challenging task. The transformations that are commonly used to simplify the mathematical representation of the system like Park Transformation are appropriate for other purposes for instance control strategy development, but inadequate for the demands on these models. Though it is certainly

possible to investigate symmetrical fault situations of wind turbines with a model system based on dq- components (i.e. the Park - transformation), it presumes very detailed knowledge about the total system configurations and has limited scope for adaptation to expansion and variations to other uses like asymmetrical simulations. Using a three phase system avoids any invalid assumptions introduced by the transformation theory and therefore introduces less error and represents more closely the physical system, which is a priority for the model. In chapter 3 the models of a three-phase two-winding, a three-phase three-winding and a three-phase autotransformer are developed, using the experiences gained from the machine modelling. The modelling method which is needed in order to connect the electrical elements generator, transformer, grid elements and source to be able to simulate the complete wind turbine were investigated but not included in this work. The development of the wind turbine model is concluded by the implementation of a model for the aerodynamics (modelling the wind obtained power, pitch of the blades and 3p- effect), the mechanical model (using two masses: representing the mass of the blades and the drive train, and including the generator axis) and the control systems. The models for the aerodynamical, the mechanical components and the control systems have been developed in different articles/papers previously and have undergone several verification processes. The main challenge encountered during this work was related to combine the existing models with the own developed advanced electrical models into an efficient complete model. Because the protection systems of the investigated wind turbine are quite different, a complete wind turbine model for the Sinovel wind turbine has been made. The protection systems of the wind turbine with a relay protection is shown and discussed in chapter. With the developed models, simulations of faults according to current grid connection requirements for wind turbine have been carried out. From the many presented requirements discussed, a two phase short circuit and a voltage sag were chosen for investigation. The two phase short circuit is an interesting case, because it occurs relatively often and presents an asymmetrical case. Further a voltage sag inside the operation limits of the turbine has been investigated. Both faults were simulated with a generator model both including and excluding saturation effects. While in the simulation of an unprotected machine, these effects play an important role, they are minimal in a protected wind turbine. In normal conditions the influence of machines saturation is minimal and can be neglected using the studied machine type. However, in fault situations the saturation



effects do have a greater influence for some machine types. The two specific examples which have been investigated do not provide suitable basis to draw a general conclusion. Because of this it is an advantage to consider saturation effects during grid fault studies until a general conclusion can be drawn.

## **5.2. Results Obtained in the Work**

The present thesis contributes to the body of research in the field of wind turbine behaviour in fault situations and their mathematical representations as well. The main contributions have been:

### **5.2.1. Overview of existing grid codes**

- Methods for comparing different grid connection requirements have been presented
- Presentation of the perspective of network operators as well as the wind turbine Manufacturer has been made.
- Emphasis of important points for the development of wind turbine grid codes is made.

### **5.2.2. Modelling and analysis of the asynchronous machine model**

- Analysis of different analytical asynchronous machine representation has been made.
- An advanced three phase ABC/abc asynchronous machine model is developed in Matlab/Simulink. The model includes a representation of leakage and main inductance saturation, as well as friction and windage losses. A discussion of the saturation influences due to faults is presented.
- Measurements on a test bench at full-scale verifies the achieved model.

### **5.2.3. Modelling of Electrical three-phase Components**

-A three phase transformer model has been developed in Matlab/ Simulink. A two winding three-phase autotransformer is presented.

### **5.2.4. Modelling of a Complete Wind Turbine System**

-The models are reliable for research in symmetrical as well as asymmetrical fault situations and short circuits due to the three phase representation of the electrical system.

-The models represent the two standard used protection and control strategies and include validated aerodynamical and mechanical models. Completed with the electrical models it is believed to have a real representation of the behaviour of the wind turbines.

-The model has particular importance for wind turbine component design and it is useful for studies of e.g. load and protection design.

-Because it models the grid, it can be used for simple grid fault simulations and therefore it is useful as documentation for customers and useful as a supportive component for larger grid connection studies.

-The model is easy to handle, since all input parameters used for the simulations are available by documentation inside the company.

-The usage of Matlab/ Simulink keeps the specific model open for adaptation to a variety of uses, for example for the purpose of harmonic studies.

### **5.2.5. Results obtained from the models**

-The generator effects like saturation are alleviated by doubly-fed operation and are more likely to be experienced with an asynchronous machine with a short-circuited rotor.

-While the Sinovel wind turbine model shows especially stresses of the electrical system during fault situations, Other wind turbines model may show more stresses of the mechanical system compared to the electrical system, this is based on the control and protection strategy.

-The investigation with the Sinovel wind turbine model also shows high stresses internally in the turbine in order to retain good power quality.

-The simulated examples show a satisfactory wind turbine operation within the accepted operation limits.

-During modelling of the turbine a review of the control and protection systems has been conducted.

#### **5.2.6. Wind turbine protection**

-An Overview of Electrical Faults in Wind Farm Systems has been investigated and presented

-The common protective schemes for wind farms as well as the basic Protection Functions has been studied.

-The investigation of Rotor protection system, Wind turbine controller role, Protection of the local step-up transformer, Collector feeder protection is made in this work.

-The analysis of the basic protection challenges has been made in this work at which the distribution system topology, protection system configuration, distributed generation effects, control system requirements, and dynamic behavior of the asynchronous generator were the main points.

-The case study of this work is Bereket Enerji-Uşak RES 54MW that shows a satisfactory wind turbine operation within the accepted operation limits at which the performance of DFIG units has been evaluated and simulated.

### 5.3. Recommendation and future work

The research captured in this work represents the state of the art and challenges of today, though it is only a step in the effort to clarify the influences of faults in wind turbines and their impact on the grid. The following are opportunities for future work:

- To include saturation and iron losses in all electrical machine models based on standard data-sheets;
- To develop an advanced 3-phase 3-winding model for transformer and include saturation in the transformer models.
- To develop Abc/abcmodels for synchronous machine both field winding and permanent magnet.
- To develop an advanced model for overhead-lines and shielded cables.
- To develop an Differential and Algebraic Equation Solver (DAE) for Simulink;
- To develop models for new topologies and components, which can be used in future in the wind turbine applications e.g. switched reluctance generator, matrix converter, new control strategies for wind turbine/farm, etc.
- An important part the wind turbine model yet to be implemented, is the total protection system of the turbine. A model encompassing this would to enable further fault studies.
- Extending the model with recently developed control strategies for fault ride through capability.
- Further validation of the transformer and the complete turbine models with measurements should be performed.

-Implementation of other machine phenomena such as slots effects, skin effects and the implementation of a realistic converter model to capture harmonic contributions to the turbine and investigate overload conditions of the converter.

-Expanding the study in order to clarify the influence of several different generator types and finding a rule for the machine phenomena.

-Measurement of an asymmetrical fault to further validate the machine and wind turbine model.

Another major challenge to modelling such a complex system with many nonlinear elements in Matlab/ Simulink is the stability of the simulation itself. Therefore one of the major issues beside the scientific work mentioned above is an optimisation of the models for the use in Matlab/ Simulink. Another possibility is to translate the achieved models from their representation in Simulink to Matlab (without Simulink) and use the graphical user interface programming which was recently introduced by Matlab or the use of another simulation platform altogether.

## REFERENCES

- [1] SIPSUR GE, Integrated Protection System for Rural Substations- Protection & Control and Union Electrica Fenosa (Spain) under a PIE research project, 1990.
- [2] M.L.REICHARD, D. FINNEY, J.T. GARRITY, Wind Farm System Protection and Stability Using Peer to Peer Communications, CIGRE Canada, Power Systems Conference, 2006.
- [3] RICH HUNT, JORGE CARDENAS, VIJAY MUTHUKRISHNAN, DAVID MCGINN, Wind Farm Protection Using an IEC 61850 Process Bus Architecture– GE Digital Energy Multilin. Presented at the 2010 DistribuTech Conference & Exposition, March 23, 2010.
- [4] H. HAZAL EDREMITLIOGLU, C. KUTHAN TOYDEMIR, OZAN BASKAN. Economical, Environmental outcomes of Wind Energy production in Turkey, Worcester Polytechnic Institute., 2007.
- [5] S. CLARKE – Engineer, Electricity Generation Using Small Wind Turbines at Your Home or Farm, Rural Environment/OMAFRA. Ontario Sept, 2003.
- [6] Infrastructure needed before wind turbines, Kate Snyder. September 21, 2013.
- [7] VEYSEL YILMAZ, H. ERAY ÇELİK, A statistical approach to estimate the wind speed distribution: the case of gelibolu region. Eskişehir Osmangazi University. Doğu Üniversitesi Dergisi, 9 (1) 2008.
- [8] AHMET DURAN ŞAHİN, İBRAHİM DİNCER, MARC A.ROSEN, Thermodynamical analysis of wind Energy, Canada Ontario 13 jan, 2006.
- [9] ADEL MOHAMMED REDHA, İBRAHİM DİNCER, MOHAMED GAD-ALLA, Erratum to “Thermodynamic performance assessment of wind energy systems: An application” [Energy (2011) 36: 4002–4010]”,. January 2012.
- [10] J.R. SAENZ, G. TAPIA, X. OSTOLAZA, A. TAPIA, R. CRIADO, J.L. BERASTEGUI, Simulation of a wind farm performance under wind speed changes, Electricity Distribution, 2001. Part 1: Contributions. CIRED. 16th International; Conference and Exhibition on (IEE Conf. Publ No. 482), Volume: Summaries , 2001.

- [11] SP TRANSMISSION & DISTRIBUTION, SCOTTISH HYDRO ELECTRIC, Guidance Note for the connection of Wind Farms, Issue No. 2.1.4, December 2002, Scotland.
- [12] A. TAPIA, G. TAPIA, X. OSTOLAZA, E. FERNANDEZ, J.R. SAENZ, Modeling and dynamic regulation of a wind farm, Power Electronics Congress, 2000. CIEP 2000. VII IEEE International , 2000.
- [13] LUBOSNY, Z., Wind Turbine Operation- Electric Power Systems. Springer, Germany.2003.
- [14] BALAS, M. FINGERSH, L. JOHNSON, K. PAO, L. (2006) Control of Variable-Speed Wind Turbines: standard and adaptive techniques for maximizing energy capture. IEEE Control Systems, Magazine, [Online] 26, 70-81, Available, from: [www3.imperial.ac.uk/library/digitalibrary/electronicjournals](http://www3.imperial.ac.uk/library/digitalibrary/electronicjournals), accessed:11.12.2014.
- [15] BONGERS, P. VAN BAARS, G. (1992) Wind turbine control design and implementation based on experimental models. *IEEE*, [Online] 2, 2454-2459 Available from:[www3.imperial.ac.uk/library/digitalibrary/electronicjournals](http://www3.imperial.ac.uk/library/digitalibrary/electronicjournals), accessed:27.10.2014.
- [16] MOHIT SINGH, Dynamic Models for Wind Turbines and Wind Power Plants, The University of Texas at Austin, USA, 2011. accessed 07.10.2014.
- [17] BUTTERFIELD, C. MULJADI, E. (2001) Pitch-Controlled Variable-Speed Wind Turbine Generation. IEEE Transactions on Industry Applications, [Online] 37, 240-246 Available from: [www3.imperial.ac.uk/library/digitalibrary/electronicjournals](http://www3.imperial.ac.uk/library/digitalibrary/electronicjournals), accessed:10.09 2013.
- [18] MAXPRO CORPORATION. 2015 Generic Direct Drive Wind Turbine with 77.5 meter Conventional Tower (online),United NRG Group available from: [www.grabcad.com/library/generic-direct-drive-wind-turbine-with-77-dot-5-meter-conventional-tower](http://www.grabcad.com/library/generic-direct-drive-wind-turbine-with-77-dot-5-meter-conventional-tower), accessed 19.12.2014.
- [19] ACKERMANN, T. SÖDER (2000) Wind energy technology and current status: a review. Renewable and Sustainable Energy Reviews, [Online] 315-374 Available from: [www3.imperial.ac.uk/library/digitalibrary/electronicjournals](http://www3.imperial.ac.uk/library/digitalibrary/electronicjournals), accessed:21.10.2014.
- [20] FUJITA, H. FUNABASHI, T SEKINE, H. SENJYU, T. SAKAMOTO, R URASAKI, N. (2006) Output Power Levelling of Wind Turbine Generator for All Operating Regions by Pitch Angle Control. IEEE Transactions on Energy Conversion, [Online] 21, 467-475 Available from: [www3.imperial.ac.uk/library/digitalibrary/electronicjournals](http://www3.imperial.ac.uk/library/digitalibrary/electronicjournals), accessed:16.12.2014.

- [21] BRITISH WIND ENERGY ASSOCIATION (2006) The technology of turbines. [Online] Available from: [www.bwea.com/ref/tech.html](http://www.bwea.com/ref/tech.html), accessed: 01.10.2013.
- [22] KARRARI, M. MALIK, O. ROSEHART, W. (2005) Comprehensive Control Strategy for a Variable Speed Cage Machine Wind Generation Unit. *IEEE Transactions on Energy Conversion*, [Online] 20,415-423, Available from: [www3.imperial.ac.uk/library/digitallibrary/electronicjournals](http://www3.imperial.ac.uk/library/digitallibrary/electronicjournals), accessed:20.01.2015.
- [23] BONGERS, P. VAN BAARS, G. (1992) Wind turbine control design and implementation based on-experimental-models.*IEEE*,[Online]2,2454-2459,Available from: [www3.imperial.ac.uk/library/digitallibrary/electronicjournals](http://www3.imperial.ac.uk/library/digitallibrary/electronicjournals),accessed 20.06.2013.
- [24] EERE (2007) Wind Power. [Online] Available from: [www1.eere.energy.gov/windandhydro/wind\\_how.html](http://www1.eere.energy.gov/windandhydro/wind_how.html),accessed 30.07.2013.
- [25] JENKINS, N. WALKER, J. *Wind Energy Technology*. Wiley, England.1997.
- [26] W.A. TIMME, *Aerodynamic characteristics of wind turbine blade airfoils at high angles-of-attack*; Crete, Greece.2010.
- [27] HARRISON, R. HAU, E. SNEL, H. *Large Wind Turbines*. Wiley, England.2000.
- [28] R VIJAY, ADITYA KUMAR SETHI, *Pitch Control of Horizontal Axis Wind Turbine*. National Institute of Technology, Rourkela,2011.
- [29] MCNERNEY, G. RICHARDSON, D. (1993) *Wind Energy Systems*. *IEEE*, [Online] 81, 378-389 Available from: [www3.imperial.ac.uk/library/digitallibrary/electronicjournals](http://www3.imperial.ac.uk/library/digitallibrary/electronicjournals),accessed 27.02.2015.
- [30] AEOLOS WIND ENERGY, Ltd-The leading small wind turbine company in the world.The comparatives parameters. *Horizontal Axis Wind Turbine VS Vertical Axis Wind Turbine*. (Europe & America).
- [31] ACKERMANN, T. (ed). *Wind Power in Power Systems*. Wiley, England,2005.
- [32] EL-TOUS, Y. *Pitch Angle Control of Variable Speed Wind Turbine*. *American J. Of Engineering and Applied Sciences* 1 (2): 118-120, 3.2008.
- [33] GOPAL, M., *Digital Control and State Variable Methods*. New Delhi: Tata McGraw Hill Education Private Limited,2010.



- [34] VORGELEGT VON, GEORGIOS PECHLIVANOGLU. Passive and active flow control solutions for windturbine blades. Germany,Berlin. 2013  
JOHN ANDERSON.AWEA, American Wind Energy Association. Siting wind farms requires choosing a proper location. Washington,DC,2013.
- [35] RELEVANSI, Offshore and Onshore: The Debate in Wind Energy. America,2011.
- [36] BWEA(2005), Wind Turbine Technology. [Online] Available from: [www.bwea.com/energy/briefing-sheets.html](http://www.bwea.com/energy/briefing-sheets.html), accessed 20.08.2013.
- [37] VLADISLAV AKHMATOV, Analysis of Dynamic Behavior of Electric Power Systems with Large Amount of Wind Power, PhD Thesis, Ørsted DTU, Denmark, April 2003 .
- [38] J.R. SAENZ, G. TAPIA, X. OSTOLAZA, A. TAPIA, R. CRIADO, J.L. BERASTEGUI, Simulation of a wind farm performance under wind speed changes, Electricity Distribution, 2001. Part 1: Contributions. CIRED. 16th International; Conference and Exhibition on (IEE Conf. Publ No. 482) , Volume: Summaries , 2001 .
- [39] E.ON NETZ, Netzanschlussregeln Hoch- und Höchstspannung, Germany, August 2003.
- [40] FENG DONG, MARIESA L. CROW, BADRUL H. CHOWDHURY , LEVENT AÇAR. Improving Voltage Stability by Reactive Power Reserve Management,IEEE. Missouri-Rolla, Rolla, MO 65409 USA, 2005.
- [41] PETER CHRISTIANSEN, JESPER R. KRISTOFFERSEN, The Wind Farm Main Controller and the Remote Control System of the Horns Rev Offshore Wind Farm, Proceedings Fourth International Workshop on Large-Scale Integration of Wind Power and Transmission Networks for Offshore Wind Farms, Billund, Denmark, October 2003.
- [42] PETER NOVAK, INGE JOVIK, BENGT SCHMIDTBAUER, Modeling and Identification of Drive-System Dynamics in a Variable-Speed Wind Turbine, IEEE 0-7803-1872-2/94,1994.
- [43] K.P.KOVACS,Symmetrische-Komponenten in Wechselstrommaschinen,Birkhäuser Verlag,1962 .
- [44] P. C. KRAUSE, O. WASYNCZUK, S. D. SUDHOFF, Analysis of electrical Machinery, IEEE PRESS, 1994 ISBN 0-7803-1101-9.
- [45] NECA, National Electricity Code, Version 1.0 Amendment 8.0, 1999 - 2003,Australia.
- [46] ION BOLDEA, S. A. NASAR, Electric Drives, CRC Press LLC, 1999, ISBN 0-8493-2521-8.

- [47] A.H. GHORASHI, S.S. MURTHY, B.P SINGH, Field Studies and Transient Analysis Related to Wind Electric Systems, Proceedings of Power Electronics, Drives and Energy Systems for Industrial Growth, Volume: 1 , 1995, p. 271 -279 vol.1, 1996.
- [48] PRABHA KUNDUR, Power System Stability and Control, McGraw-Hill Inc. 1993, ISBN 0-07-035958-X.
- [49] W. LANGREDER, Models for Variable Speed Wind Turbines, Risø 1996.
- [50] K. VOGT, Berechnung elektrischer Maschinen, VCH Verlag, 1996, ISBN 3-527-28391-9.
- [51] RUDOLF RICHTER, Elektrische Maschinen/ Die Transformatoren,3. Band, Birkhäuser Verlag, 1963.
- [52] ZHONGMING YE, BIN WU, Simulation of Electrical Faults of Three Phase Induction Motor Drive System, Power System Technology, Proceed. of PowerCon, Vol. 2 pp. 789-794, 2000.
- [53] P. PILLAY, V. LEVIN, Mathematical models for asynchronous generators, Proceed. of IAS- 95, Vol.X.pp.606-616.
- [54] C. GOLDEMBERG, A. DE ARRUDA PENTEADO, F. A. M. SALOTTI, Induction motor analysis in the ABC/abc reference frame including saturation effects, Proceed. of the ICEM 2000,pp.397-401, 2000.
- [55] A.E.FITZGERALD,CHARLES KINGSLEY,JR.,STEPHEN D. UMANS, Electric Machinery, McGraw-Hill Book Company, 1992, ISBN 0-07-112946-4.
- [56] JULIJA MATEVOSYAN, THOMAS ACKERMANN, SIGRID BOLIK, LENNART SÖDER, Comparison of International Regulations for Connection of Wind Turbines to the Network, NWPC '04, Grid Integration and Electrical Systems of Wind Turbines and Wind Farms.
- [57] JØRGEN KAAS PEDERSEN, SKJOLD SAXE, Magnetiske Kredse og Transformere, Den private ingeniørfond ved Dth, Laboratoriet for Almen Elektroteknik, Danmarks tekniske Højskole, 2800 Lyngby,1974.
- [58] Iov F, Hansen A.D., Sørensen P., Cutululis N.A.,” Mapping of grid faults and grid codes”, Risø report, Risø-R-1617(EN), 2007, 40p.
- [59] D. HORNAK, N. CHAU, “Green power - wind generated protection and control considerations”, Protective Relay Engineers, 57th Annual Conference for 30 Mar-1 Apr 2004, pp. 110 – 131.,2004.
- [60] S. MUSUNURI,"Protection requirements for a large scale wind park", Protective Relay Engineers Conference, pp. 478 – 491, 30.03.2009 to 04.02.2009

- [61] TEIAŞ, Grid Access and Integration of Renewable Energy Resources (RES), Turkish Electricity Transmission Corporation (TEIAS), 2011.
- [62] ANDREAS DITTRICH ALEXANDER STOEV, "Comparison of fault ride-through strategies for wind turbines with DFIM generators", Power Electronics and Applications, European Conference on, Dresden, Germany, 2005.
- [63] NIIRANEN, J. "Voltage Dip Ride Through of Doubly-Fed Generator Equipped with Active Crowbar", Nordic Wind Power Conference, 1-2 March 2004, Chalmers University of Technology, Göteborg, Sweden. 2004.
- [64] NIIRANEN, J. 2005. "Experiences on Voltage Dip Ride through Factory Testing of Synchronous and Doubly Fed Generator Drives", Proceedings of 11th European Conference on Power Electronics and Applications. Dresden, Germany, 11-14, September 2005.
- [65] XIANG, D., RAN, L., TAVNER, P.J., BUMBY, J.R. 2004. "Control of a Doubly-fed Induction Generator to Ride-through a Grid Fault", Proceedings of ICEM 2004, Cracow, Poland, 5-8 September 2004.
- [66] ERLICH, W. WINTER, A. DITTRIC, "Advanced Grid Requirements for the Integration of Wind Turbines into the German Transmission System", IEEE General Meeting, GM2006.
- [67] S. HASLAM, P. CROSSLEY AND N. JENKINS, "Design and evaluation of a wind farm protection relay", Generation, Transmission and Distribution, IEE Proceedings, Volume 146, Issue 1, pp. 37 – 44, Jan. 1999.
- [68] TAMER KAWADY, "An Interactive Simulation of Grid-Connected DFIG Units for Protective Relaying Studies", IEEE PES/IAS Sustainable Alternative Energy Conference-2009, Valencia, Spain, 28-30 Sept., 2009.

## **RESUME**

Eric NDUWAYEZU was born in Rwanda on 16.10.1986. He received the B.Sc. degree in electrical engineering from Kigali Institute of Science and Technology that is currently College of Science and Technology, University of Rwanda in 2012, and the M.Sc. degree in electrical and Electronics Engineering still from Sakarya University, Turkey in 2015. His research interests include renewable energy systems, electrical power systems and its protections, and detection of imbalances in wind turbine generators. In 2012 he was the Technical Development Services Engineer at E.quinox where he involved in many solar projects implementation. In 2015 he involved in different research papers and currently he works as an engineer in ELIMSAN, a leading Turkish company in Switchgears production.